To the Graduate Council:

I am submitting herewith a dissertation written by Richard Ray Kemmerer entitled "Matrix Isolation Fourier Transform Infrared Spectroscopy of Polycyclic Aromatic Hydrocarbons." I recommend that it be accepted in partial fulfillment of the requirements for the degree of Doctor of Philosophy, with a major in Chemistry.

Gleb Mamantov, Major Professor

Earl L. Wehry, Major Professor

We have read this dissertation and recommend its acceptance:

Accepted for the Council:

Vice Chancellor
Graduate Studies and Research

Thesis
Ph
.K455
c.1-2

MATRIX ISOLATION FOURIER TRANSFORM INFRARED SPECTROSCOPY OF POLYCYCLIC AROMATIC HYDROCARBONS

A Dissertation

Presented for the

Doctor of Philosophy

Degree

The University of Tennessee, Knoxville

Richard Ray Kemmerer

June 1977

1324223

ACKNOWLEDGMENTS

The author would like to express his thanks to Dr. Gleb Mamantov and Dr. Earl L. Wehry for their help and guidance during the course of this work.

The financial assistance received by the author from the Electric Power Research Institute is greatly appreciated.

The author would like to give a special thanks to his wife, Becky, for her support and encouragement during his years at The University of Tennessee.

ABSTRACT

The application of matrix isolation Fourier transform infrared (MI-FT-IR) spectroscopy to the qualitative and quantitative analysis of polycyclic aromatic hydrocarbons was demonstrated.

Matrix isolated samples were prepared by codeposition of polycyclic aromatic hydrocarbon (PAH) vapors and a large excess of nitrogen at 15 K. PAH's were vaporized and directed to the deposition surface by means of a Knudsen effusion cell.

MI-FT-IR absorption spectra for 18 PAH's were obtained. The IR absorption bands between 900-700 cm^{-1} for the PAH's studied were sufficiently narrow to resolve several isomers and complex (10-component) mixtures. Spectral subtraction of PAH mixtures which contained similar spectral features permitted identification of individual components. The PAH content in synthetic liquid fuel (Synthoil) and shale oil fractions prepared by high pressure liquid chromatography was partially determined by MI-FT-IR.

Beer's law was shown to apply to MI-FT-IR PAH samples over a wide concentration range (1-2 decades). Using beam condensing optics, a detection limit of 50 ng of perylene (2×10^{-10} moles) was achieved. Precision was dependent on the sampling arrangement used and varied from 15% to 5%.

TABLE OF CONTENTS

CHAPTER		PAGE
I.	INTRODUCTION	1
	A. Overview of the Problem	1
	B. Carcinogenesis of PAH's	3
	C. Analytical Methods	4
	D. Fourier Transform Infrared Spectroscopy	13
	E. Low Temperature Matrix Isolation	23
	F. Statement of the Problem	27
II.	EXPERIMENTAL TECHNIQUES	28
	A. Materials	28
	B. Equipment	28
	C. General Sampling System	34
	D. Microsampling System	40
	E. Ultramicrosampling System	40
III.	RESULTS AND DISCUSSION	45
	A. General	45
	B. Qualitative Studies	60
	C. Quantitative Studies	88
	D. Comparison with Conventional Sampling Techniques	102
IV.	SUMMARY	106
LIST OF REFERENCES		110
APPENDIX		116
VITA		133

LIST OF TABLES

TABLE		PAGE
I.	Occurrence of PAH's in the Environment	2
II.	Comparison of UV-Visible Absorption Spectrophotometry, Fluorescence, and GC-MS for PAH Analysis	11
III.	Sources and Purity of Compounds	29
IV.	Strong and Medium MI-IR Absorption Bands of Polycyclic Aromatic Hydrocarbons	46
V.	PAH's Grouped by Vaporization Temperature	48
VI.	Matrix Shifts for Three PAH's in Different Matrices	50
VII.	The Ten-Component Mixture: Compounds and Weights	68
VIII.	PAH's Suspected to Be in HPLC Fractions	71
IX.	Detection Limits for Six PAH's	95
X.	Comparison of Peak Height and Integrated Area Methods for Quantitative Determinations	97
XI.	Effect of Annealing on the Absorbance of the 846 cm^{-1} Band of Pyrene	99
XII.	Precision Using the Ultramicrosampling System	101
XIII.	FT-IR Absorption Band Positions for N_2 and KBr Matrices	104
XIV.	Structures of Polycyclic Aromatic Hydrocarbons	118

LIST OF FIGURES

FIGURE		PAGE
1.	Analytical Scheme for Fractionation, Separation, and Identification of PAH's	7
2.	Michelson Interferometer	14
3.	Interferogram and Computed Spectrum of a Broadband IR Polychromatic Light Source	18
4.	Instrument Line Shape, $f(\bar{\nu})$, Resulting From the Fourier Transform of a Truncated Waveform	20
5.	Cryogenic Technology, Inc. Spectrim^{TM} Cryostat	30
6.	Optical diagram of the FTS-20V Infrared Spectrometer	33
7.	Block Diagram of the FTS-20V Infrared Spectrometer	35
8.	Knudsen Cell and Support for the General Sampling System	36
9.	Complete Oven Assembly Interfaced to the Sample Chamber	38
10.	Cryostat with the Sample Chamber in Place	39
11.	Knudsen Cell and Oven Assembly for Microsampling	41
12.	Optical Diagram of the 6X Beam Condenser Used with the FTS-20V Spectrometer	43
13.	Ultramicrosampling Assembly	44
14.	Comparison of Bandwidths as a Function of N_2/Pyrene Mole Ratio	53
15.	Transmittance Spectra of Carbazole and Benz[a]anthracene, 500-250 cm^{-1}	56
16.	Transmittance Spectra of Phenanthrene and Pyrene, 500-250 cm^{-1}	57

FIGURE PAGE

17. Transmittance Spectrum of a Mixture of Anthracene and Phenanthrene 62

18. Transmittance Spectrum of a Mixture of $C_{18}H_{12}$ Isomers . . 63

19. Transmittance Spectrum of a Four-Component Mixture 65

20. Absorbance Spectrum of a Five-Component Mixture 66

21. Absorbance Spectrum of a Ten-Component Mixture 69

22. Absorbance Spectrum of Synthoil Fraction III Prepared with Microsampling System 72

23. Absorbance Spectrum of Synthoil Fraction IV Prepared with Microsampling System 73

24. Absorbance Spectrum of Synthoil Fraction V Prepared with Microsampling System 74

25. Absorbance Spectrum of Synthoil Fraction IV Prepared with Ultramicrosampling System 76

26. Absorbance Spectrum of Shale Oil Fraction IV Prepared with Ultramicrosampling System 77

27. Absorbance Spectrum of Synthoil Fraction V Prepared with Ultramicrosampling System 78

28. Absorbance Spectrum of Shale Oil Fraction V Prepared with Ultramicrosampling System 79

29. Absorbance Spectrum of NBS Sample with Expanded 900-835 cm^{-1} Region 83

30. Spectral Subtraction of Benz[a]anthracene from a Six-Component Mixture 85

31. Spectral Subtraction of Benzo[e]pyrene from a Six-Component Mixture 86

FIGURE		PAGE
32.	Beer's Law Plot for the 753 cm^{-1} Band of Benzo[e]pyrene .	90
33.	Beer's Law Plot for the 846 cm^{-1} Band of Pyrene	91
34.	Beer's Law Plot for the 764 cm^{-1} Band of Chrysene . . .	92
35.	Beer's Law Plots for Benz[a]anthracene and Benzo[a]pyrene	93
36.	Transmittance MI-FT-IR Spectra of Acenaphthene, Fluorene, Phenanthrene, and Anthracene	121
37.	Transmittance MI-FT-IR Spectra of Fluoranthene, Pyrene, Benzo[a]fluorene, and Benzo[b]fluorene	122
38.	Transmittance MI-FT-IR Spectra of Naphthacene, Chrysene, Benz[a]anthracene, and Triphenylene	123
39.	Transmittance MI-FT-IR Spectra of Benzo[a]pyrene, Benzo[e]pyrene, Perylene, and 1,3,5-Triphenylbenzene . .	124
40.	Transmittance MI-FT-IR Spectrum of Carbazole	125
41.	Transmittance Spectrum of Pyrene, 3200-500 cm^{-1}	126
42.	Transmittance Spectrum of Benz[a]anthracene, 3200-500 cm^{-1}	127
43.	Expanded Spectra for the Compounds Shown in Figure 36, p 121, 900-700 cm^{-1}	128
44.	Expanded Spectra for the Compounds Shown in Figure 37, p 122, 900-700 cm^{-1}	129
45.	Expanded Spectra for the Compounds Shown in Figure 38, p 123, 900-700 cm^{-1}	130
46.	Expanded Spectra for the Compounds Shown in Figure 39, p 124, 900-700 cm^{-1}	131
47.	Expanded Spectrum for Carbazole, 900-700 cm^{-1}	132

CHAPTER I

INTRODUCTION

A. Overview of the Problem

In recent years, polycyclic aromatic hydrocarbons have become the subject of intensive research.[1] Polycyclic aromatic hydrocarbons (also known as polynuclear aromatic hydrocarbons) comprise a large group of compounds consisting of fused benzene rings. Several representative polycyclic aromatic hydrocarbon (PAH) compounds are shown in Table XIV (Appendix).

The reasons for the interest in these compounds are that several of them have been shown to be carcinogenic[1] (as indicated by + designations in Table XIV, Appendix), and that they are widely distributed in our environment.[2] The product of incomplete combustion or pyrolysis of carbonaceous material at high temperature,[3,4] PAH's have been identified in automobile exhaust,[5-7] tobacco smoke,[8,9] and in the emisssions from home furnaces, fossil fuel power plants, and factories[10] (Table I). With the recent increase in research activity in coal conversion processes, it has become necessary to consider the environmental consequences of the PAH byproducts of these processes. In preliminary studies, extremely high concentrations of PAH's have been found in the atmosphere in the vicinity of these conversion plants.[11] The products (i.e., liquid fuels) also contain significant quantities of PAH's.[12] Due to their widespread presence, PAH's constitute a serious health hazard. It is therefore necessary that accurate and sensitive routine analytical

TABLE I

OCCURRENCE OF PAH'S IN THE ENVIRONMENT

Source	Benzo[a]pyrene	Benz[a]anthracene
Urban air (particulates)[10]	5.1-130 μg/1500 m^3 air[a]	13.1 μg/1500 m^3 air[b]
Automotive exhaust[5]	6.6 $\mu g/m^3$	$\sim$ 26.4 $\mu g/m^3$
Tobacco smoke[3]	1 μg/40 cigarettes	--
Air sampled near coal conversion plants[11]	19 $\mu g/m^3$	--
Power plant stack[10]	320 μg/1000 m^3	--
Coal tar emissions[10]	486 $\mu g/m^3$ air[a]	1601 $\mu g/m^3$ air[b]

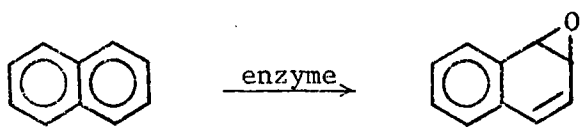
[a]Includes benzo[e]pyrene.

[b]Includes isomers chrysene and triphenylene.

methods be available for the evaluation of the environmental impact of PAH's.

B. Carcinogenesis of PAH's

It has been known for many years that the agents responsible for the carcinogenic properties of soot, coal tar, and particulate matter are polycyclic aromatic hydrocarbons. Despite the intensive research in this area, however, the mechanisms for their carcinogenic activity have yet to be fully understood. The most accepted mechanism is that PAH's are metabolically converted to a highly reactive form, either an arene oxide or epoxide.[13,14] The conversion is catalyzed by a complicated microsomal enzyme system; aryl hydrocarbon hydroxylase (AHH) and hepatic monoxygenase are two such enzymes that have been identified.



(1)

It is believed that it is this reactive species which is carcinogenic and that the PAH is a precursor.

The arene oxide species can undergo a number of activating and deactivating reactions. The deactivation reactions (isomerization, rearrangement, hydration, etc.) serve to diminish the cytotoxicity of the epoxide. The covalent bonding of the epoxide with a variety of cellular macromolecules, such as DNA, RNA and protein, appears to be the critical reaction for carcinogenic activation. Toxic, carcinogenic, and mutagenic effects often correlate to the extent of binding of aromatic compounds to biopolymers. There is evidence that possibly bioactivated intermediates

other than arene oxides have a role in the carcinogenicity of PAH's. The "K-region," the prototype of which is the 9,10-bond of phenanthrene, appears to be an important structural feature for the carcinogenic activity of PAH's.[15] Many questions remain to be answered in this research area before the mechanisms for bioactivation of PAH's are fully understood.

Polycyclic aromatic hydrocarbons alone may not promote carcinogenesis but may produce tumors in conjunction with a "cocarcinogen." These synergistic effects are important concepts in the carcinogenic properties of PAH's in complex mixtures such as atmospheric particulates.[16] Many materials which are present in particulates are capable of acting as inhibitors, promoters, or cocarcinogens with PAH's. It thus becomes important to the understanding of the problem that these effects are properly assessed. Accurate analytical information on the PAH's and their associated materials is necessary for a thorough evaluation of this complex problem.

C. Analytical Methods

The analysis of PAH's in atmospheric particulates is a difficult and complex problem. In a single air sample, over 100 PAH's have been identified.[17] The sheer number of these compounds requires that the analytical method be a high resolution technique. The concentration levels of PAH's in environmental samples are often quite low (μg range/1000 m^3 of air), requiring a technique with high sensitivity.[18,19] The chemical and physical properties of PAH's are very similar, which makes separation difficult. PAH mixtures often contain several structural isomers and alkylated derivatives which are difficult to resolve. In

atmospheric samples, PAH's are adsorbed on particulate matter[20] which complicates the sampling and recovery of these compounds. Finally, the presence of a multitude of other compounds in the sample increases the analytical difficulty.

1. Separation

The current analytical methodologies for PAH analysis are consequently complex, tedious, and multi-faceted.[3,21-23] The determination of virtually all PAH samples begins with solvent extraction. In order that atmospheric PAH's be in a form compatible with common analytical methods, they must be extracted from the particulate matter. This also accomplishes a primary separation from other materials by proper selection of the solvent. Benzene and cyclohexane are the most popular solvents. Comparisons of the numerous solvents have been made.[23,24] Solvent extraction is a long (eight hour or more) procedure with a recovery of less than 100%. The problem of contamination by the solvent also exists.

The extract which contains PAH's is a complex mixture which truly taxes analytical ingenuity. Further separation is now required to successfully identify all the PAH's present. Consequently, the largest area of investigation in the field of PAH analysis is the development of separation methods. By partitioning the mixture into fractions with fewer or single components, the complete analysis becomes feasible. Chromatographic procedures for PAH separation have received much attention.[25] Paper chromatography,[26] capillary gas chromatography,[27,28] thin layer chromatography (TLC),[29] gel permeation,[30] gas-solid

chromatography,[31] and high pressure liquid chromatography (HPLC)[32-34] have all been utilized for this problem. Often more than one separation or technique is necessary to achieve total separation of the individual components. The degree of separation and the method used will depend on the resolution of and compatibility with the detection method used. For instance, UV and fluorescence are most compatible with TLC, paper chromatography, and HPLC, while gas chromatography fractions may best be analyzed by interfacing with mass spectrometry. Figure 1 outlines an analytical scheme for PAH analysis which incorporates the basic components of a complete analysis.[35] The separation scheme and detection may vary, but the general procedure is universal at the present state of the art.

The methods of detection used to identify PAH's include most all modern techniques capable of multicomponent analysis. Voltammetry,[36] X-ray fluorescence spectroscopy,[37] and nmr[38] are just a few of the methods explored with varying degrees of success. Fluorescence, UV absorption, and mass spectrometry are, however, the methods which have found the most utility and application to the routine analysis of PAH.

2. Detection

a. Ultraviolet-visible. Historically, ultraviolet-visible absorption spectrophotometry has been the method of choice for routine PAH analysis. Compilations of UV-visible spectra of PAH are readily available.[39] Column chromatography with UV-visible spectrophotometry was used as early as 1950 for PAH analysis.[40] The "standard" methods outlined for the complete and/or routine analysis of PAH's consist of column chromatography followed by UV-visible detection.[2,41] This method,

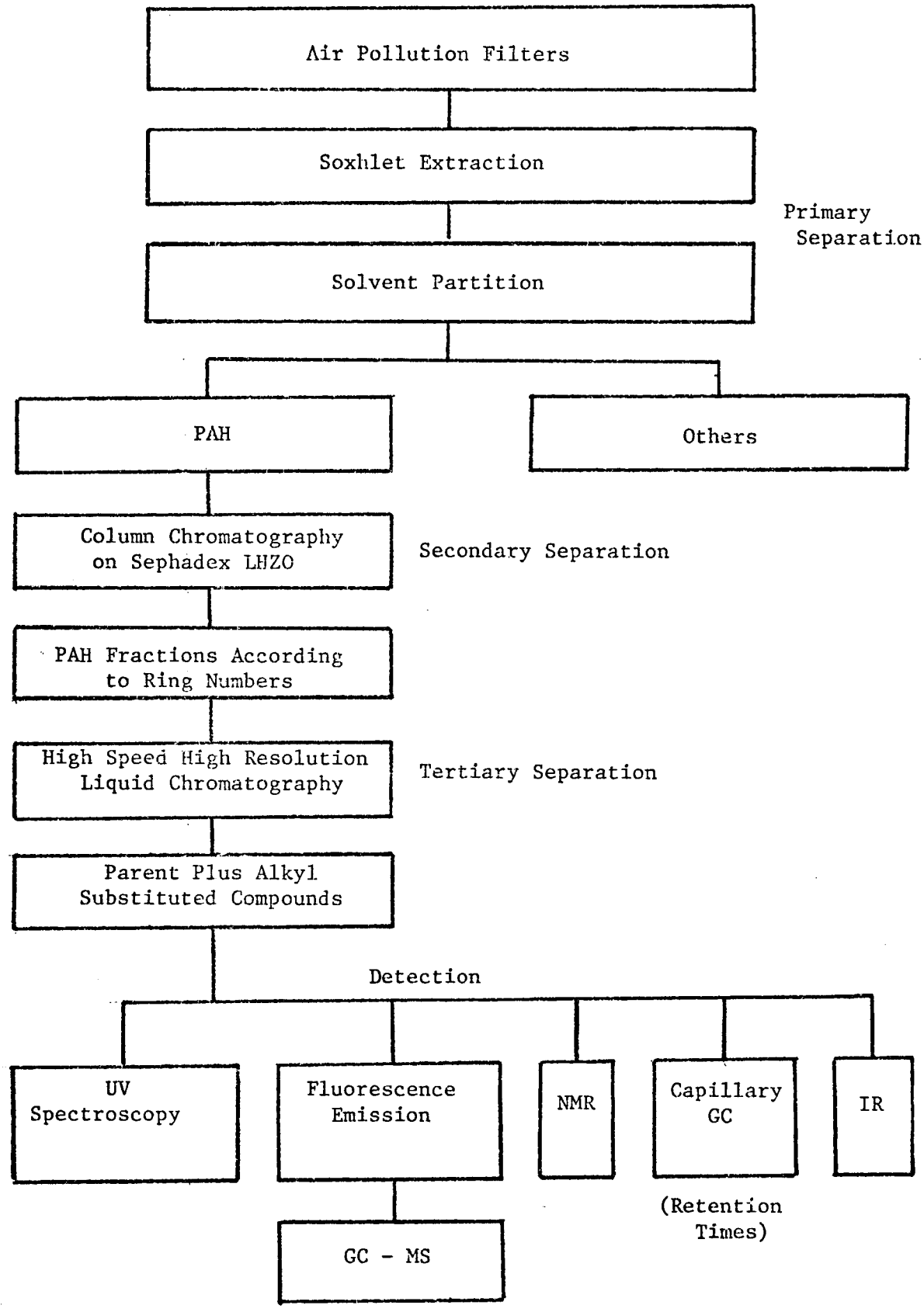


Figure 1. Analytical scheme for fractionation, separation, and identification of PAH's.[35]

however, requires large samples and does not lend itself to the routine analysis of atmospheric PAH's.[22] Results are often unreliable. The sensitivity is on the order of μg/1000 m^3 of air. The UV spectra of alkyl derivatives are often very similar to the parent compound, which makes their characterization difficult.

With the recent advances in HPLC, this technique has found extensive application to the analysis of PAH's. UV-visible absorption in combination with HPLC provides a versatile tool.[42,43] Using a variable wavelength UV detector, the utility of this technique in analyzing atmospheric and coal tar samples has been shown. Identification is made by retention times, UV-visible spectra, and quantitation done by standard addition. High (sub-μg) sensitivity is obtainable and calibration plots are linear over a wide range. The capability of this method to resolve isomers has not been demonstrated. HPLC with UV-visible detection does have great potential and may well supplant column chromatography with UV-visible spectrophotometry in routine analysis.

UV-visible spectrophometry combined with column chromatography is a low-cost method with little special equipment needed. The improvements in HPLC with UV-visible detection make it more competitive with other methods for routine analyses of low levels of PAH's.

b. Fluorescence. Virtually all polycyclic aromatic hydrocarbons fluoresce, making fluorescence an important technique for PAH detection.[44] The advantages of fluorescence over UV-visible spectrophotometry are greater sensitivity and usually greater selectivity.[41] The disadvantages are poorer reproducibility due to instrumental, quenching, and

fluorescence-enhancement problems. Also, fluorescence is highly sensitive to impurity effects. Room temperature fluorescence spectra consist of broad bands which make resolution of mixtures difficult. Thus most applications of fluorescence detection require adequate prior separation of the mixtures of PAH's. Two-dimensional TLC with fluorescence detection has been successfully employed for the qualitative and quantitative analysis of isomeric groups of PAH's.[19]

In order to reduce much of the time-consuming separation requirement for fluorescence detection, two main techniques have been explored. Characteristic fluorescence spectra with a large number of distinct, sharp bands can be obtained if the PAH measurements are carried out in a low temperature, solid paraffin matrix.[3] The sensitivity using this technique is as low as 0.1 to 10 ng/ml and mixtures of very similar isomers can be resolved. The major drawbacks of this technique are poor reproducibility and limited linear working range. The selectivity of fluorescence can also be enhanced by special fluorescence quenching effects.[45] These techniques also allow the determination of mixtures difficult to separate by conventional chromatographic methods. Quantitative results are poor for these methods.

Conventional fluorescence and its complementary technique, phosphorescence, offer sensitivity and selectivity advantages but may be difficult to use for quantitative work.

c. Gas chromatography - mass spectrometry. Probably the method which has shown the most promise as a complete analytical technique for PAH analysis is gas chromatography coupled with mass spectrometry (GC-MS).

This method was established as a powerful tool for PAH analysis by Lao et al. in 1973.[46] In this study, over 70 PAH's were identified in air filter samples. The method has been refined in subsequent studies[17] and utilized by others for PAH analysis in the environment.[20,47] Computerization has been incorporated to permit peak identification, library compilation, and background subtraction.

In addition to high sensitivity (ng level), the greatest advantage of this method is its ability to identify PAH's for which there may not be standards available. All other major techniques require standards for identification of PAH's. The biggest drawback of GC-MS is the inability of mass spectrometry to distinguish isomers. Thus, for this method to be useful, isomeric separation must precede analysis. Quantitative work is done by gas chromatography.

A comparison of the three techniques described above — ultraviolet and fluorescence spectroscopy, and GC-MS — is shown in Table II.

d. Infrared spectroscopy. Infrared spectroscopy (IR) is a universal and widely applied technique for qualitative and quantitative analysis,[49] but unlike fluorescence, UV spectrophotometry, and mass spectrometry it has been virtually ignored for the analysis of PAH's. There are several reasons for this. First, the sensitivity of IR is largely inadequate for determination of the low levels found in the environment. IR sources are relatively weak and band strengths of vibrational spectra typically equal only 1/100 o[illegible] electronic bands.[1] Second, the IR spectra of PAH's are very complex, making resolution of large mixtures difficult. Finally, the quantitative results by common

TABLE II

COMPARISON OF UV-VISIBLE ABSORPTION SPECTROPHOTOMETRY, FLUORESCENCE, AND GC-MS FOR PAH ANALYSIS

Characteristic	UV-Visible	Fluorescence	GC-MS (Computerized)
Sensitivity	1 μg[41]	0.1 ng[3]	1 ng[46]
Resolution of isomers[29]	yes	yes[a]	no
Resolution of alkyl derivatives[29]	not always	yes	yes
Universal (applicable to compounds other than PAH's, i.e. aliphatics)[48]	no	no	yes
Necessity for standard references	yes	yes	no
Initial cost[48]	$30,000-$40,000	$10,000-$20,000	$100,000
Interferences[22]	overlapping bands	self-absorption, solvent contamination	few
Applicability to routine analysis[48]	1 sample/day	8 samples/day	6 samples/day
Accuracy[1]	10%	5-10%	poor
Reproducibility[1]	7%	--	poor

[a]In a low temperature matrix.

IR techniques are generally not good at high concentrations due to molecular interactions. The universality of IR, however, makes it attractive for analyzing environmental samples as this method allows determination of a variety of compounds, not just PAH's. In addition, IR spectra of compounds with very similar structures differ considerably, allowing resolution of isomeric mixtures. Analysis of multicomponent systems by IR can be complicated, but is usually possible.

Results of early IR studies on PAH's have shown very little utility for environmental samples.[50-52] These studies tended to reinforce the problems mentioned. In solutions, up to 1 M concentrations of PAH's were utilized.[50] In another study, quantities of PAH's in the 20-200 μg range were determined.[52] Recently, two studies have demonstrated improvements in IR techniques which enhance its feasibility for PAH analysis.[53,54]

Boiteau et al.[53] have done virtually the only study of the utility of IR for PAH analysis of real samples. The detection limit obtained by this group using beam-condensing optics was 1 μg for several compounds. Their reproducibility was 4.8 to 7.8% for the compounds studied. They also showed that IR can be very valuable for qualitative identification of PAH's.

Brotherton[54] investigated the utility of Fourier transform IR spectroscopy for analyzing PAH's by a number of conventional sample preparation methods (liquid solutions, KBr pellets, and attenuated total reflectance). At high concentration levels (i.e., mg), a four-component mixture could be resolved. However, some of the most intense bands overlapped, indicating problems for low level determinations. Beer's law plots of PAH in solution and in KBr were linear over

concentrations of less than one order of magnitude. Detection limits were approximately 2-7 μg, depending on the medium and compound. It should be noted that these low detection limits were obtained without the use of microsampling optics or techniques.

Both studies demonstrate the utility of IR spectroscopy for the PAH problem even though they fall short in some regards. The enhancement of sensitivities, better quantitative capabilities, and the resolution of complex mixtures remain to be improved before IR can play a useful role in PAH analysis. A combination of two new techniques have made these improvements a real possibility and opened the way for application of IR to the PAH analysis problem. Fourier transform IR spectroscopy has been demonstrated to provide higher sensitivities than conventional spectroscopy. Low temperature matrix isolation can simplify spectra and reduce sample interactions to produce better precision of quantitative data.

D. Fourier Transform Infrared Spectroscopy

Although the theory of interferometry has been known since the 19th Century,[55] only in the last eight years has this technique been incorporated into commercially available Fourier transform spectrometers.[56] At present the technical problems associated with producing a reliable, high-resolution instrument have been solved, making this equipment available to the analytical laboratory.

1. Theory

The basic component of a Fourier transform spectrometer is a Michelson interferometer, shown in Figure 2.[57] The function of the

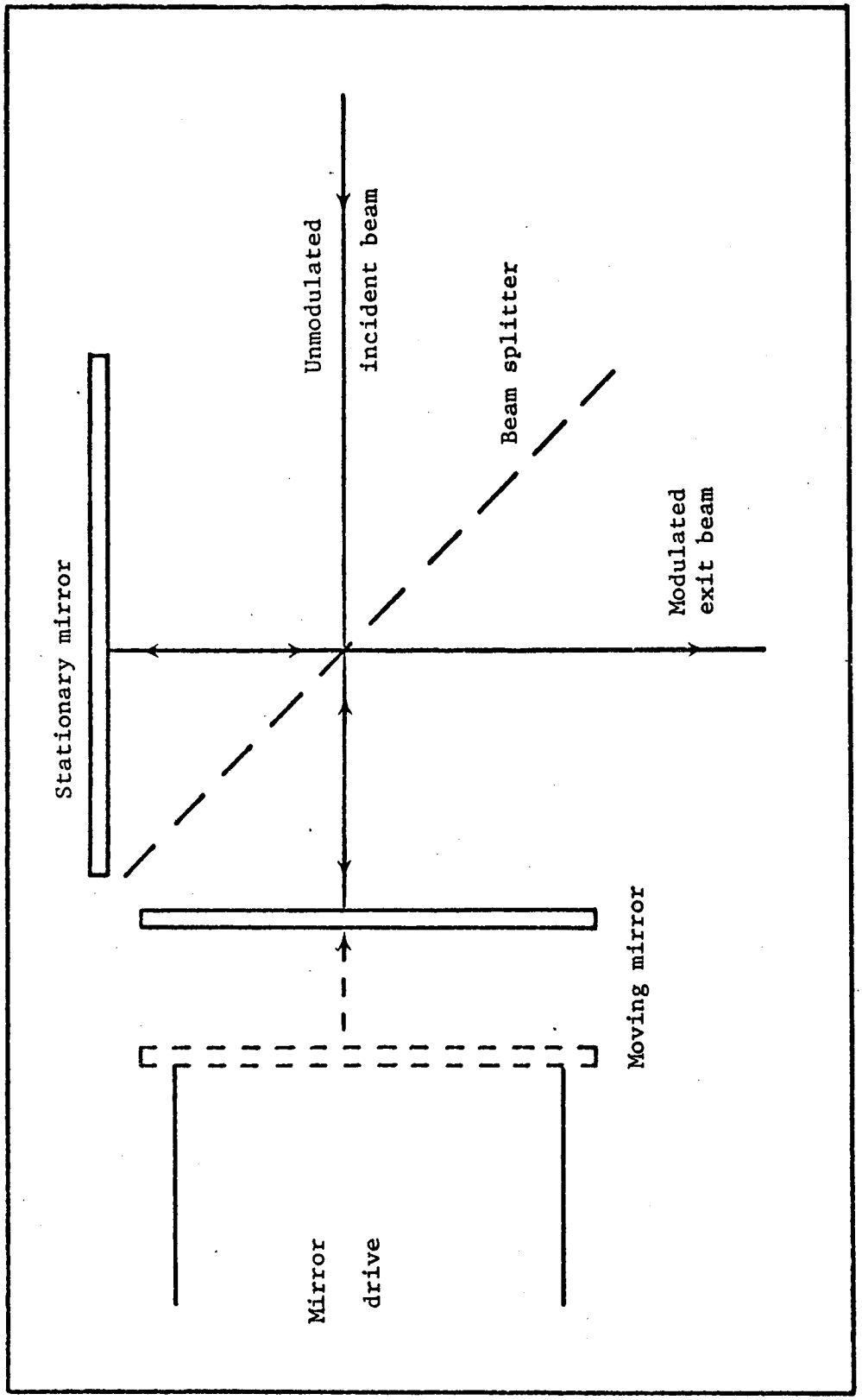


Figure 2. Michelson interferometer.

interferometer is to optically transform incoming radiation from high frequencies (typically 10^{14} Hz in the IR) to signals of low frequencies in the audio range.[57,58] This modulation (heterodyning) transforms the signal to a frequency range where both amplitude and frequency can be detected.[58] This is as opposed to normal grating IR spectroscopy where slits and a monochromator select the frequency and only the signal amplitude is detected. Since the interferometer permits amplitude and frequency response, all resolution elements can be observed at the same time. This is called multiplexing. The number of resolution elements (M) in a spectral region ($\bar{\nu}_{max} - \bar{\nu}_{min}$) is given by:[59]

$$M = (\bar{\nu}_{max} - \bar{\nu}_{min})/\Delta\bar{\nu} \quad , \tag{2}$$

where $\Delta\bar{\nu}$ = resolution. In a grating instrument, only one resolution element is observed per unit of time. This arrangement is particularly wasteful of energy, as slits and a monochromator severely diminish the signal. The multiplex capability of interferometry is believed to be the most important advantage of this approach.[56,57]

For a grating instrument, each small band of width $\Delta\bar{\nu}$ is observed for a time T/M where T is the total scan time. The signal proper is directly proportional to the observation time. The noise, being random, is proportional to the square root of T/M. Thus, for a grating instrument:[60]

$$(S/N)_G \propto (T/M)^{1/2} \quad . \tag{3}$$

In FT-IR all resolution elements are observed at once, so the integrated signal in a small band $\Delta\bar{\nu}$ is proportional to T. The $(S/N)_I$ is thus proportional to $(T)^{1/2}$. The advantage is:[60]

$$(S/N)_I/(S/N)_G = M^{1/2} \quad . \tag{4}$$

Thus in the same observation time, FT-IR spectroscopy provides a better S/N ratio than does dispersive spectroscopy.

The relationship between incoming radiation and the transformed signal can be understood by referring to Figure 2. Incoming radiation impinges upon a beamsplitter which ideally reflects and transmits 50% of the incident energy. The beamsplitter consists commonly of a thin film of germanium on a CsI or KBr substrate. Mylar films are also used in the far IR spectral regions. The transmitted and reflected beams are incident upon a moving mirror and a stationary mirror, respectively. The two beams are subsequently recombined and as the moving mirror scans, the recombined beam forms a series of constructive and destructive interferences. At path differences (retardation = δ) of an odd number of half-wavelengths, the signals cancel to zero. At retardations of integral multiples of λ, the signal is a maximum. The signal that the detector sees is thus a sinusoidal function whose intensity is related to the incoming frequency by:[61]

$$I(\delta) = 0.5I(\bar{\nu})\cos 2\pi\bar{\nu}\delta, \tag{5}$$

where $I(\bar{\nu})$ is the intensity of a beam of monochromatic light and frequency $\bar{\nu}$. The function $I(\delta)$ is referred to as an interferogram. The amplitude of $I(\delta)$ must be modified for beamsplitter efficiency, detector response, and amplifier characteristics, yielding:[61]

$$I(\delta) = 0.5\ H(\bar{\nu})I(\bar{\nu})\cos 2\pi\bar{\nu}\delta, \tag{6}$$

where $H(\bar{\nu})$ is a frequency-dependent correction factor. The equation for the interferogram in its simplest form is then:[61]

$$I(\delta) = B(\bar{\nu})\cos 2\pi\bar{\nu}\delta, \tag{7}$$

where $B(\bar{\nu})$ is the intensity versus frequency function.

For a polychromatic source, the interferogram is given by:[61]

$$I(\delta) = \int_{0}^{+\infty} B(\bar{\nu})\cos 2\pi\bar{\nu}\delta \cdot d\bar{\nu}, \qquad (8)$$

where $B(\bar{\nu})$ = the intensity vs. frequency spectrum (power spectrum)

and δ = retardation.

This function is recognized as one-half of a Fourier transform pair, the other half being:[61]

$$B(\bar{\nu}) = \int_{-\infty}^{+\infty} I(\delta)\cos 2\pi\bar{\nu}\delta \cdot d\delta, \qquad (9)$$

which is an expression for the familiar intensity vs. frequency form of a spectrum. Thus the power spectrum of the radiation, $B(\bar{\nu})$, is given by the Fourier transform of the interferogram.[57]

$$B(\bar{\nu}) = \widetilde{I(\delta)} \qquad (10)$$

Figure 3 shows a typical interferogram of a polychromatic source and the spectrum obtained by taking its Fourier transform.[62,63]

The expression for an interferogram (Equation 8) requires that the moving mirror be scanned over an infinite distance. This is physically impossible, so a modification of this expression must be made. The finite mirror travel results in the multiplication of the interferogram by a boxcar truncation function, $D(\delta)$;[61]

$$D(\delta) = 1 \qquad -\Delta < \delta < +\Delta$$

$$D(\delta) = 0 \qquad \begin{cases} \delta < -\Delta \\ \delta > +\Delta \end{cases} \qquad (11)$$

where Δ is the retardation at the end of a scan. The spectrum is then given by:[61]

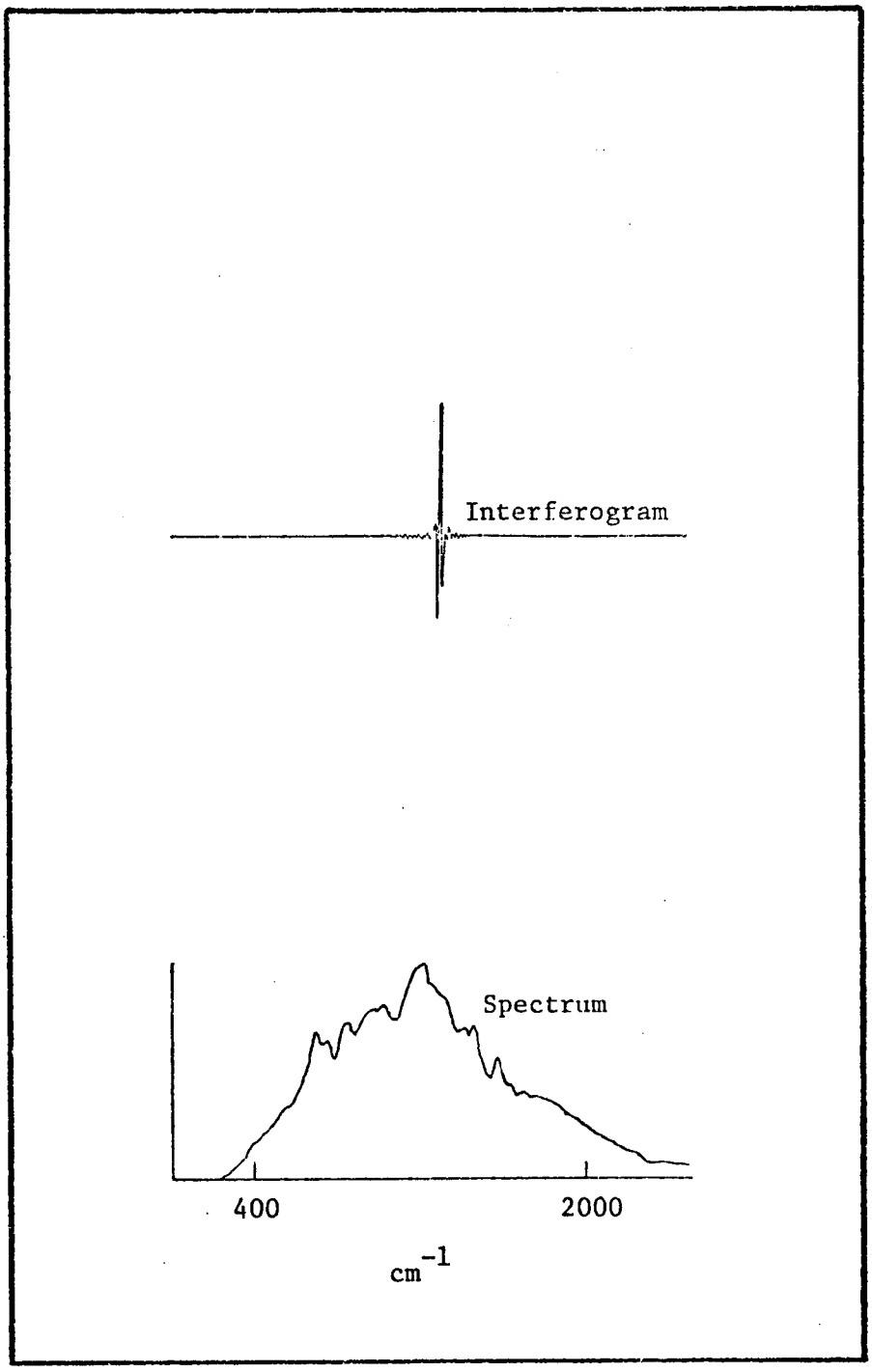


Figure 3. Interferogram and computed spectrum of a broadband IR polychromatic light source.

$$B(\bar{\nu}) = \int_{-\infty}^{+\infty} I(\delta)\, D(\delta)\, \cos 2\pi\bar{\nu}\delta \cdot d\delta. \qquad (12)$$

The Fourier transform of the truncated wave is of the form sin x/x which means that the infinitely narrow line resulting from infinite mirror travel now has a finite width. This function, $f(\bar{\nu})$, is referred to as the instrument line shape (ILS),[61]

$$f(\bar{\nu}) = 2\Delta \cdot \frac{\sin(2\pi\bar{\nu}\Delta)}{2\pi\bar{\nu}\Delta} \quad . \qquad (13)$$

Another consequence of this truncation is the production of side lobes, shown in Figure 4. To eliminate these side lobes, apodization is performed by weighting the interferogram by an appropriate function. A triangular function is most commonly used since it decreases the amplitude of the side lobes and generates an ILS which is the same as that of a diffraction-limited grating spectrometer.

To calculate a Fourier transform in a reasonable length of time, a limited number of data points should be sampled from the analog interferogram. To sample unambiguously, the interferogram must be digitized at a frequency of $4V\bar{\nu}_{max}$ Hz, where V is the mirror velocity. Using this Nyquist criterion, it is possible to completely reconstruct the signal without any loss of information or S/N (signal/noise) ratio.[61]

2. Practice

In practice, there were several technological problems to be solved before the FT-IR spectroscopy (Fourier transform infrared spectroscopy) instrumentation became a part of the analytical laboratory.[56] These should be mentioned, for they are the key to the advancement of this technique.

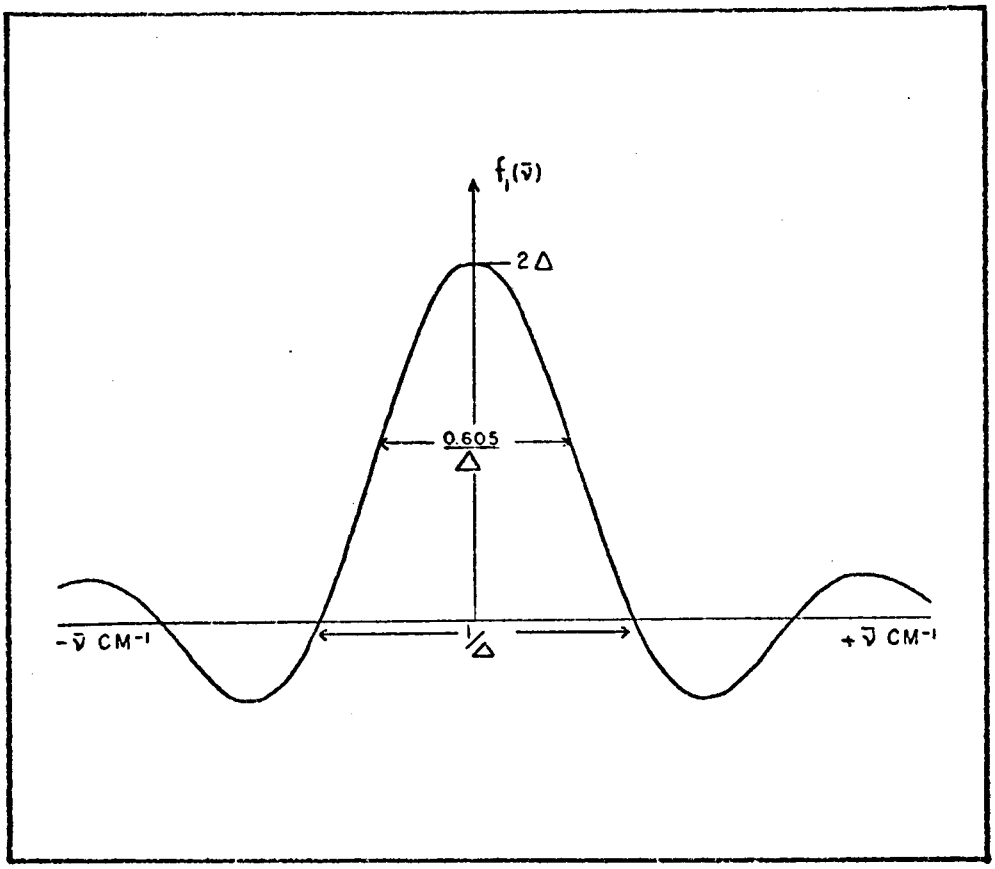


Figure 4. Instrument line shape, $f(\bar{\nu})$, resulting from the Fourier transform of a truncated waveform.

First was the design of an air-bearing mirror drive with tilt of less than half the shortest wavelength in the spectrum being observed. The second problem was developing a method of digitizing the interferogram at equal intervals of mirror travel. This was achieved by use of a He-Ne laser reference beam which is monitored at the same time as the main signal. The interferogram is sampled each time the reference signal crosses zero. To be sure that the first data point is collected at the same mirror position for every scan (important for signal averaging), a white light signal is sent through the interferometer. Sampling is initiated when the white light interferogram reaches a certain maximum value, V_t.

As described, FT-IR is a multiplex technique in which a wide range of frequencies is observed at the same time. Common thermal detectors have a response time too long to permit measurement of all frequencies. The development of sensitive pyroelectric bolometers, i.e. triglycine sulfate, has permitted these mid-IR spectra to be measured.

Finally, advances in data handling systems have streamlined data processing. The development of the fast Fourier transform (by Cooley-Tukey algorithm) has expedited the retrieval of spectral data from the interferogram.[64] Mini-computers have proved to be essential in a complete system.

Infrared spectrometers should have high energy throughput since they suffer from energy-limited sources and noise-limited detectors. With FT-IR instrumentation which lacks energy-wasting slits and monochromators, the energy throughput can be 80 to 200 times greater than for a dispersion

instrument.[65] The throughput and multiplex advantages provide greatly enhanced sensitivity. It has been estimated that quantities as low as 1 ng can be detected by this method.[66] In practice, IR studies have shown quantities from 50 to 10 ng to be detectable.[67,68] The improved sensitivity of FT-IR over conventional IR improves IR's utility for the PAH problem.

The use of a mini-computer to handle the digitized form of the data provides several advantages.[69] The most common use of the computer is to improve the S/N ratio of spectra by coadding of successive interferograms.[70] Since the signal increases with the number of scans and the noise with the square root of the number of scans, the S/N should increase with the square root of the number of scans.[69] A sacrifice of time may be necessary to attain the S/N desired. Spectra can be subtracted, ratioed, and stored for future reference. The computer also has control of plotting of the spectra. These functions can be very useful for unraveling complex mixtures such as those containing PAH's.

Speed is also a potential advantage of FT-IR. An interferogram can be obtained in less than a second. It should be remembered that there is a trade-off between speed, resolution, and S/N ratio.[61] To increase resolution, scan time is decreased since resolution is proportional to retardation. To improve S/N ratios, coaddition may be necessary which again sacrifices speed. It is important to understand and define the problem to be solved so that the appropriate parameter is emphasized. The rapid collection of data has the potential of making FT-IR spectroscopy useful for routine analysis, which is important for PAH analysis.

E. Low Temperature Matrix Isolation

Poor quantitative results obtained by standard IR techniques, particularly KBr pellets, and finding a suitable transparent matrix in the IR region are problems which can potentially be solved through the use of low temperature matrix isolation. In low temperature matrix isolation,[71-73] the sample is mixed with an excess of host inert gas and codeposited on a cold (15 K) IR-transparent substrate. Temperatures must be low enough to prevent diffusion. A temperature of approximately 0.3 of the matrix melting point is necessary. At large matrix/sample ratios (10^2 to 10^5/1), the molecules are effectively isolated from one another. Interactions between the sample and rare gas matrices are weak; therefore, spectroscopic analysis of the sample will be similar to gas phase spectra. It is important to note that the matrix-isolated spectra are simpler than room temperature gas phase spectra since rotational contributions to the spectra are frozen out. This is particularly important in analyzing complex mixtures such as PAH samples.

If the sample is gaseous or liquid at room temperature, matrix isolation is a relatively simple procedure. The matrix and sample are premixed in a vacuum system at an appropriate ratio and delivered at a controlled rate to the cold surface. If the sample is solid, however, it must be vaporized prior to deposition. This is accomplished by use of the Knudsen cell.[74-77] This device takes on a number of forms but is essentially a resistively heated cell with a small effusion hole. As the sample migrates from the cell, it is cocondensed on the window with a separate stream of matrix gas. Since PAH's are solid, analysis

must be carried out by this method. Vapor pressures of PAH's are high and consequently these materials vaporized easily.[78]

A matrix-isolated (MI) sample spectrum also has relatively narrow bandwidths (4 cm^{-1}) since interactions are eliminated and rotation frozen out.[71] This is also of obvious help in simplifying the resolution of a complex mixture. Greater sensitivities are also obtainable in MI samples due to the sharpness of the bands of isolated molecules.

Common matrix host (solvent) materials utilized are rare gases or nitrogen which provide an IR-transparent medium. Only crystal lattice vibrations are IR-absorbing.[71] These are in the far IR, however, and therefore, do not interfere in the mid-IR (4000-400 cm^{-1}) where most work is performed.

When matrix isolation was first introduced in 1954, it was designed to allow observation of radicals and high temperature species for structural analysis.[79] In its early applications,[80] only molecular spectroscopists utilized the method since it was time-consuming and required cumbersome and sophisticated refrigerators to attain very low temperatures. Early devices consumed large quantities of liquid He or H_2 and, in addition to being dangerous, were expensive. It has only been in the last few years that relatively inexpensive and reliable closed-cycle refrigerators have been developed.[71] This development has made low temperature matrix isolation practical in any laboratory.

Consequently, matrix isolation has been adapted to a number of practical applications. Rochkind has applied matrix isolation to the

qualitative and quantitative analysis of multi-component gas mixtures. The experimental technique developed by Rochkind is described as pseudo matrix isolation.[81] In this method, the premixed sample and matrix are delivered in short duration pulses. This method appears to have certain advantages over the continuous deposition. The deposition can be achieved more quickly without affecting isolation. Samples prepared by pseudo matrix isolation are less prone to IR light scattering. This method is not without its disadvantages, however, since it requires the assumption that effects such as incomplete condensation and intermolecular interactions will affect a species equally. Using the technique, eight compounds were analyzed simultaneously. Beer's law plots of absorbance vs. amount deposited yielded straight lines with accuracy better than 5%.

Snelson tested Beer's law using Knudsen effusion of LiF molecules.[82] Beer's law was obeyed within $\pm$ 5% over a small concentration range.

Ball and Purnell applied Rochkind's method and slow deposition to the identification and measurement of airborne amines.[83] They demonstrated linearity over one order of magnitude for absorbance vs. amount deposited.

The method of matrix isolation has been demonstrated, then, as a useful tool for quantitative and qualitative analysis of single components and mixtures, but does have some inherent problems which should be considered.[80]

Vibrational spectra of matrix-isolated materials may be markedly different from those in other media. It is important to understand the various effects of the matrix environment on the spectrum of a molecule. Singlet absorption bands of molecules may become multiplets for a number of reasons. A common problem with matrix-isolated samples is multiple trapping sites. A solute molecule trapped in more than one distinguishable site in a matrix will exhibit more than one band. The distinguishing feature of doublets due to alternate trapping sites is that the relative intensity of the bands is unaffected by changing the solute concentration. By annealing — warming to allow some movement — intensities do change. This problem is common for large molecules (such as PAH's) which dislocate two or more lattice molecules on being trapped as well as for most all vapor-deposited matrices.[71] Quantitative work can be severely affected by this phenomenon especially if depositions result in varying quantities in the different trapping sites.

Multiple bands are most commonly caused by aggregation. If molecules are not completely isolated, multiple bands due to monomer, dimer, trimer, etc., may be present. Extremely high ratios may be necessary to obtain adequate isolation. Particularly in Knudsen effusion, the rate of deposition may be very important for good isolation.[82] Aggregation (solute-solution interaction) may influence the position, shape, and intensity of the solute absorption frequencies which would render this method useless for quantitative or qualitative work.

If properly utilized, then, MI has a number of desirable features as applied to the problem of PAH analysis. These may be summarized as follows:

1. Sharp, narrow bands may be obtained, simplifying the resolution of the spectrum of a complex mixture.

2. Better sensitivities are attained due to the lack of guest-guest interaction which decreases band intensity.

3. Due to reduced interaction, linearity of Beer's law plots is more likely.

F. Statement of the Problem

The objective of this study was to develop a new infrared analytical technique for the determination of polycyclic aromatic hydrocarbons. Matrix isolation coupled with Fourier transform infrared spectroscopy was investigated with regard to its qualitative and quantitative capabilities for PAH analysis. Specific objectives were to improve the sensitivity of infrared spectroscopy, to develop capabilities to analyze complex mixtures, and to establish linear relationships between absorption and PAH quantity. Provided these objectives are attained, this method would find application to PAH analyses important to a number of environmental problems.

CHAPTER II

EXPERIMENTAL TECHNIQUES

A. Materials

Sixteen PAH's, one heterocycle, and one related aromatic compound were utilized in this study. Table III lists the compounds and their sources. Where possible, zone-refined materials were obtained. Vacuum sublimation was used to enhance the purity of phenanthrene and anthracene. Standard solutions of PAH's were made, utilizing only spectroscopic grade solvents. Matrix gases were research grade (99.995% pure), obtained from Matheson Gas Products.

B. Equipment

1. Cryostat

The cryostats used in this study were Cryogenic Technology Inc. Spectrim^{TM} units (Figure 5). These devices are closed-cycle refrigerators operating on a modified Gifford-McMahon cycle.[84] Gaseous helium (99.999% pure) is compressed and delivered to the cold head where it expands. The gas cools and takes heat from the cold head area. The gas is passed through an absorber to remove any hydrocarbons and returned to the compressor. The system is rated at 15 K with no thermal load and a temperature stability of $\pm$ 1.5 K at 22 K.

A sample chamber (cryostat head) is attached to the cryostat, its function being to provide a vacuum environment so that low temperatures can be obtained (described in detail later). To obtain 20 K, a

TABLE III

SOURCES AND PURITY OF COMPOUNDS

Compound	Source	Purity
Acenaphthene	Duke Standards Palo Alto, Calif.	ZR[a]
Fluorene	Duke Standards	ZR
Anthracene	B. Pauric Philadelphia, Pa.	ZR
Phenanthrene	James Hinton Columbia, S.C.	ZR
Fluoranthene	Duke Standards	ZR
Pyrene	B. Pauric	ZR
Benzo[a]fluorene	ICN Life Standards Plainview, N.Y.	95-99%
Benzo[b]fluorene	ICN Life Standards	95-99%
Napthacene	J. Hinton	ZR
Benz[a]anthracene	Fluka AG Switzerland	Purum
Chrysene	J. Hinton	ZR
Triphenylene	Aldrich Chemical Co. Milwaukee, Wis.	98%
Benzo[a]pyrene	Aldrich Chemical Co.	98%
Benzo[e]pyrene	Environ. Canada	Unknown
Perylene	Aldrich Chemical Co.	Puriss
1,2,5,6-Dibenzanthracene	Aldrich Chemical Co.	97%
1,3,5-Triphenylbenzene	Aldrich Chemical Co.	98%
Carbazole	J. Hinton	ZR

[a]Zone refined.



Figure 5. Cryogenic Technology, Inc. Spectrim™ cryostat.

vacuum of 10^{-4} torr must be obtained, thus the cryostat must be capable of holding a high vacuum (leak rate no greater than 1×10^{-8} std. cc He/sec). The temperature was monitored by a digital temperature controller calibrated for use with a chromel vs. gold (0.07% iron) thermocouple. The thermocouple was located on the sample mount. The temperature controller also incorporates a heating unit which permits warming up to and maintaining any temperature up to approximately 360 K. This was especially convenient for sample conditioning (i.e. annealing). The deposition surface can be warmed without breaking the vacuum, which was convenient for routine work. Window mounts holding the deposition surface were fashioned from oxygen free high conductivity (OFHC) copper which provides excellent thermal conductivity. Indium was used to seal all mechanical connections.

2. Vacuum System

A vacuum line was designed for the matrix isolation experiments with two functions in mind. The line was utilized to rough the cryostat and cryostat head to 50 μm of Hg. This was necessary to reduce the load that the cryostat handled to achieve low (10^{-4} torr) pressures. A Hastings vacuum gauge (model VT5B) was used to monitor these pressures. A Welch 1400 vacuum pump was used to evacuate the line.

The other function of the vacuum line was to store and deliver the matrix gas. The line was made of glass with teflon stopcocks, in order to minimize the amount of grease needed. A mercury manometer measured the pressure of the matrix gas and was used to calculate the amount delivered during an experiment. Matrix volumes were converted to moles using the ideal gas law. The matrix supply volume was

1.5 liters and the pressure was $(P_1-P_2)/760$ mm, where P_1 is the starting pressure and P_2 is the pressure after deposition. The flow was metered by a Fisher-Porter, Tri-flat flowmeter preceded by a teflon metering valve. Interfacing to the cryostat was accomplished by converting the glass line to metal tubing (1/8" stainless steel Kovar) and ending with the female section of a Swagelok quick connect. The small diameter tubing provided great flexibility to the matrix delivery line. The cryostat head contained a shut-off valve and a male quick connect.

3. Fourier Transform Infrared Spectrometer

The infrared spectrometer used was a Digilab FT-20V (Digilab, Inc., Cambridge, Massachusetts). The optical components, consisting of the interferometer (Model 496), focusing optics, and detector (triglycine sulfate) are shown in Figure 6. The diameter of the beam at focus was approximately 25 mm. As described previously, an He-Ne laser and white light were also included in this unit. The whole unit was mounted in a vacuum box which can be evacuated to eliminate all but traces of atmospheric water and CO_2 which may interfere with desired spectral data. The interferometer was interfaced with a dedicated minicomputer system. A Nova 1200 computer (Data General Corporation, Southboro, Massachusetts) with a 4K memory controlled the interferometer and performed the fast Fourier transform (FT) of the data. The computer was fitted with a 256K Alpha Data disk on which the FT programs were stored and the digital data were collected. Accessories included a synchronous digital magnetic tape recorder (Model 9700, Kennedy Co., Altadena, California), digital plotter (Houston Instruments, Austin, Texas), and an oscilloscope read-out (Tektronix, Inc., Portland,

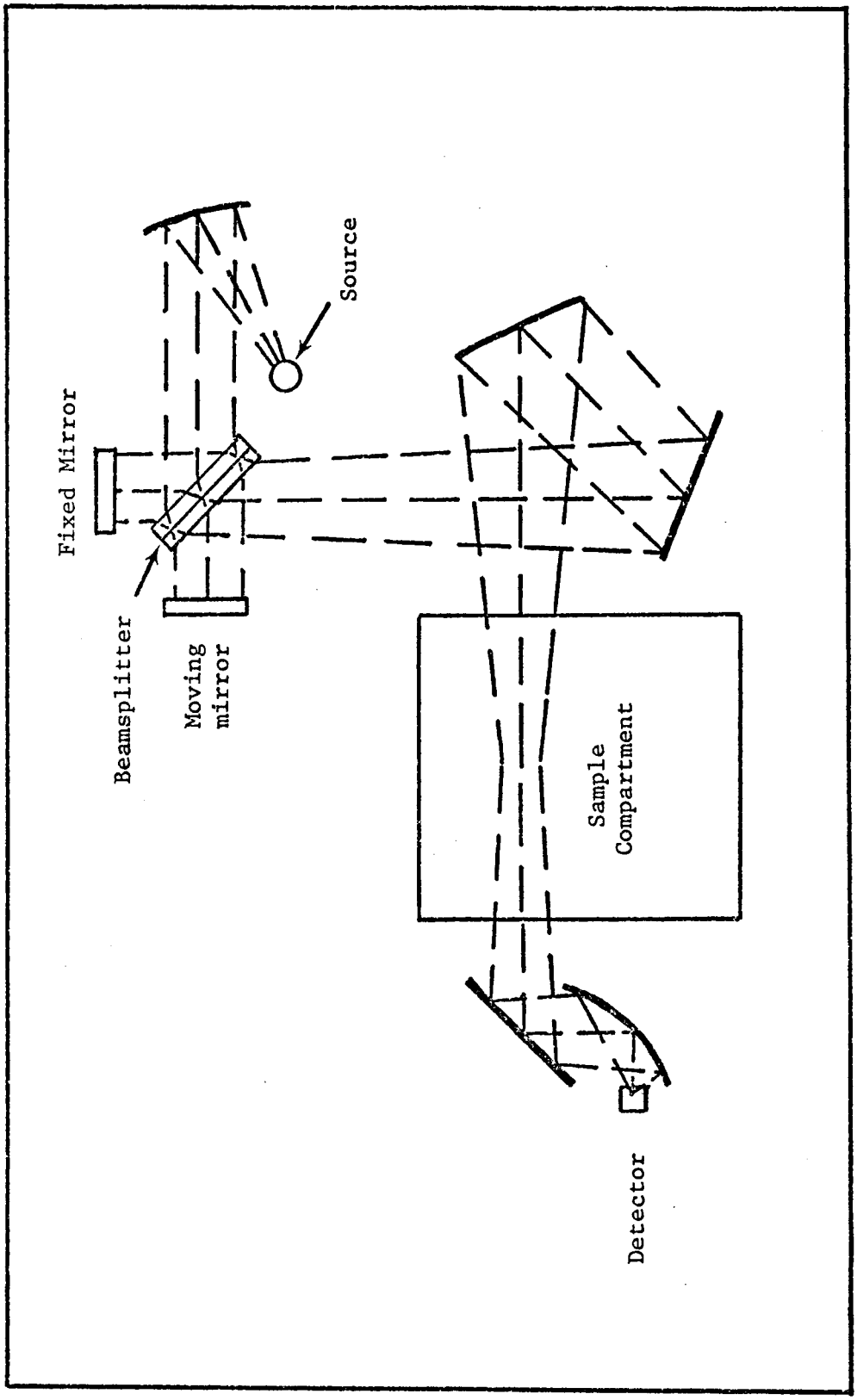


Figure 6. Optical diagram of the FTS-20V infrared spectrometer.

Oregon). All functions were controlled through a teletype (Teletype Corp., Skokie, Illinois). A block diagram of the FTS system is shown in Figure 7.

The Digilab FTS-20V is a high-resolution instrument capable of resolutions of 16 cm^{-1} to 0.125 cm^{-1}. Scan time varied from 0.4 seconds for resolution equal to 8 cm^{-1} to 26 seconds for 0.1 cm^{-1} resolution. Computation time to produce a spectrum varied depending on whether the data were collected in single or double precision (two 16-bit words). Computation time for a resolution of 1.0 cm^{-1}, double precision spectrum was about fifteen minutes.

For mid-IR work, a Ge/KBr substrate beamsplitter (4000-400 cm^{-1}) was used. A Ge/CsI substrate beamsplitter overlapped the mid- and far-IR regions with a range from 1200-200 cm^{-1}. The IR source was a nichrome wire. For far-IR work, a Mylar film beamsplitter (220-40 cm^{-1}) was utilized and a mercury lamp was used as the source.

C. General Sampling System

Matrix isolated samples were prepared by vaporizing the PAH by means of a Knudsen cell. The cell consisted of a 7 mm diameter pyrex glass tube which was 2 cm in length, with a 7/25 female joint at one end and a 0.5 mm effusion hole at the other end. The cell was placed on a 7/25 male joint attached to the front of a 29/45 ground glass joint (Figure 8). The Knudsen cell was resistively heated by a wound coil of nichrome wire connected to tungsten feedthroughs in the 29/45 joint. The heater was powered by a variable auto-transformer. The complete oven assembly was seated in a 29/42 female stainless steel

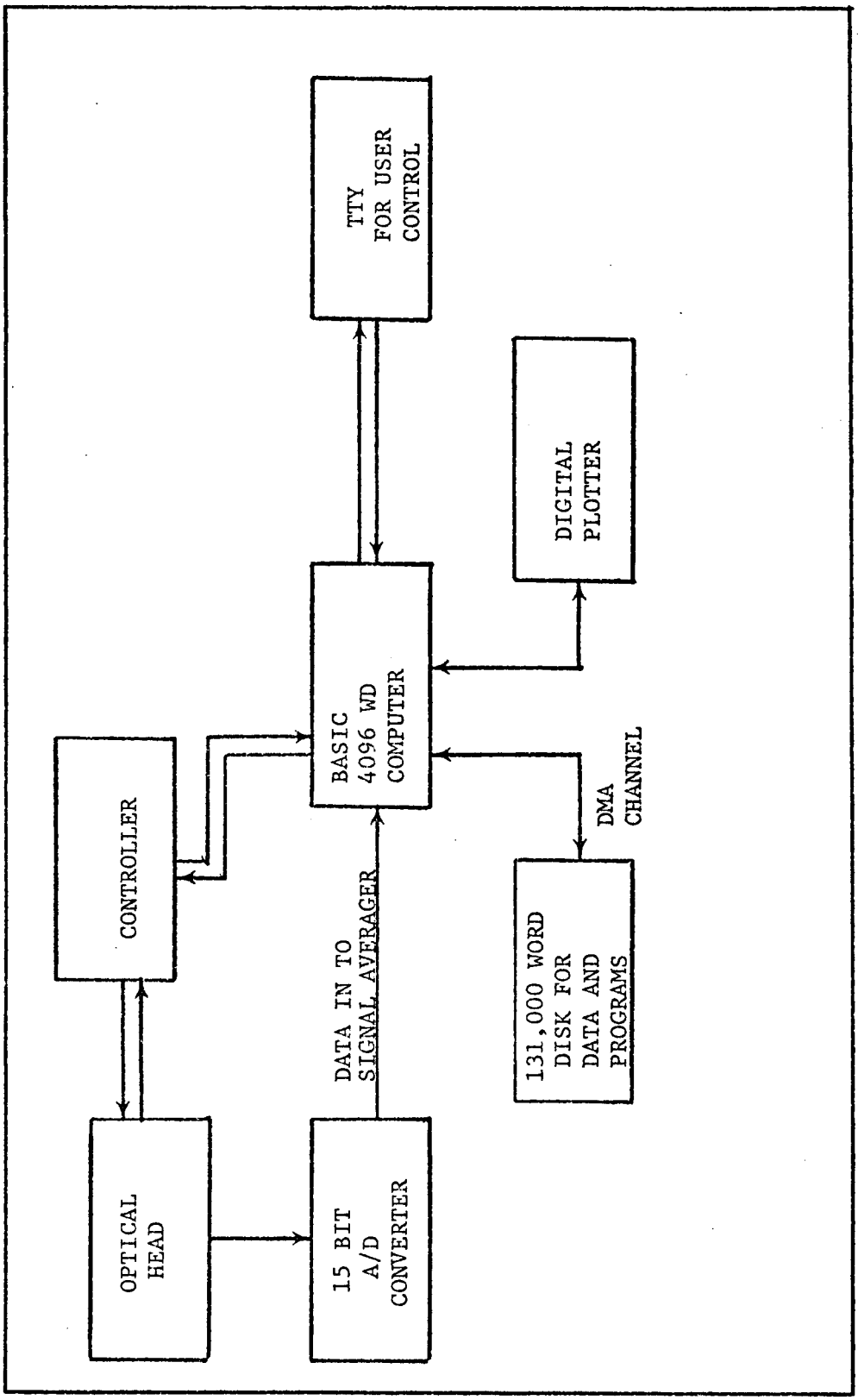


Figure 7. Block diagram of the FTS-20V infrared spectrometer.

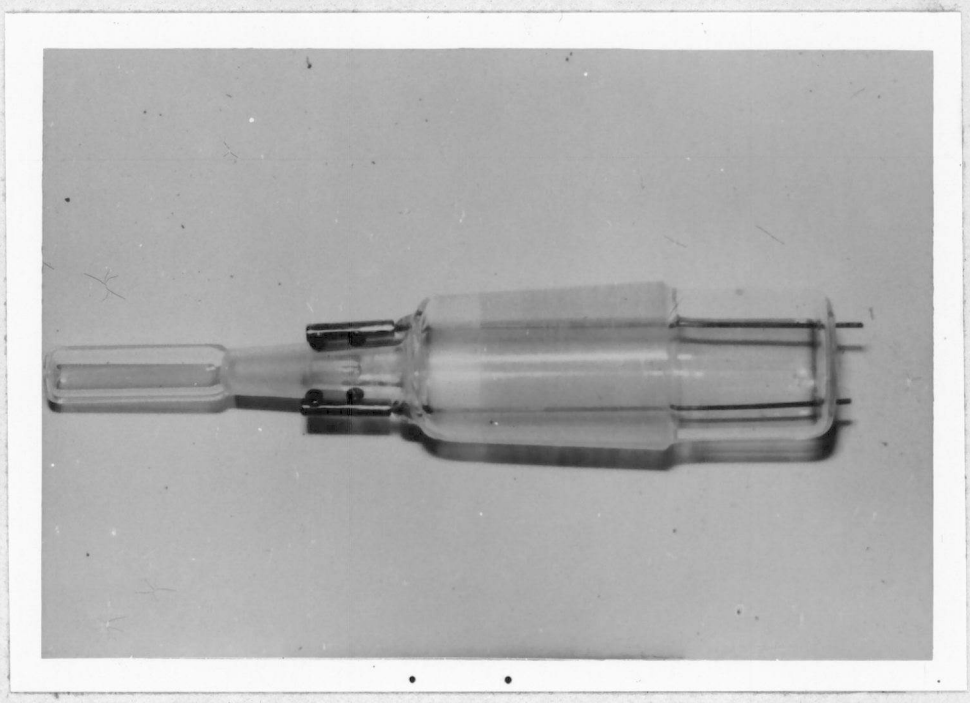


Figure 8. Knudsen cell and support for the general sampling system.

joint which was silver soldered to an interface plate sealed by an o-ring to the sample chamber. The matrix port entered the cryostat head through this interface plate. The port was preceded by an on-off valve in line with a quick connect. The sample chamber with the oven in place is shown in Figure 9. After deposition the flow was shut off, the matrix line disconnected, and the entire cryostat unit placed in the interferometer unit. In addition to the oven assembly, the cryostat head was fitted with two 1 1/4" CsI windows for optical viewing. The cryostat with sample chamber in place is shown in Figure 10.

The Knudsen oven was calibrated periodically at operating conditions by a chromel-alumel thermocouple placed in the Knudsen cell through the effusion hole. The thermocouple entered the head through an interface plate, using ceramic feedthroughs.

The deposition surface was a 1" CsI window mounted in a gold-plated OFHC copper mount. This arrangement was used for accumulation of a library of PAH spectra. Milligram quantities of PAH's at matrix to sample ratios of approximately 1000:1 were used to obtain complete spectra. Deposition efficiency for this arrangement was poor (25-30%), mainly due to the large distance of the oven from the window (approximately 30 mm). Deposition times were typically one hour.

It is important to mention that several of the first spectra obtained showed copious amounts of aggregated water (strong, broad bands at 3700-3200 cm^{-1}, 1800-1400 cm^{-1}, and 900-700 cm^{-1}). These severely affected the baseline and spectral quality. It was discovered that this was not due to a leaking system, but to desorption of adsorbed water from the cryostat walls. This was remedied by baking out the



Figure 9. Complete oven assembly interfaced to the sample chamber.

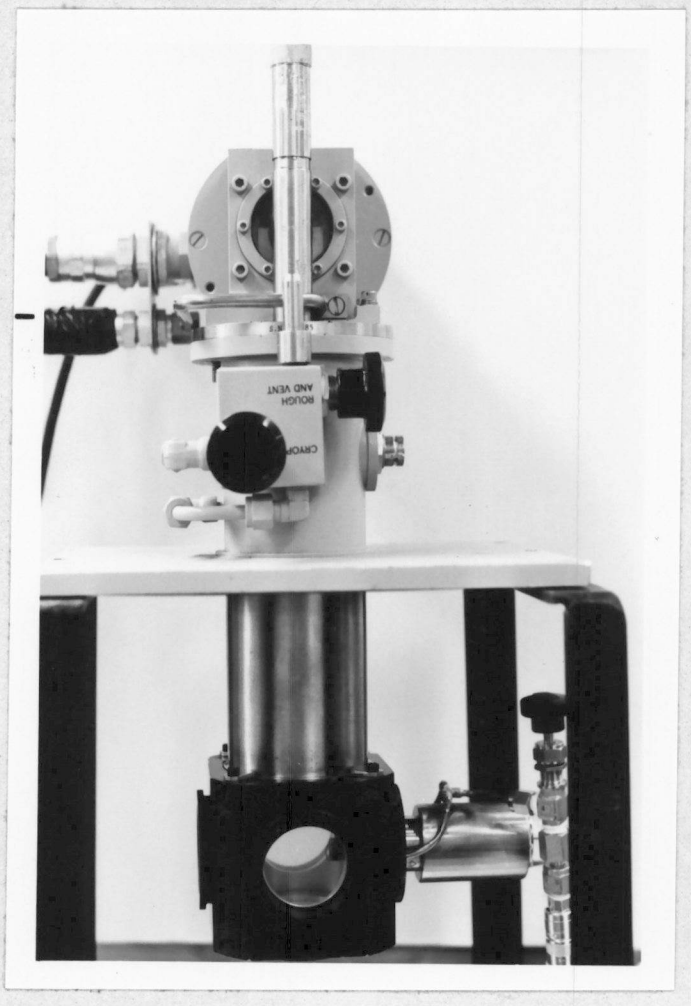


Figure 10. Cryostat with the sample chamber in place.

system under vacuum prior to beginning a deposition (the unit was wrapped with a heating tape).

D. Microsampling System

The general sampling system proved to be inadequate for sampling low (sub-milligram) quantities, since the Knudsen cell was by necessity a large distance (1-2 in.) from the deposition surface. Consequently, the efficiency of deposition was found to be very poor. In order to enhance the efficiency, the oven was moved closer to the deposition surface. This was made possible by reducing the window size to 12 mm in diameter. The deposition efficiency was improved to approximately 50% by this modification. Also, the Knudsen cell was modified to accomodate liquid solutions by sealing one end and placing a delivery hole, sealed with a glass plug, in the side of the cell. The cell mount (7/25 male joint) was eliminated (Figure 11).

Though detection limits were improved, the system was still very inefficient due to an optical mismatch. The window diameter was 12 mm while the beam at focus was 25 mm. Much of the incident light was stopped by the window mount and much passed by unabsorbed. Thus the absorbance was an average of absorbed and unabsorbed light, decreasing the sensitivity.

E. Ultramicrosampling System

A final modification of the sample preparation system provided significant increases in sensitivity. A 6X beam condenser (Harrick Scientific Corp., Ossining, New York) was incorporated into the system

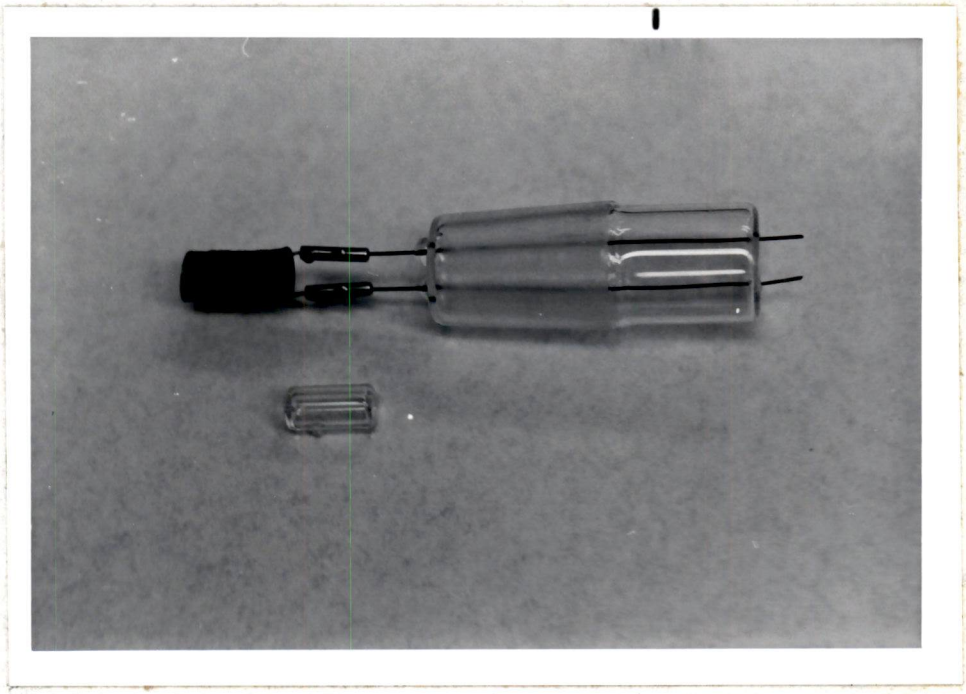


Figure 11. Knudsen cell and oven assembly for microsampling.

which reduced the size of the beam at focus to approximately 4 mm in diameter. This is shown in Figure 12. In order to employ this device, a cryostat was constructed to fit the sampling area of the beam condenser (shown in Figure 13). In order to prepare ultramicrosamples, the Knudsen oven was mounted on a 1/2 in. glass tubing which was sealed in an Ultra Torr fitting. This allowed the oven to be moved very close to the window, so that the deposit could be directed to a spot. The same window was used as in microsampling, but was masked off with a 0.01 in. thick teflon sheet with a hole cut to match the diameter of the condensed beam. This position was determined by viewing the beam at focus with a far-IR beamsplitter in place. The teflon mask, being a poor thermal conductor, appeared to condense little of the PAH vapor species.

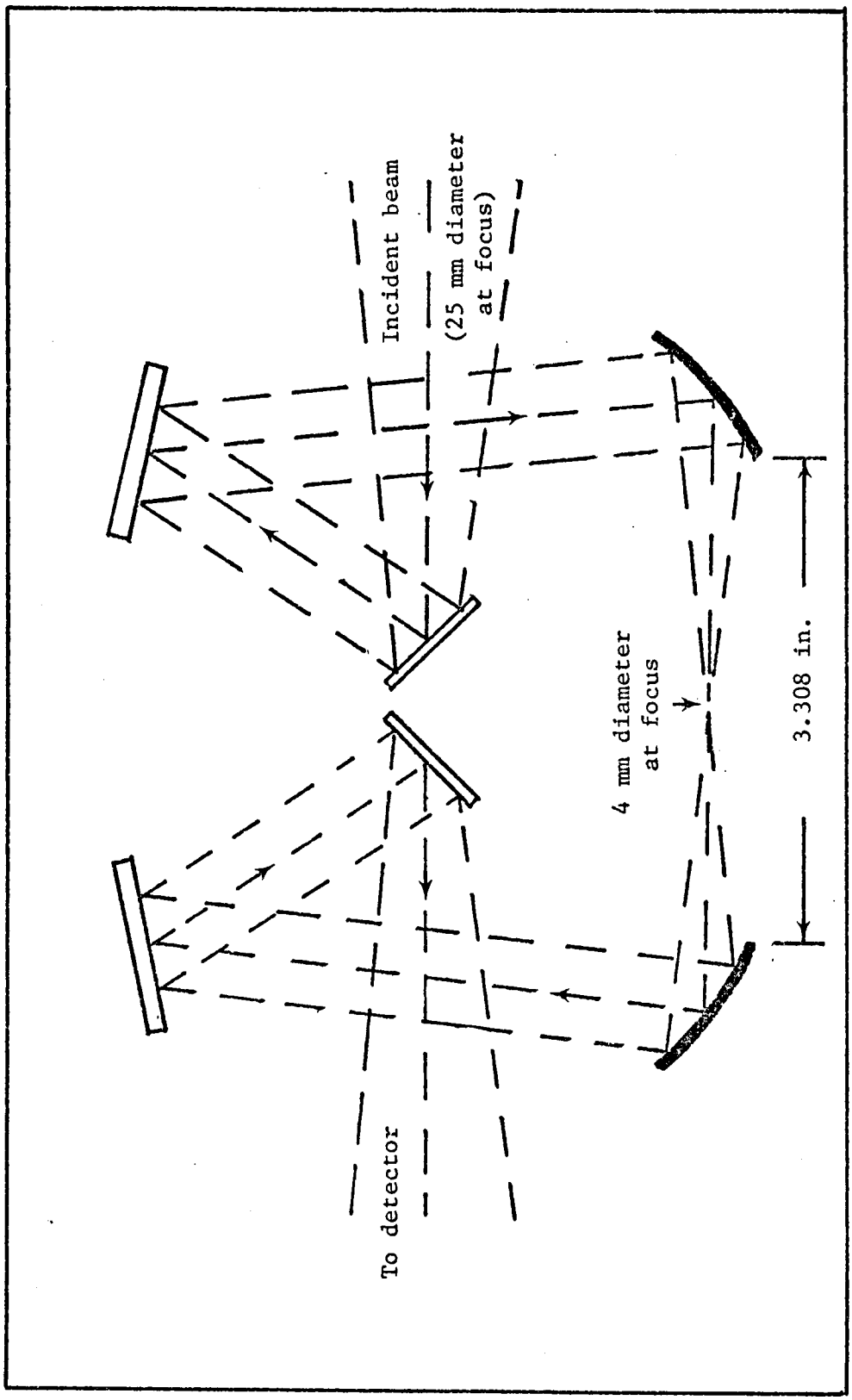


Figure 12. Optical diagram of the 6X beam condenser used with the FTS-20V spectrometer.

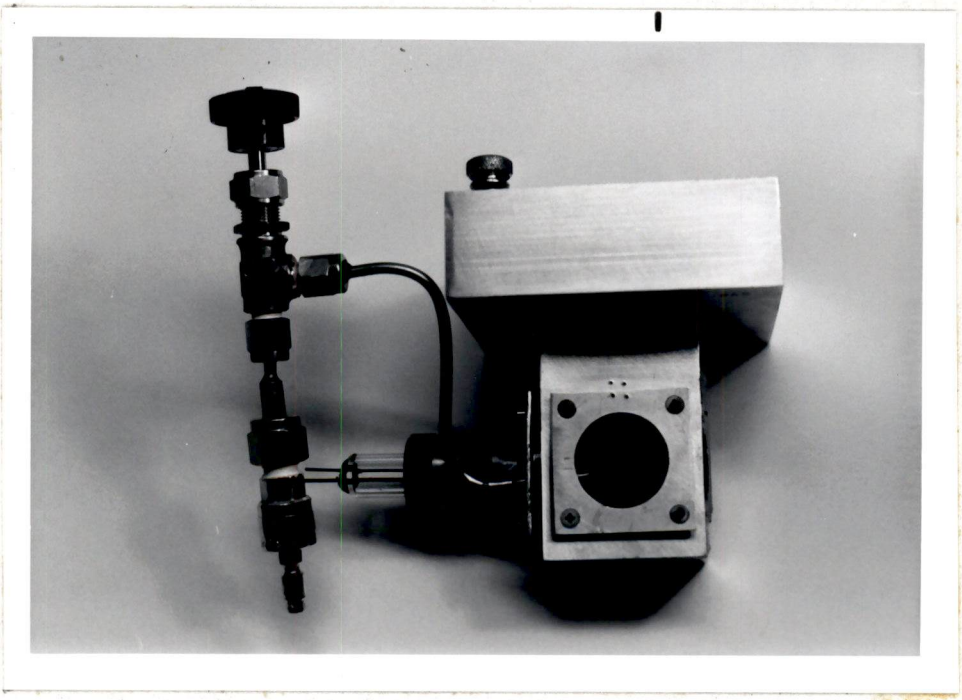


Figure 13. Ultramicrosampling assembly.

CHAPTER III

RESULTS AND DISCUSSION

A. General

1. Library of Standard Spectra

Matrix-isolated Fourier transform infrared (MI-FT-IR) spectra of sixteen polycyclic aromatic hydrocarbons, a nitrogen heterocycle (carbazole), and a related compound (1,3,5-triphenylbenzene) (see Figures 36-40 in the Appendix) were obtained using nitrogen as the matrix gas and 1 mg samples, at a nitrogen to PAH mole ratio (N_2/PAH) of approximately 10^3. The spectral region above 1500 cm^{-1} is not included because the PAH spectra did not exhibit any characteristic absorption bands above this frequency. Bands due to C-H stretches observed between 3000 and 3100 cm^{-1} for the PAH's studied, were broad (approximately 80 cm^{-1}) and weak in intensity as compared to absorption bands in the 1500-500 cm^{-1} region (Figures 41 and 42, Appendix). This region would be useful in identifying the presence of aromatic compounds in an unknown sample, but was of no use in identifying the specific PAH present.

Table IV lists the major absorption bands of the compounds studied. The vaporization temperatures for these compounds were determined during the library accumulation (Table V). The compounds are grouped according to their vaporization temperatures and form thermal fractions which are consistent with the number of rings in the PAH. The fewer the number of rings comprising the PAH, the lower was the vaporization temperature.

TABLE IV

STRONG AND MEDIUM MI-IR ABSORPTION BANDS
OF POLYCYCLIC AROMATIC HYDROCARBONS

Compound	IR Absorption Bands (cm^{-1})
Acenaphthene	(1431, 1422 doublet), 1374, 1017.5, 843, 792,[a] 750
Fluorene	(1483.5, 1480 doublet), (1456.6, 1451.5 doublet), 1408, 1301, 1190, 1005, 958, 746,[a] 696, 622
Phenanthrene	1504, 1462, 870, 818, 740.5,[a] 617
Anthracene	881, (733, 730 doublet),[a] 603
Fluoranthene	1461, 1455.5, 1444, 1138, 830, (782, 778 doublet),[a] 750, 620
Pyrene	1436, 1185 (850, 846 doublet),[a] (715, 713 doublet)
Benzo[a]fluorene	1223, 1020 (828, 826 doublet), (763, 760.5 doublet)[a]
Benzo[b]fluorene	957, 872, 775,[a] 764, 728, 570, 475
Naphthacene	900.5,[a] (747, 744.5 doublet), 551.5
Chrysene	1365, 1234 (817, 814 doublet), (766, 764 doublet)[a]
Benz[a]anthracene	1504, 1365, 886, 809, 785, 752[a]
Triphenylene	1502, 1438, 746[a]
Benzo[a]pyrene	1184 (888, 886 doublet), 853, 841, 830, 764[a]
Benzo[e]pyrene	1480, 1444, 1415, 883 (755, 753 doublet)[a]
Perylene	1498, 1385, 818,[a] (776, 774 doublet)
1,3,5-Triphenylbenzene[b]	1580, 1558, 1503, 1417, 1080, 1032, 884, 758.5,[a] 702, 632, 623 (614, 611 doublet), 509

TABLE IV (Continued)

Compound	IR Absorption Bands (cm^{-1})
Carbazole[b]	1496, 1464.5, 1454, 1397.5, 1338,[a] 1328, 1241, 754, 729.5, 618, 569
1,2,5,6-Dibenzanthracene[c]	1513, 1458, 893, (813, 809 doublet),[a] (750, 745 doublet), 667, 649, 529

[a]Strongest IR band.

[b]Not a PAH.

[c]Not stored in the magnetic tape library.

TABLE V

PAH'S GROUPED BY VAPORIZATION TEMPERATURE

Fraction	PAH	Vaporization Temperature Range (°C)[a]
I	Acenaphthene	< 40
	Fluorene	
II	Phenanthrene	40 - 55
	Anthracene	
	Fluoranthene	
	Pyrene	
	Benzo[a]fluorene	
	Carbazole	
III	Chrysene	70 - 75
	Benz[a]anthracene	
	Triphenylene	
IV	Benzo[a]pyrene	80 - 85
	Benzo[e]pyrene	
	Perylene	
	Benzo[b]fluorene	
V	1,3,5-Triphenylbenzene	90 - 100
	Naphthacene	
	1,2,5,6-Dibenzanthracene	

[a]The pressure under sample preparation conditions was 10^{-4} torr.

Naphthalene (a diaromatic) volatilized at room temperature in the sample chamber and could not be studied by the sampling methods used in this study. Its vaporization temperature was, however, consistent with the trend noted in Table V. The data indicated that separation by thermal fractionation was certainly possible. This could help to eliminate some sample pretreatment, thus simplifying the analysis scheme. It should be noted that the vaporization temperatures were obtained with milligram samples and that with smaller (μg or less) samples, the vaporization temperatures were lower by about 10 to 15°C. However, a temperature gradient did exist between the fractions.

With the exception of carbazole (a nitrogen heterocycle), the strongest IR absorption bands for the PAH's studied were those due to the out-of-plane C-H bending vibrations in the spectral region 900-700 cm^{-1}.[85] For this reason, these absorption bands were chosen for analytical studies. Spectra for this region of the compounds studied are shown in Figures 43-47 (Appendix). The absorption bands are sharp (maximum half-band widths 4-8 cm^{-1}), and the spectra are sufficiently different in this region to be useful in qualitative analysis of mixtures of these PAH's.

2. Comparison of Different Matrix Gases

Three different matrix gases — krypton, argon, and nitrogen — were examined to determine their utility for the matrix isolation of PAH's. The positions of the absorption bands for carbazole, benzo[a]-pyrene, and pyrene were consistently shifted from matrix to matrix as shown in Table VI. This was as expected since, although the matrices

TABLE VI

MATRIX SHIFTS FOR THREE PAH'S
IN DIFFERENT MATRICES

Matrix	Absorption Bands (cm^{-1})[a]					
	Carbazole		Pyrene		Benzo[a]pyrene	
N_2	754	730	846	715	765	747
Ar	750	724	843	712	761	742
Kr	749	725	842	711	--	--

[a]Matrix/sample mole ratio approximately 10^4.

are inert, they perturb the vibrational levels to a differing extent.[71] Based on the frequencies, none of the three matrices provided any advantage over the others for analytical work. Absorption band intensities for the same-sized (50 μg) sample were the same and bandwidths at half maximum were consistent in the three matrices examined.

In order to obtain good detection limits and flat baselines, it was important to produce a clear deposit. A clear deposit had better energy throughput and less scatter. Nitrogen and argon produced clear deposits while krypton deposits were cloudy and highly scattering of incident light. Thus, nitrogen and argon were superior in this regard.

An important consideration in choosing a matrix is the effect, if any, the matrix has on the simplicity of an absorption band. As discussed previously, deposits of PAH's by Knudsen vaporization are highly favorable to multiple site trappings. Multiple sites lead to different perturbations of the molecule and result in splitting the singlets into multiplets. For resolving complex mixtures of PAH's using MI, the less splitting one observes, the more favorable is the matrix. Another cause of splitting of spectral features is aggregation. During the determination of which matrix resulted in the least splitting, preliminary work was done to ascertain the origin of band splitting.

Multiplet features were observed for the strongest absorption bands for nearly all of the compounds studied. Some of the less intense bands showed no splitting at all. The frequency difference between the splitting patterns varied little from matrix to matrix for carbazole, pyrene, and benzo[a]pyrene. Argon produced more splitting than krypton or nitrogen, although the multiplet bands were often less

intense as compared to the major band intensity. Evidence of the origin of the splitting came from annealing at high temperatures (i.e. 0.5 the melting point of the matrix), which allowed sample diffusion. Peak intensities changed drastically, with minor multiplet peaks growing in intensity, which indicated that these peaks were due to aggregate forms of the PAH.

Different matrix/sample ratios resulted in the same splitting but due to the narrower bandwidths at high ratios, the multiplets were often baseline resolved. Annealing at temperatures (i.e., 0.4 of the melting point of the matrix) to enhance site selection did not remove multiple bands, but often changed their relative intensities. The splitting observed at high N_2/PAH ratios was indicative of multiple trapping sites. A very careful study of the effects of N_2/PAH ratios on splitting using premixed nitrogen and PAH vapors would be necessary to substantitate this.

Nitrogen was chosen as the best matrix based on the considerations described above. It produced clear deposits and formed a rigid matrix at the deposition temperature used (15 K). However, if the cooling capacity of the refrigerator were not sufficient to use nitrogen, argon would be an adequate substitute for matrix isolation of PAH's with little sacrifice in spectral quality.

3. Bandwidths as a Function of N_2/PAH Mole Ratio

The bandwidth at half maximum for the 846 cm^{-1} peak of pyrene was studied as a function of N_2/PAH ratio. The results showed that the higher the N_2/PAH, the better the isolation, as indicated by the narrower bandwidths (Figure 14). The bandwidth decreased from 6 cm^{-1} at a ratio of 10^3, to 1.7 cm^{-1} at a ratio of 10^4, to a very narrow width of 0.7 cm^{-1}

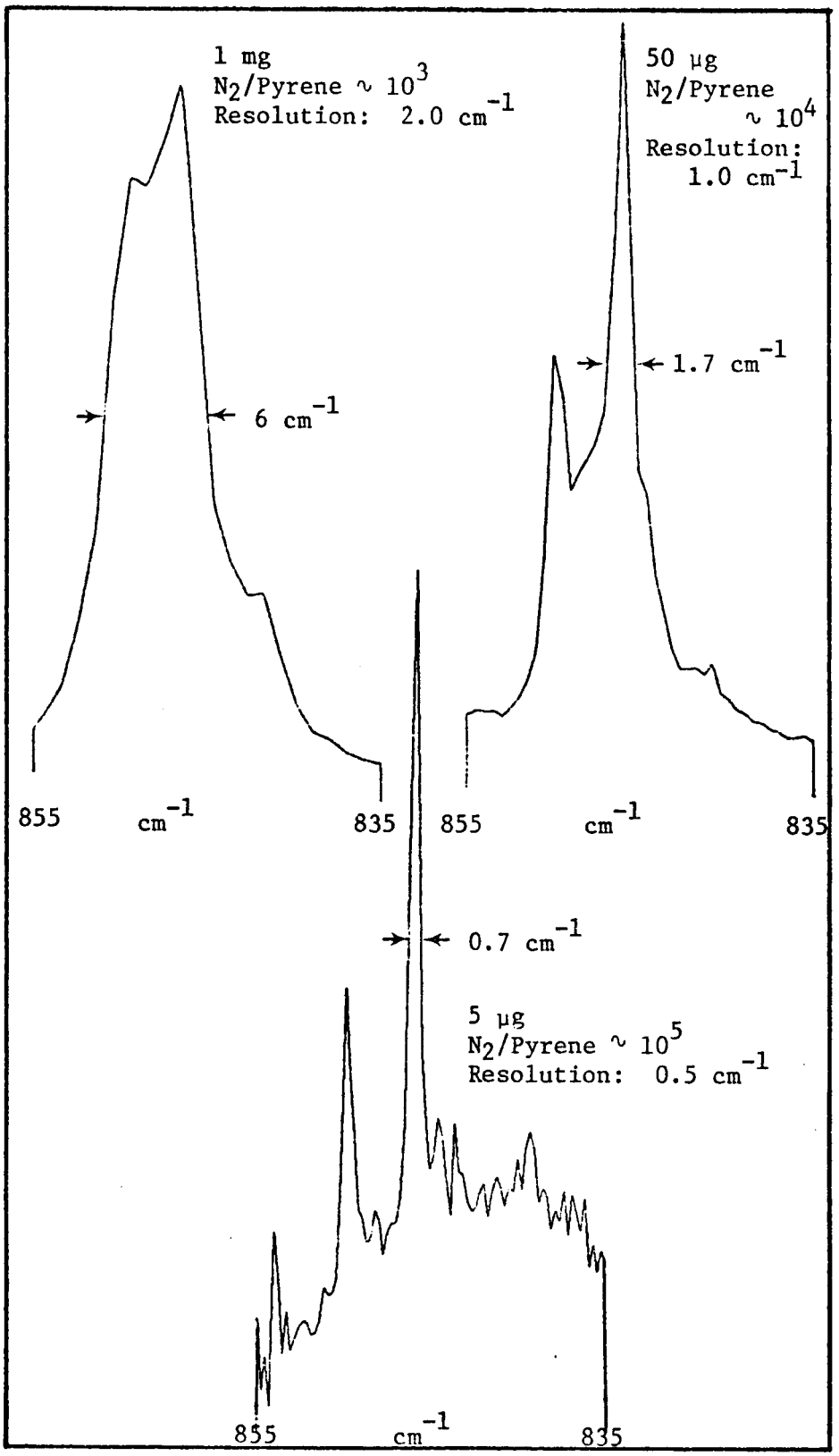


Figure 14. Comparison of bandwidths as a function of N_2/pyrene mole ratio.

at a ratio of 10^5. These results were obtained using the microsampling system. Bandwidths using the ultramicrosampling system were larger than for the same-sized sample using the microsampling system. For example, a 5 μg sample of pyrene using the ultramicrosampling system had a 846 cm^{-1} bandwidth of 1.5 cm^{-1}. Larger bandwidths using the ultramicrosampling system were noted for all compounds studied with both sampling systems. The larger bandwidths were undoubtedly due to the proximity of the Knudsen cell to the deposition surface and the resultant high density of sample obtained with the ultramicro system. In this case, optimum isolation was sacrificed to achieve an increase in deposition efficiency.

This study showed that, to achieve narrow bandwidths, high matrix/sample ratios should be employed. The narrow absorption bands thus obtained would facilitate the analysis of complex mixtures of PAH's. There were, however, experimental difficulties which limited the attainment of high matrix to sample ratios for samples of all sizes. The rate of molecular effusion could not be precisely controlled, so that to obtain large ratios, very high nitrogen flow rates were necessary. This often resulted in warming of the window, which was detrimental to good isolation. High flow rates also dispersed the sample throughout the sample chamber, leading to poor deposition efficiency and precision. When the sample size was 50 μg or less, attainment of sufficient ratios for narrow bandwidths (2 cm^{-1} or less) was no problem at moderate gas flows (3-5 mmoles N_2/hr).

4. Deposition Efficiencies

The deposition efficiencies of the three different sampling systems were estimated by comparison of the absorption of a 1 mg

sample of pyrene prepared by MI to that of a same-sized sample prepared with a KBr pellet. The KBr pellet was mounted on the deposition surface in the sample chamber to assure that the optical arrangements were equivalent. Using the general sampling system, the collection efficiency of a one milligram sample was only 20%. Use of the micro-sampling arrangement increased the efficiency to 50%. The efficiency of the ultramicrosampling system was estimated at close to 100% for samples less than 5 μg in size. The efficiencies were undoubtedly sample size dependent, so that these efficiencies should be taken only as representative values.

5. Utility of the Far-IR Region, 500-40 cm^{-1}

The KBr beamsplitter was energy deficient between 500-400 cm^{-1} and consequently the S/N ratio was severely degraded in this region. Spectral information in this range was virtually useless. The KBr beamsplitter did not transmit radiation below 400 cm^{-1}, leaving that region unexplored. Using other beamsplitters, the spectra of several PAH over the region 500-40 cm^{-1} were obtained to determine if there were any absorption bands which would be useful for qualitative or quantitative determinations. A CsI beamsplitter with a range from 1200-230 cm^{-1} was utilized to observe bands below 500 cm^{-1} for carbazole, pyrene, benz[a]anthracene, and phenanthrene (Figures 15 and 16). For these compounds, additional bands in this region were few and relatively weak as compared to the most intense band in the mid-IR region. The strongest pyrene far-IR band (303 cm^{-1}) was only 6% as intense as the 846 cm^{-1} peak for this compound. Similarly, the strongest far-IR peaks for benz[a]-anthracene (471 cm^{-1}), phenanthrene (427 cm^{-1}), and carbazole (424 cm^{-1}),

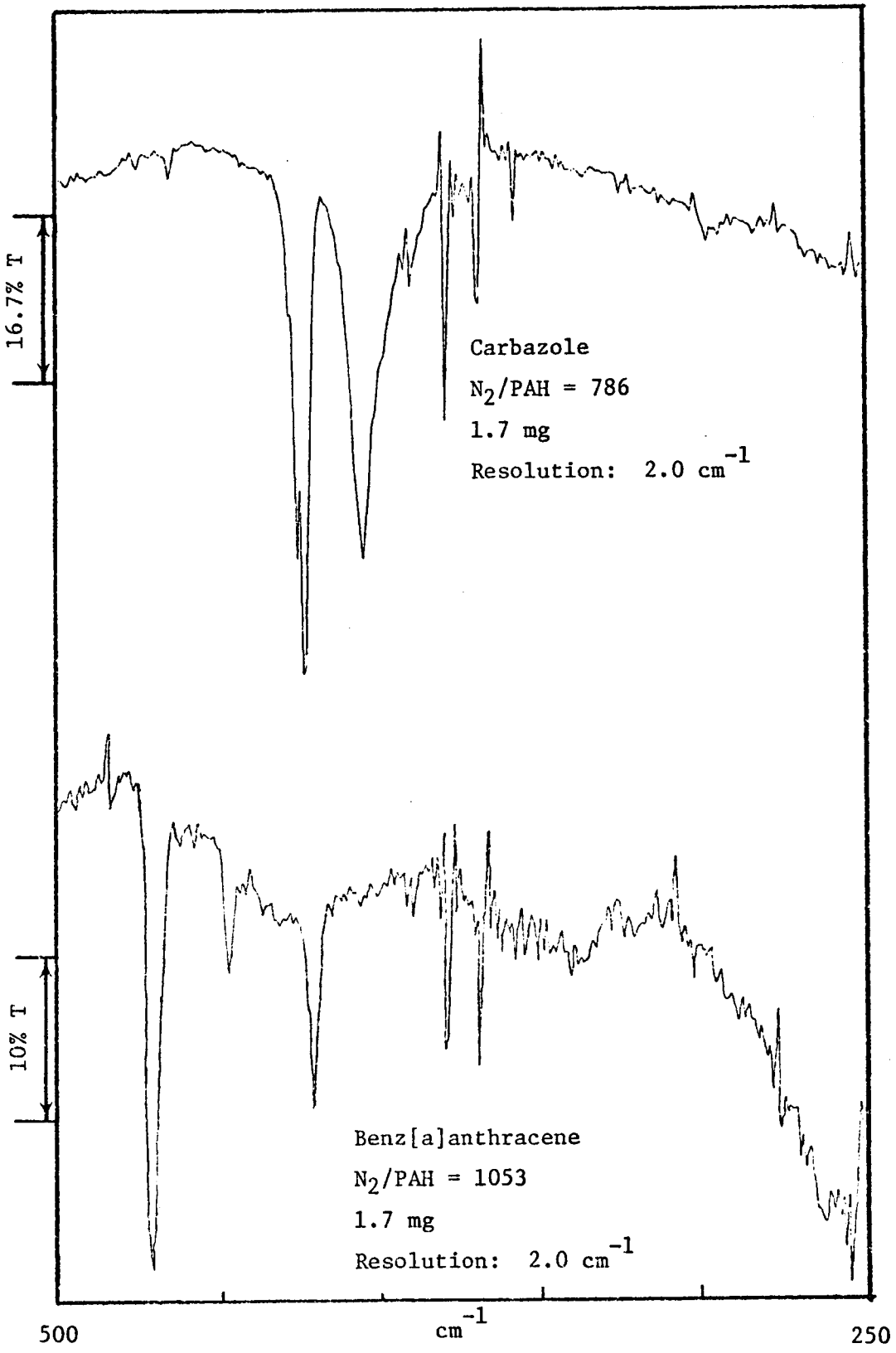


Figure 15. Transmittance spectra of carbazole and benz[a]anthracene, 500-250 cm^{-1}.

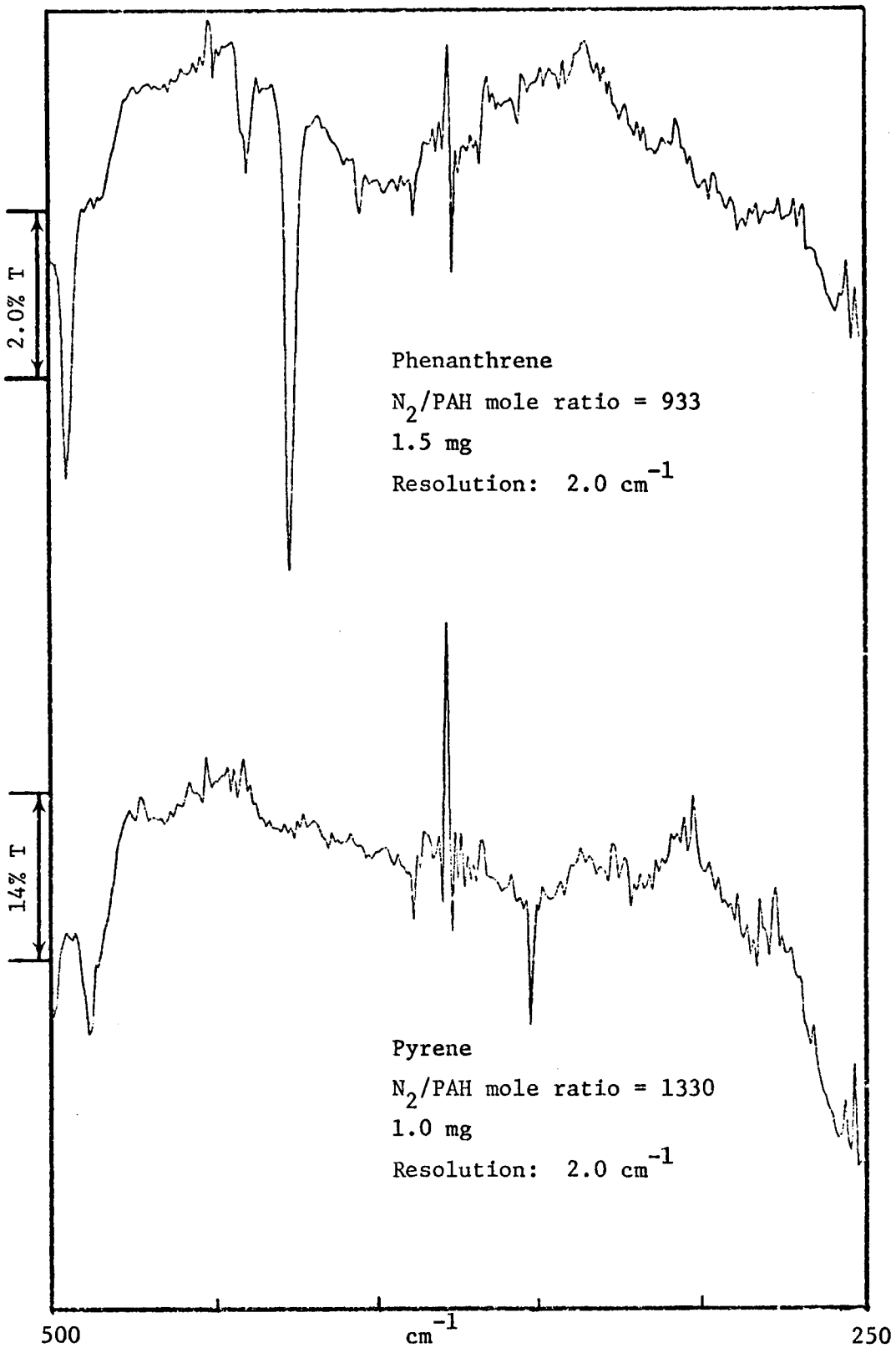


Figure 16. Transmittance spectra of phenanthrene and pyrene, 500-250 cm^{-1}.

were 26%, 28%, and 50% as intense as the strongest bands for these PAH's. Except for carbazole, a nitrogen heterocycle, these bands would be useful only for highly absorbing samples (0.02 absorbance or more). For the purposes of analyzing very small PAH quantities, it was concluded that this region had very little utility.

These far-IR spectra were obtained utilizing a Nernst glower source, obtained from a Perkin-Elmer IR grating instrument. This source was investigated in an attempt to improve the source energy and enhance the sensitivity of the MI-FT-IR method. However, the Nernst source could not be powered by the spectrometer's DC power supply. AC operation of the source generated 60-cycle noise evident throughout the spectra as spurious signals. One such spectral anomaly was seen at 378 cm^{-1}. In addition to this problem, the Nernst glower did not provide more energy, and was subsequently no longer used.

Occasionally, spurious signals were observed in spectra using the DC nichrome source. The origin of these spurious signals was never absolutely identified, but was presumed to be due to several instruments operating in the same laboratory. Signal averaging was used to reduce the severity of these spectral anomalies.

The far-IR region from 200-40 cm^{-1} was explored utilizing a 12.5 μm-thick Mylar beamsplitter and a mercury source. Polyethylene windows were used in the sampling chamber. Large (mg) samples of pyrene and phenanthrene were prepared and no absorption bands due to the PAH's were detectable. Absorbance coefficients, ε, in the far-IR are smaller than those for the mid-IR by a factor of $\sim$ 1/5, requiring

that much larger samples be used to observe these bands.[86] The situation for MI samples was severely energy-limited, since the IR radiation had to pass through three polyethylene surfaces. The amount of sample necessary to observe any bands in this region was beyond the scope of this application, and therefore this region was no longer investigated.

Polyethylene exhibits a lattice vibration at 72 cm^{-1} which was observed in these studies. It was interesting to note that at low temperatures (approximately 15 K), an additional strong polyethylene band was activated at 80 cm^{-1}. No explanation for this phenomenon has apparently been given.

6. Peak Position

Since only one or two bands may be observed for a particular PAH at very low levels, it was important to establish that peak positions remained constant under matrix-isolation conditions. In cases where the peaks were split, the positions of the multiplets must remain constant.

Comparison of the spectra for compounds deposited individually and in mixtures showed no variation in peak position provided that the samples were well isolated. Determination of the exact peak position was dependent on the degree of x-scale expansion and the pen positioning. By scaling to 10 cm^{-1}/inch, spectral features were much better defined. Except for a few specific absorption bands, when the peak did not fall directly on an integral wavenumber marking, the position of the band was rounded off to the nearest wavenumber. Small peak position differences (less than 0.5 cm^{-1}) were sometimes observed, but

these errors were of a magnitude that could be introduced in pen positioning and visual inspection.

The use of a digital plotter caused some problem with askew or flattened peaks due to the linear interpolation between the spectral points. This stepping effect can cause a loss of photometric precision which can often be overcome by a technique known as "zero filling." To zero fill, one adds zeros to an interferogram to increase the number of points which define the spectrum.[61] This helps to smooth the absorption bands. The Digilab instrument was programmed to perform this operation, expediting what would otherwise be a very lengthy procedure.

Zero filling was utilized extensively and was found to provide very little improvement in the shape of absorption peaks. In fact, four times zero filling (increasing the number of points by four) increased the bandwidths of the absorption bands. It was concluded that the best way to achieve well-defined peaks was to collect the spectrum at sufficient resolution. A resolution of 1.0 cm^{-1} proved to be the most useful. To insure photometric accuracy, full double precision collection and computation was used for quantitative work.

B. Qualitative Studies

1. Resolution of Two and Three Component Synthetic Mixtures

One of the possible advantages of the MI-FT-IR method for PAH analysis was that isomers and complex (greater than four compound) mixtures could be easily resolved. The capability of this method to resolve

both isomers and complex mixtures was important to the overall evaluation of the method.

The first mixture studied by MI-FT-IR was an equimolar sample of phenanthrene and anthracene, $C_{14}H_{10}$ isomers. Figure 17 shows the MI-FT-IR spectrum of this isomeric pair. Each compound was easily identified by a number of distinctive absorption bands. It is important to note that the strongest MI bands (the 740 cm^{-1} band of phenanthrene and the 730 cm^{-1} band of anthracene) are resolved even at these very large quantities (i.e. 1 mg). Resolution of these two bands was not possible by conventional sampling methods.[54]

A particularly difficult group of isomers to separate is benz[a]anthracene, triphenylene, and chrysene ($C_{18}H_{12}$). Without prior separation, several detection methods cannot adequately resolve these compounds (see Table II, p 11). The standard spectra indicated that these compounds should be easily resolved by MI-FT-IR and this was shown to be the case (Figure 18). As with the $C_{14}H_{10}$ isomers, bands for each isomer were readily assigned. This mixture contained very large quantities (i.e. 1 mg) of each isomer, and it can be expected that at low quantities (μg levels), the resolution of this mixture would be even more distinct.

Benzo[a]pyrene and benzo[e]pyrene are very difficult isomers to separate. Benzo[a]pyrene is highly carcinogenic and benzo[e]pyrene is not carcinogenic, so it is very important to distinguish the two. Standard spectra indicate their separation to be easy and in six-component mixtures, these two isomers were readily identified.

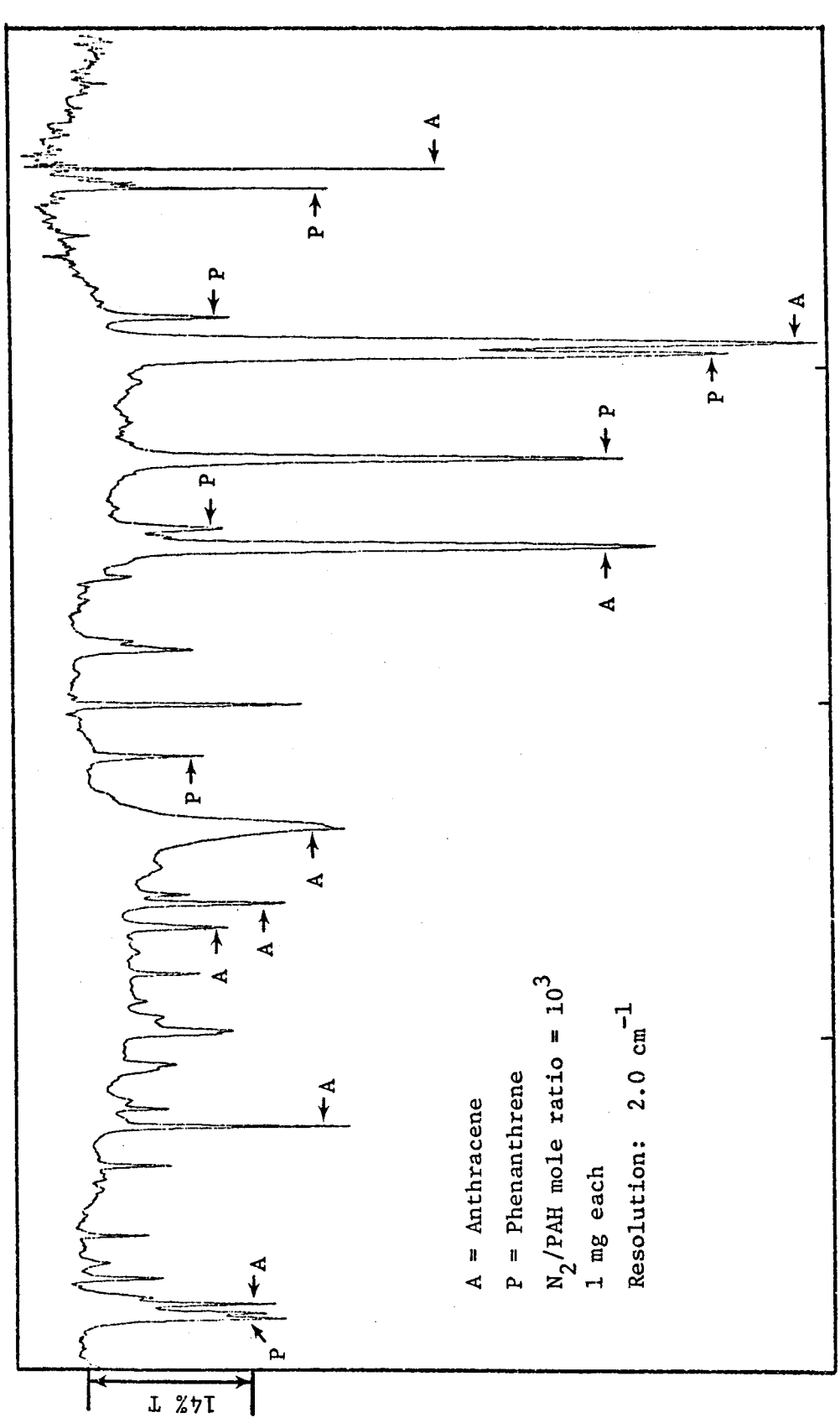


Figure 17. Transmittance spectrum of a mixture of anthracene and phenanthrene.

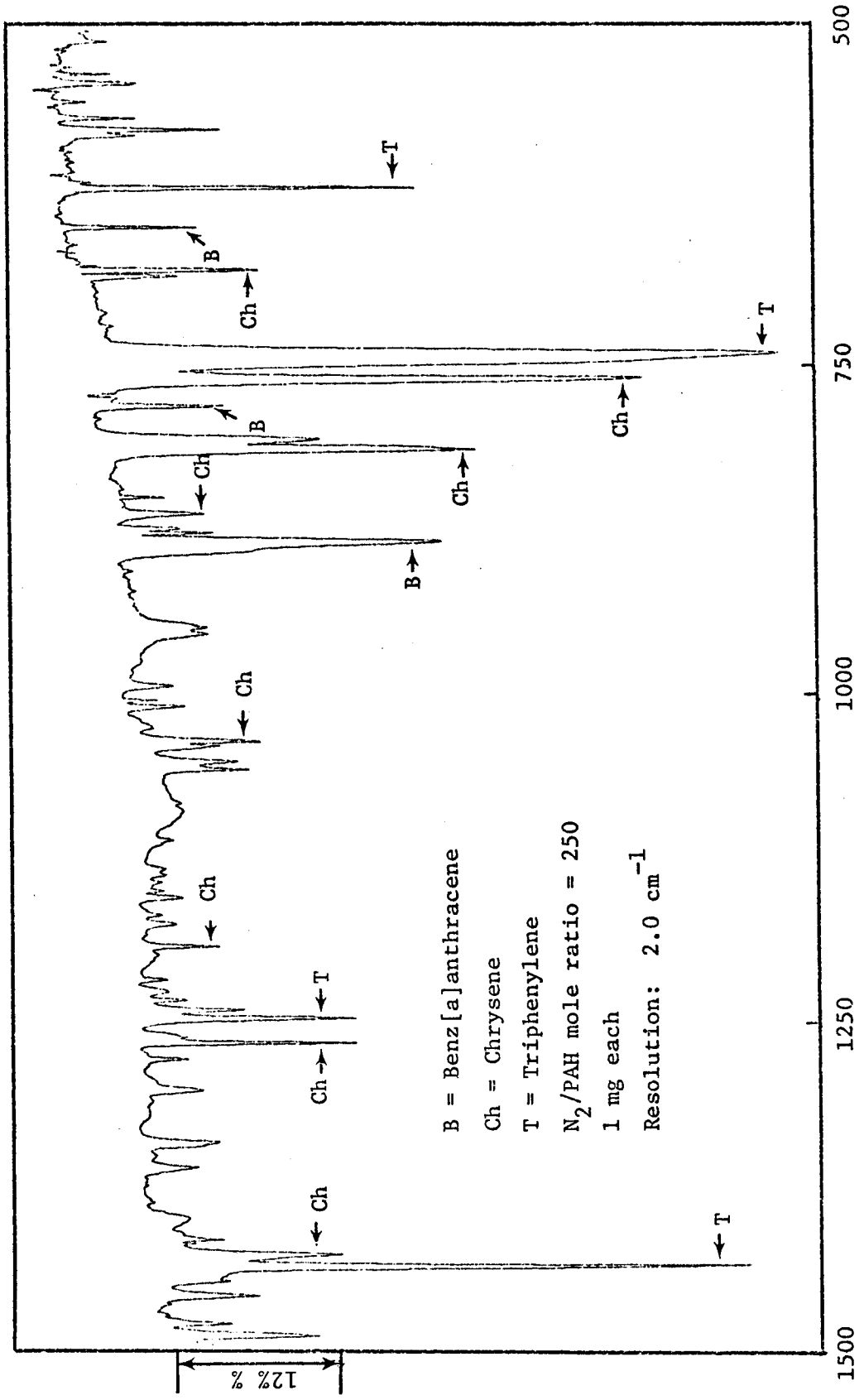


Figure 18. Transmittance spectrum of a mixture of $C_{18}H_{12}$ isomers.

The form in which the spectrum was plotted had much to do with identification of mixture components. By scale expansion along the x-scale of the region of interest, the bands become much more separated. As previously discussed, this scale expansion was also necessary in order to determine the band position accurately.

2. Resolution of More Complex Mixtures

Another advantage of the MI-FT-IR method over other detection methods is its ability to resolve complex mixtures. This has the potential to reduce overall analysis time by eliminating some of the prior separations.

A spectrum of a four-component mixture is shown in Figure 19. In the presence of carbazole (which has a very rich spectrum), pyrene, anthracene, and phenanthrene can readily be identified. This mixture and the $C_{18}H_{12}$ isomers (Figure 18) indicated that at high PAH levels (i.e. mg), spectra of several compound mixtures could become very complicated. As demonstrated in the bandwidth vs. N_2/PAH study, low level mixtures of PAH should result in much simpler spectra due to the reduced bandwidths and the reduction in the number of detectable bands. Low level mixtures are in fact more typical of environmental samples, which commonly contain µg or lower quantities of PAH's (Table I, p 2).

Figure 20 is a spectrum of a mixture of five components at µg levels: 7 µg benzo[b]fluorene, 7 µg benzo[a]fluorene, 10 µg anthracene, 10 µg phenanthrene, and 7 µg 1,3,5-triphenylbenzene. In the region where the strongest absorption bands appear (900-700 cm^{-1}), all five compounds are readily identified by one or more distinct bands. At these low

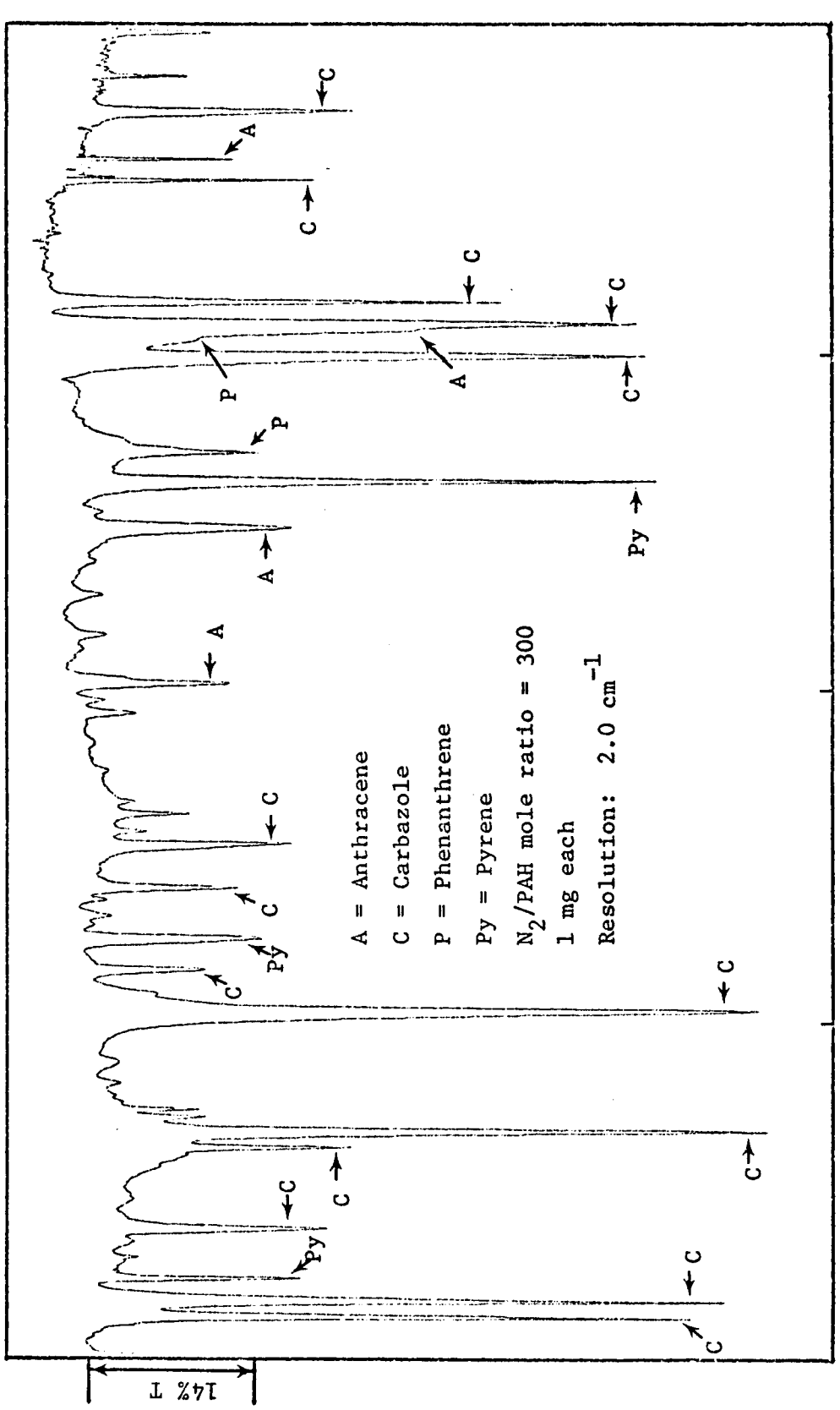


Figure 19. Transmittance spectrum of a four-component mixture.

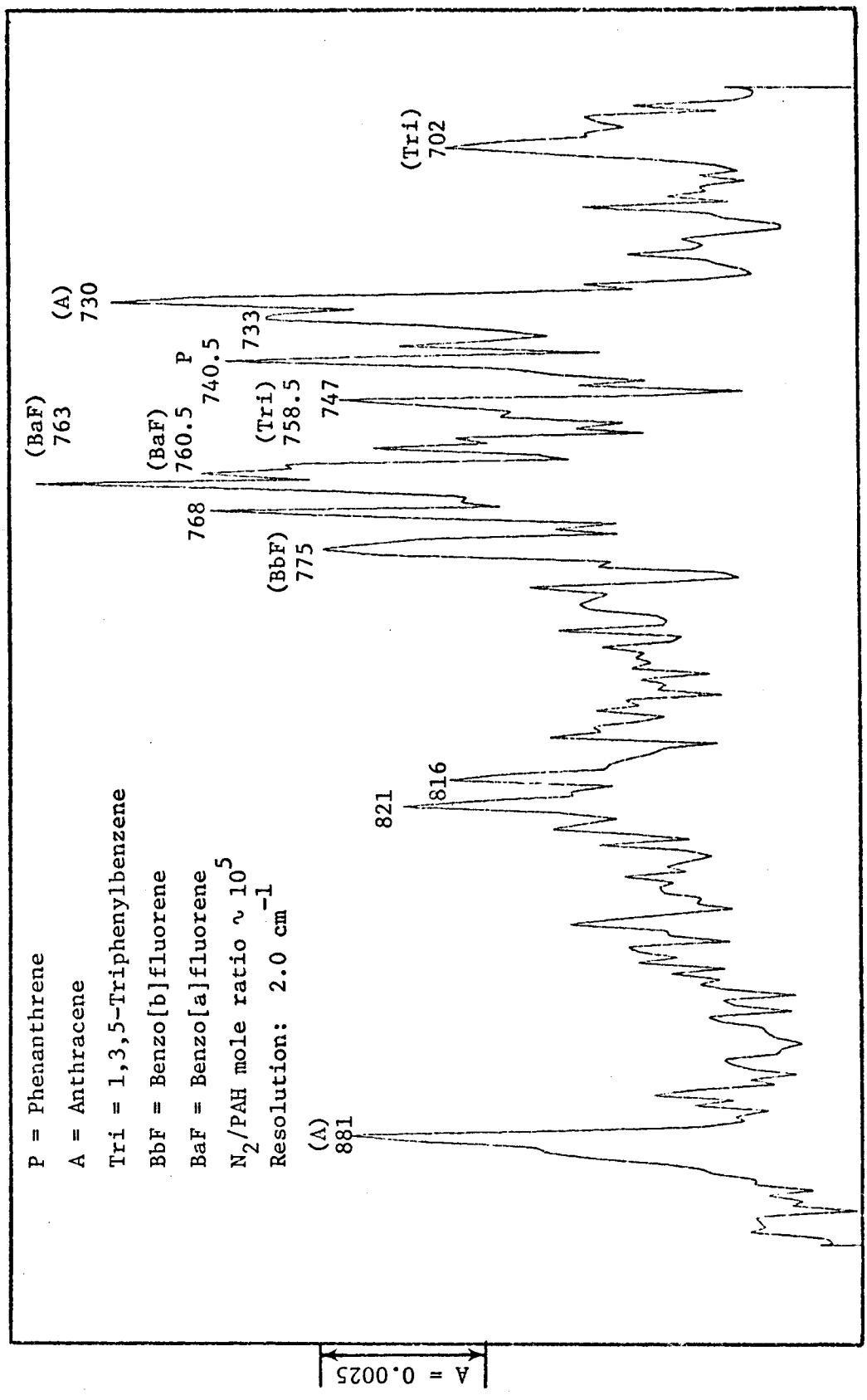


Figure 20. Absorbance spectrum of a five-component mixture.

levels the bandwidths are much narrower (2-5 cm^{-1}) than in large quantity mixtures, making the resolution of neighboring bands more complete. This mixture was examined because it simulated the PAH components expected in a "real" liquid chromatography fraction of a synthetic fuel, Synthoil.[12] Provided that the sensitivity is adequate, resolution of PAH in such fractions by MI-FT-IR should be feasible.

A six-component mixture was also prepared and all compounds, benzo[a]pyrene, benzo[e]pyrene, anthracene, phenanthrene, carbazole, and benz[a]anthracene, were identified. The spectrum of this mixture is shown later in this chapter.

In an attempt to determine the ultimate capability of this method for resolving complex mixtures, the MI-FT-IR spectrum of a ten-component mixture was run at very low levels (1 μg or less) using the ultramicro-sampling system. The compounds and their weights are shown in Table VII.

As the spectrum (Figure 21) shows, all the compounds except phenanthrene were unambiguously identified. Phenanthrene could certainly have been seen at 740 cm^{-1} as there were no interferences, but it was not observed due to its high volatility at this low level. Future work using a cryogenic Knudsen cell should provide a means by which all ten compounds can be simultaneously determined.

3. Real Samples

High pressure liquid chromatographic fractions of Synthoil (a coal liquefaction product) and shale oil were analyzed for PAH's by MI-FT-IR. The chromatographic separations were performed by G. Goldstein of the Oak Ridge National Laboratory.[12] Polyvinylpyrrolidone (PVP) was

TABLE VII

THE TEN-COMPONENT MIXTURE:
COMPOUNDS AND WEIGHTS

PAH	Weight (μg)
Pyrene	0.5
Fluoranthene	1.0
Anthracene	1.0
Phenanthrene	1.0
Benzo[e]pyrene	0.5
Chrysene	0.5
Triphenylene	0.5
Perylene	0.5
1,3,5-Triphenylbenzene	1.0
Naphthacene	1.0

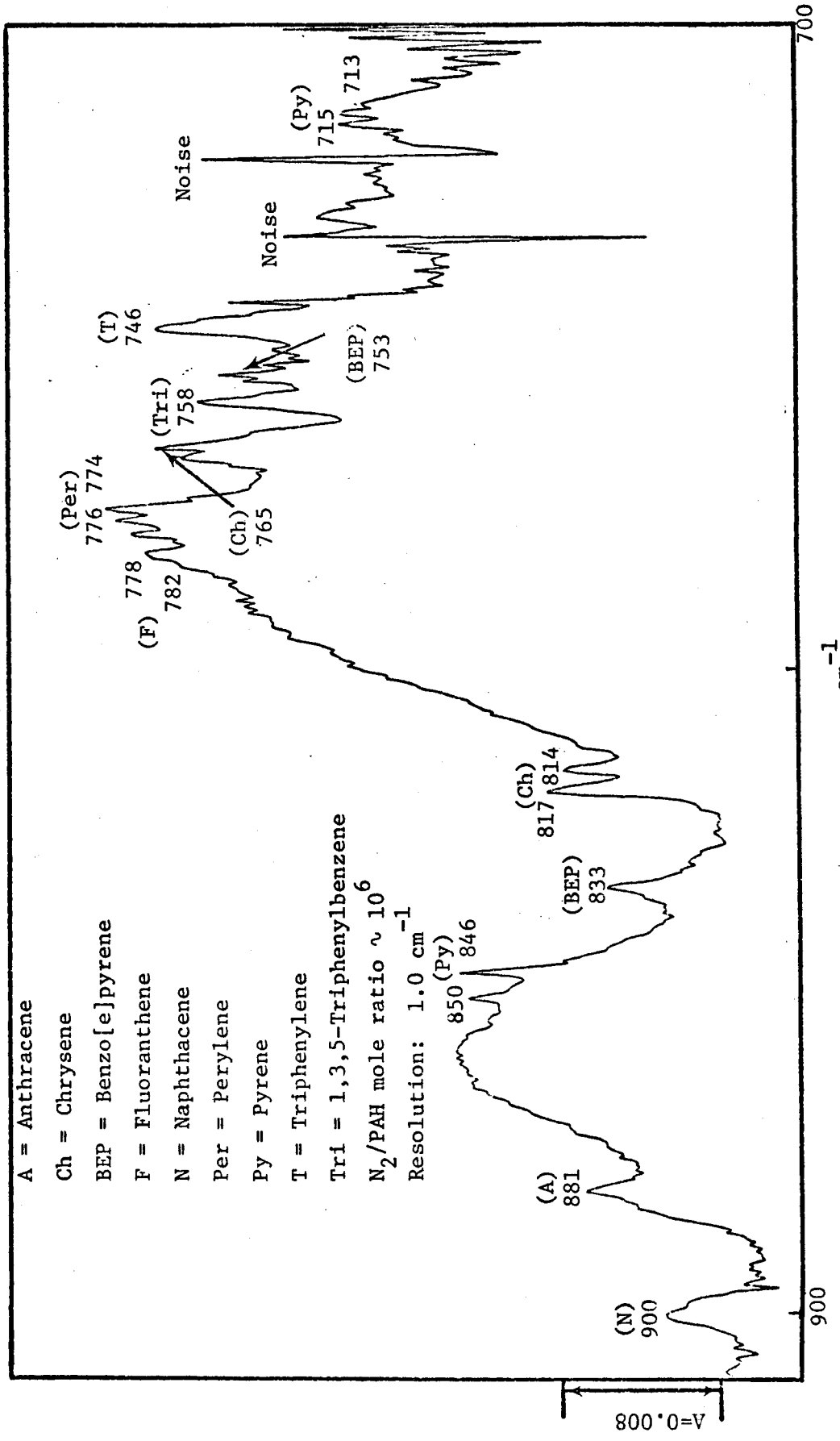


Figure 21. Absorbance spectrum of a ten-component mixture.

used as the stationary phase and isopropanol as the eluent. The size of the initial oil samples was 0.3 ml. Two milliliters of each fraction were collected. The presumed constituents of seven fractions are shown in Table VIII.

Two different HPLC lots were investigated. The first lot, received in January 1976, consisted solely of Synthoil fractions. These fractions were analyzed with the general sampling system and the microsampling system. The second lot, received in September 1976, consisted of HPLC fractions of Synthoil and shale oil. These fractions were analyzed by means of the ultramicrosampling system. All fractions were loaded into the Knudsen cell and evaporated to dryness prior to deposition.

Large volumes (0.5-0.6 ml) of HPLC fractions III and IV were analyzed with the general sampling system, but no PAH's were detected due to the poor sensitivity of this arrangement.

The improved deposition efficiency of the microsampling system met with more success. MI-FT-IR spectra of fractions III, IV, and V contained several distinct absorption bands (Figures 22-24). Phenanthrene (740.5 cm^{-1}) and pyrene (750, 746 cm^{-1}) were identified in fractions III and IV, respectively. The other absorption bands in these spectra could not be attributed to any of the PAH's presumed to be present (see Table VIII). Absorption bands between 3000 and 2920 cm^{-1} in these spectra were indicative of the presence of alkyl groups in these samples. Alkanes could account for some of the unknown absorption bands in the spectra. Neither benz[a]anthracene nor chrysene was detected in fraction V. The only absorption bands seen were in

TABLE VIII

PAH'S SUSPECTED TO BE IN HPLC FRACTIONS

Fraction	PAH
I	Monoaromatics
II	Acenaphthene, biphenyl, naphthalene, fluorene
III	Phenanthrene, anthracene, benzofluorenes, possibly 1,3,5-triphenylbenzene
IV	Pyrene, fluoranthene
V	Benz[a]anthracene, chrysene, triphenylene
VI	Benzo[a]pyrene, perylene, benzo[e]pyrene
VII	Dibenzanthracenes

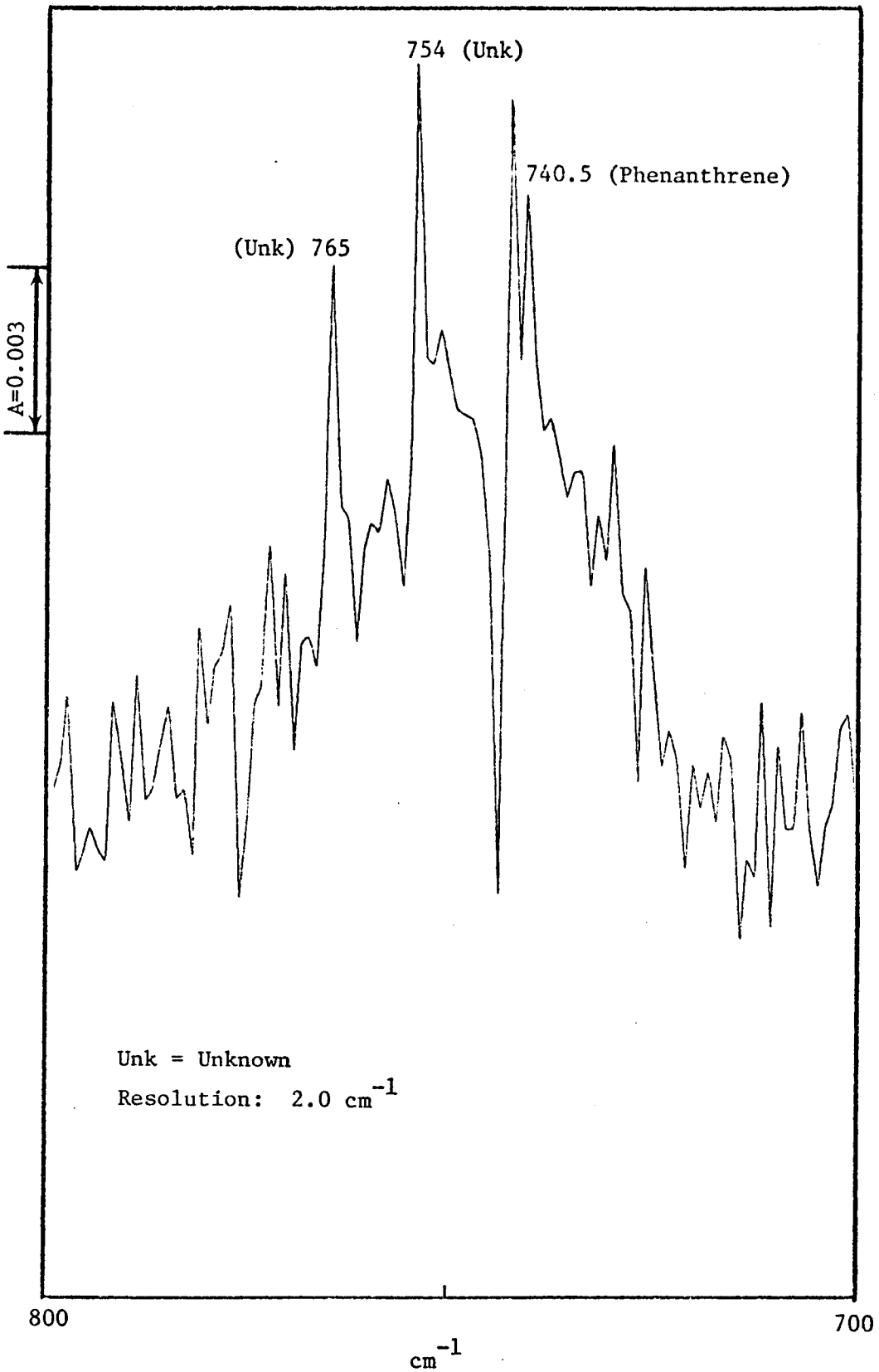


Figure 22. Absorbance spectrum of Synthoil fraction III prepared with microsampling system.

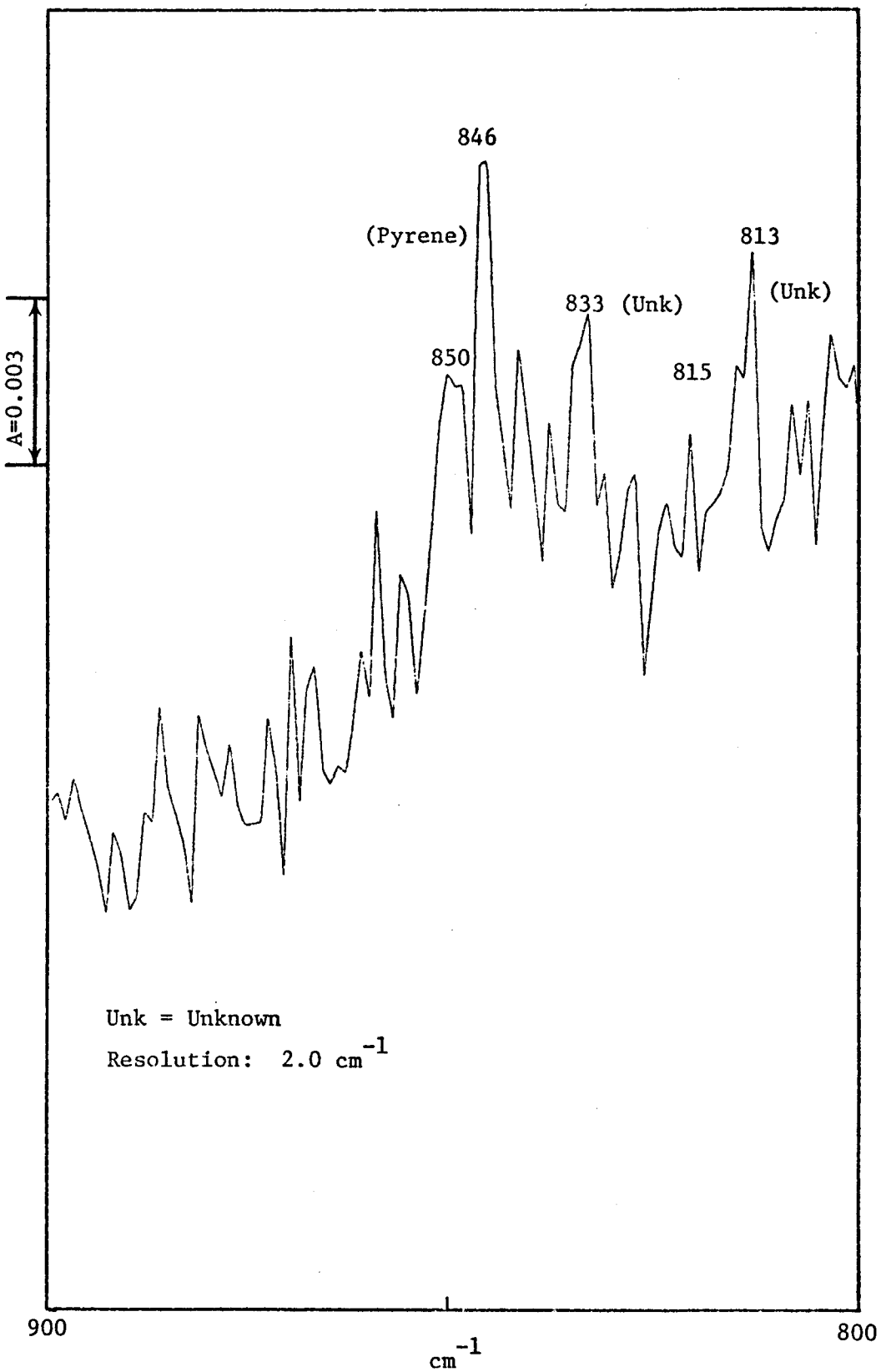


Figure 23. Absorbance spectrum of Synthoil fraction IV prepared with microsampling system.

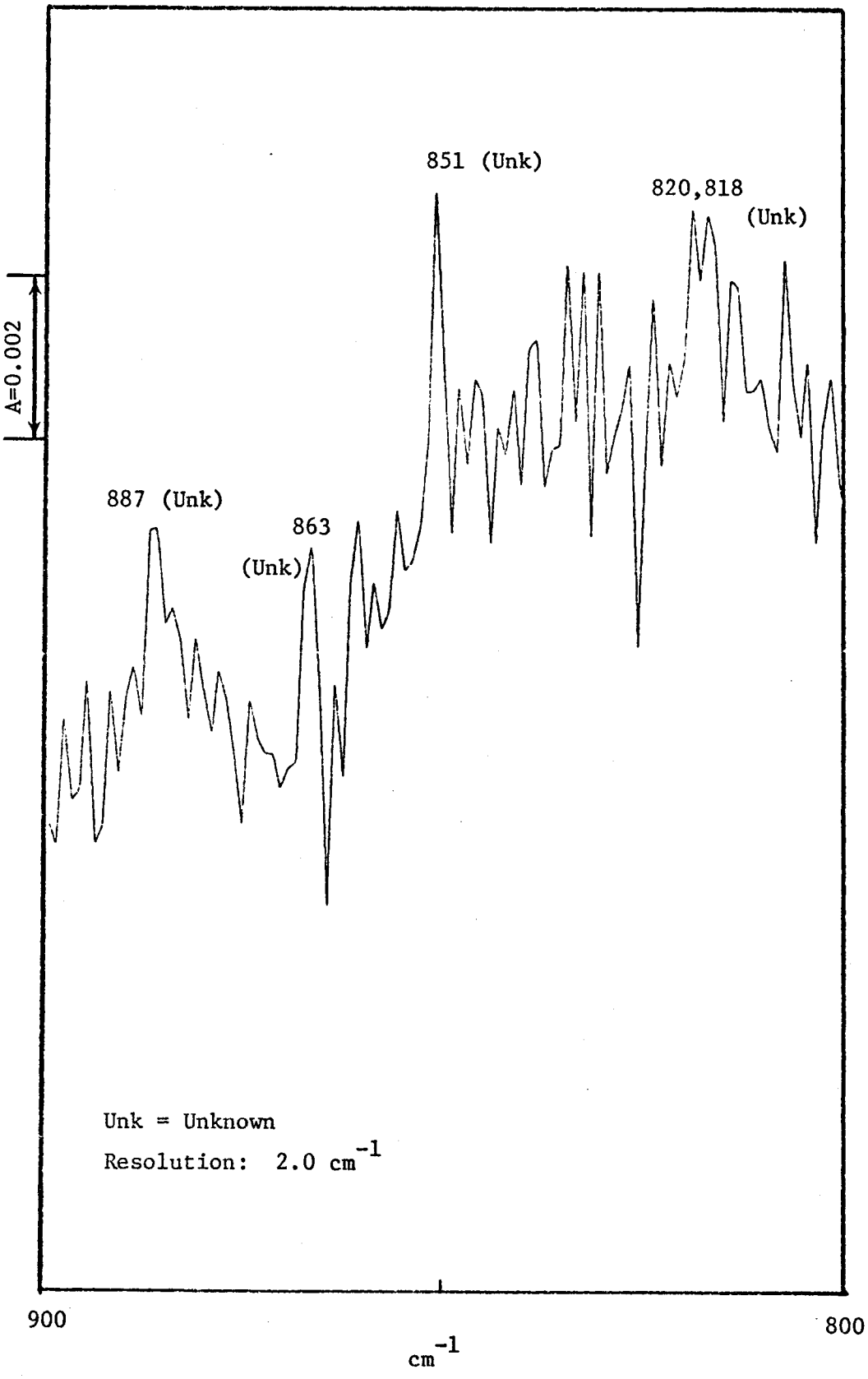


Figure 24. Absorbance spectrum of Synthoil fraction V prepared with microsampling system.

in the spectral region 900-800 cm^{-1} (Figure 24). The concentrations of these PAH's in fraction V were too low to be detected in 100 µl sample volumes. The limited amount of the fraction prohibited the use of larger volumes.

HPLC fractions IV of both Synthoil and shale oil from the second lot were determined to contain pyrene (Figures 25 and 26) as evidenced by absorption bands at 850, 846 cm^{-1} and 715, 713 cm^{-1} in the MI-FT-IR spectra of these oils. No fluoranthene was detected. Using standard addition and by referring to calibration plots, the concentrations of pyrene were determined to be approximately 67 ppm in Synthoil and 9.3 ppm in shale oil. In the volume of the fractions analyzed, these concentrations were equivalent to 1.0 µg pyrene in the Synthoil and 0.7 µg pyrene in the shale oil.

The MI-FT-IR spectra of fraction V of Synthoil and shale oil were much more complex than those of fraction IV, which made identification of PAH constituents difficult. The spectra included a number of broad, intense absorption bands which blocked large spectral regions (Figures 27 and 28). The large absorption at 750 cm^{-1} overlaps the region where the major absorption bands of benz[a]anthracene and triphenylene would be seen. Secondary bands were not detectable for these compounds in either oil. Chrysene was detectable in both fractions at very low quantities. Chrysene has two strong absorption bands in this region, the doublets at 766, 764 cm^{-1} and 817, 814 cm^{-1}. In the Synthoil fraction V, the 817, 814 cm^{-1} band provided the key to identification, while in shale oil, the 766, 764 cm^{-1} band was most obvious. The entire HPLC fraction was used for both these analyses, so only an

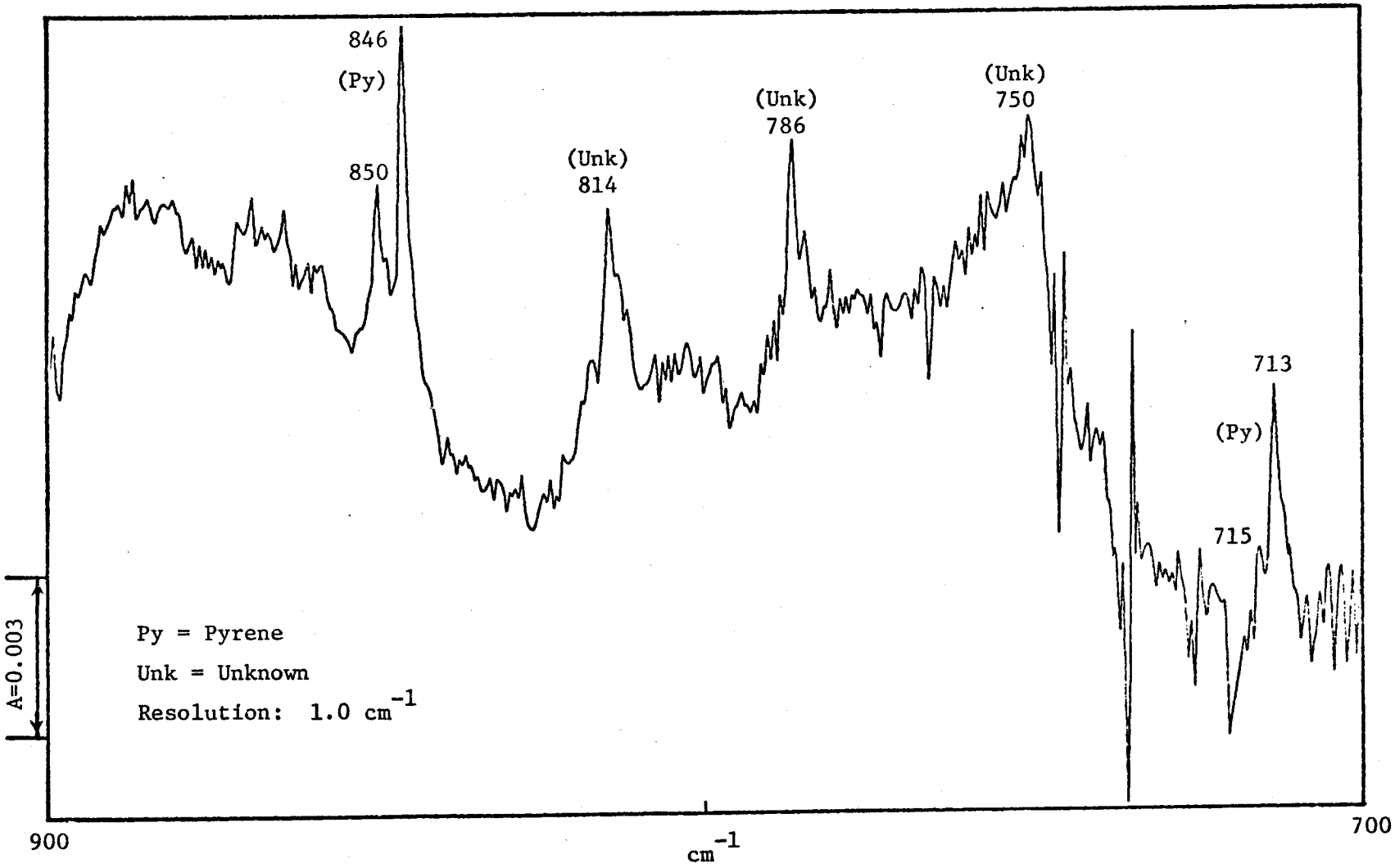


Figure 25. Absorbance spectrum of Synthoil fraction IV prepared with ultramicrosampling system.

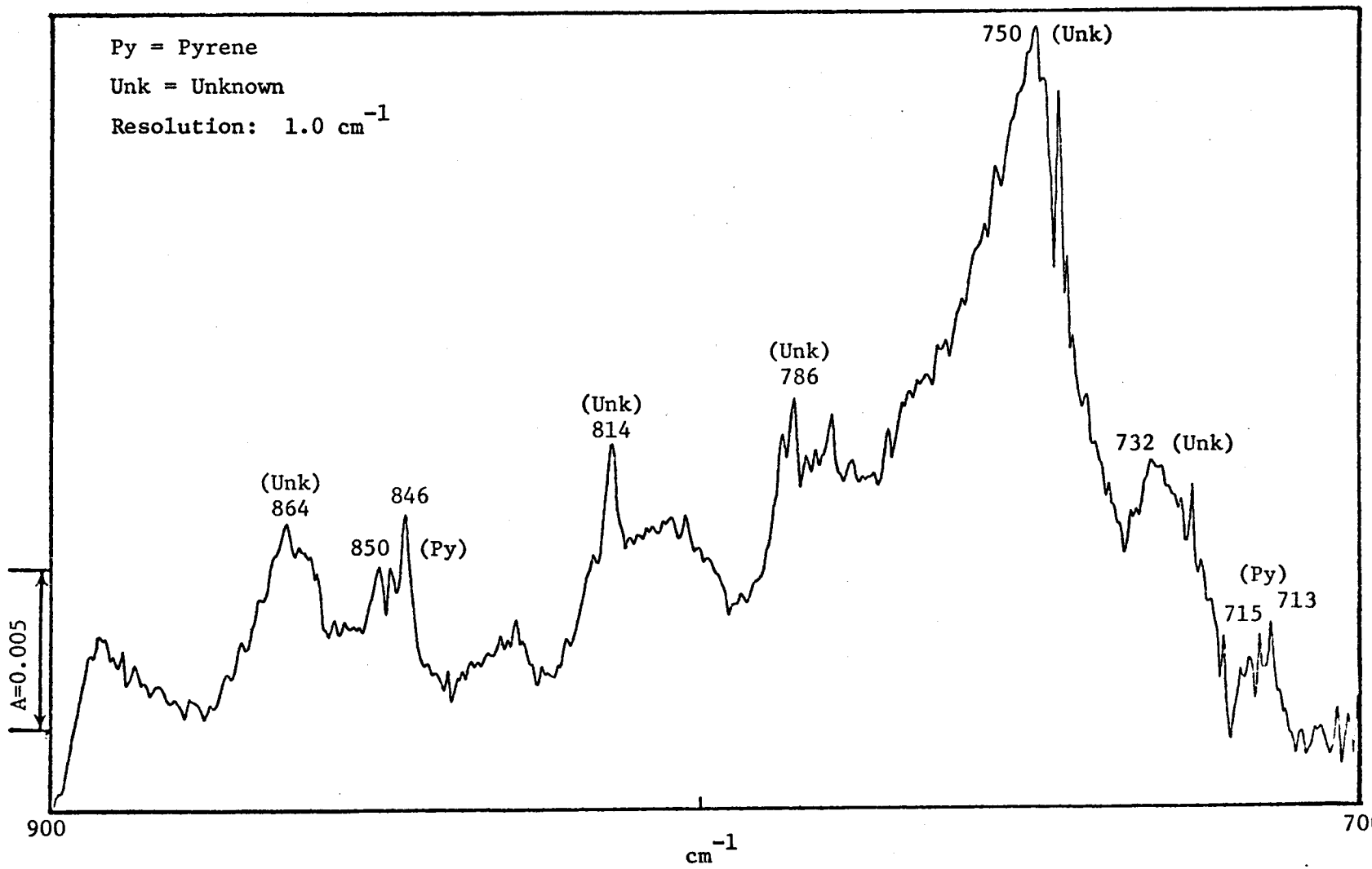


Figure 26. Absorbance spectrum of shale oil fraction IV prepared with ultramicrosampling system.

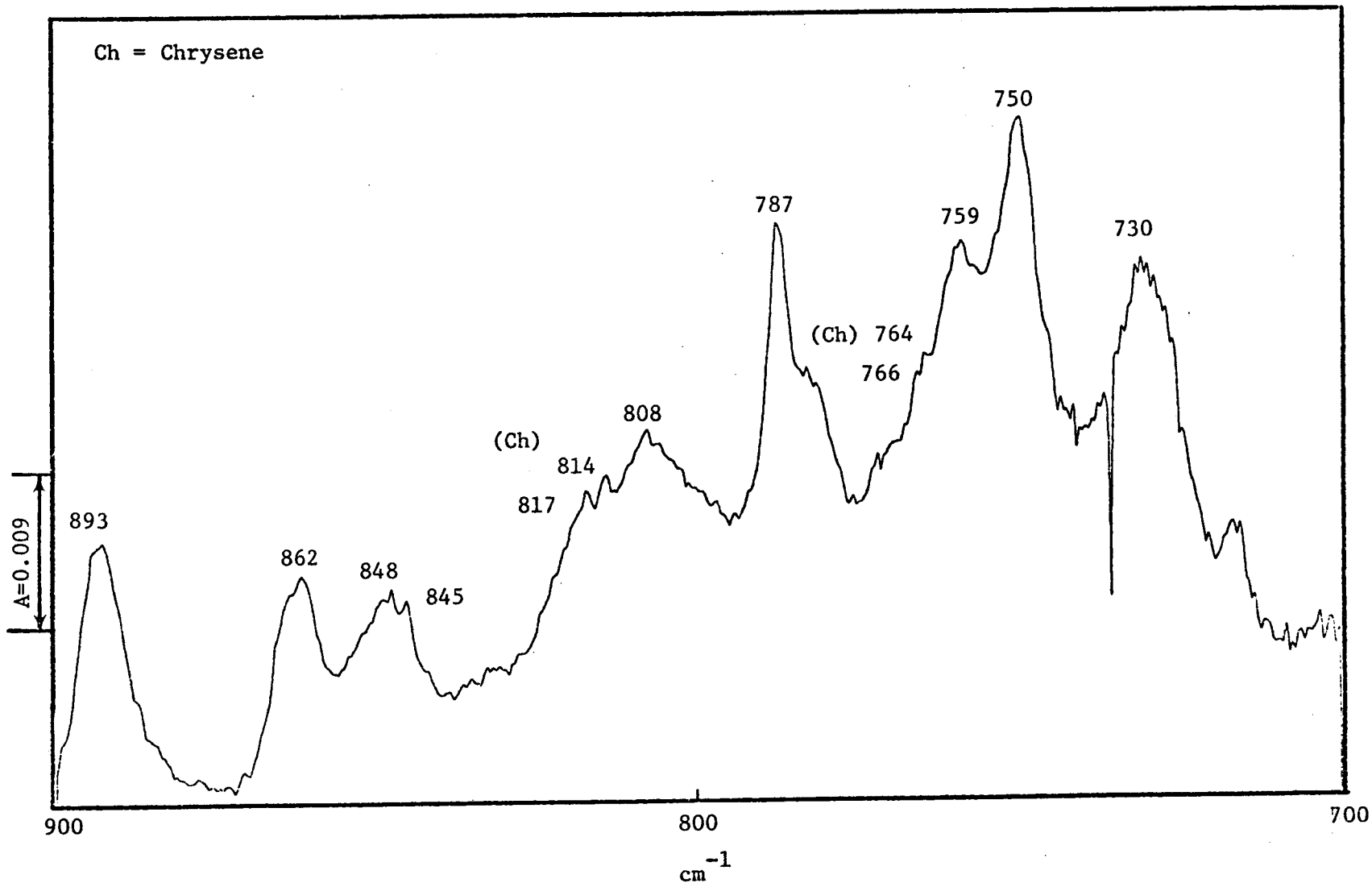


Figure 27. Absorbance spectrum of Synthoil fraction V prepared with ultramicrosampling system.

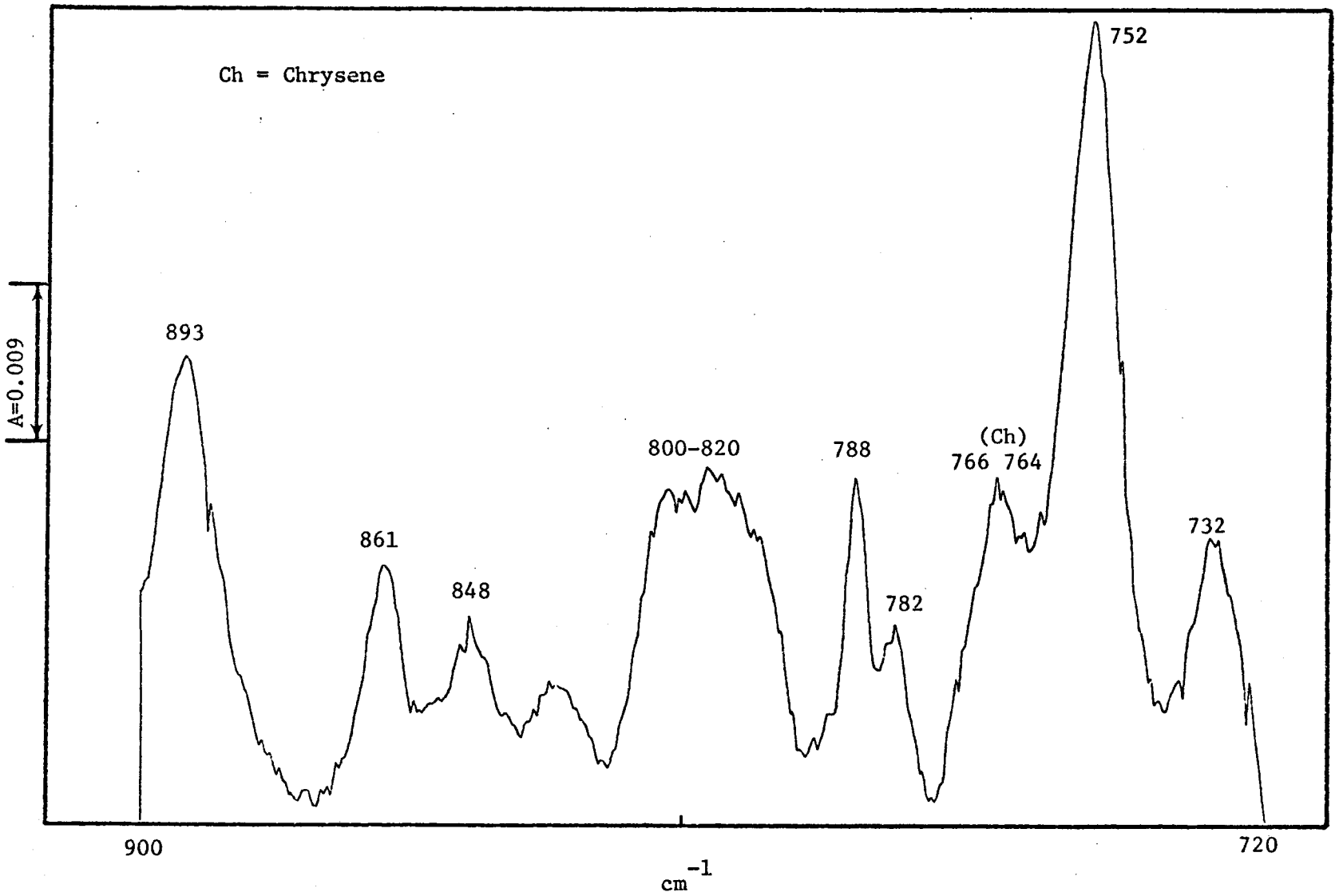


Figure 28. Absorbance spectrum of shale oil fraction V prepared with ultramicrosampling system.

estimate of the concentrations of chrysene could be made from Beer's law plots. Chrysene in Synthoil was estimated at 0.56 ppm, and in the shale oil sample at 2.0 ppm.

None of the suspected PAH's in fraction VI could be detected by MI-FT-IR. The spectra were very complex, containing broad, intense bands centered over the regions 840-800 cm^{-1} and 760-740 cm^{-1}. Other intense bands were observed at 893, 878, 844, 783, and 730 cm^{-1}. Except for the band at 878 cm^{-1}, this series of bands was common to all fractions run in this lot except Synthoil fraction IV.

Oils are known to contain many compounds in addition to PAH's which infrared spectroscopy can be helpful in identifying. For instance, nitrogen and sulfur heterocycles, phenols, olefins, and of course, paraffins have been found in Synthoil.[87] Several of the MI-FT-IR absorption bands not attributable to the PAH's suspected in the Synthoil and shale oil fractions were due to these materials.

Strong C-H stretch vibrations were noted below 3000 cm^{-1}, which indicated a significant amount of paraffin materials in several of the fractions. The intensities of the bands at 890 and 730 cm^{-1} were related, which indicated they were due to the same compounds. The absorptions at 890 cm^{-1} were in the region common for C-C stretch absorptions.[85] Methylene ($-CH_2-$) rock can be assigned to the region around 730 cm^{-1}.[85] These bands were consequently attributed to paraffins.

The strong absorption band at 750 cm^{-1} and the absorption band at approximately 820 cm^{-1} were related in intensity and could be due to a number of groups of compounds. Strong absorptions in this region are often due to C-H wag vibrations in aromatic compounds. Both phenols and

nitrogen heterocycles have strong absorptions in this region.[85] The key to identifying the compounds which give rise to these bands was the 3500-3000 cm^{-1} region of the spectra. Strong absorptions were noted at 3495 cm^{-1} for all fractions which had strong bands at 750 cm^{-1}. The 3495 cm^{-1} band is indicative of N-H stretch and thus the other major components in these fractions were probably N-heterocycles. Comparison with a standard MI-FT-IR spectrum of carbazole confirmed that this was where N-H stretch would be observed. The assignment was consistent with previous studies which indicated that large concentrations of indole (210 ppm) and skatole (128 ppm) were present in Synthoil.[87] Other strong absorptions at 1040 and 1065 cm^{-1} could also be assigned to N-heterocycles.

The spectra of Synthoil and shale oil fractions IV indicated that less paraffins and N-heterocycles were present than in fractions V and VI. However, this was certainly due in part to the much smaller fraction samples utilized to obtain these spectra. Only 0.1 and 0.5 ml were used for Synthoil and shale oil fractions IV, respectively. Fractions V and VI samples were 1.0 ml or more. It could be expected, however, that due to H-bonding, the heterocycles with a free hydrogen may come off the PVP column in higher fractions.[88] Thus, these materials would be more prevalent in these fractions (i.e. V and VI).

Oil samples for which the PAH concentrations were relatively high (greater than 10 ppm) could be analyzed for PAH's with little problem. When the PAH concentrations are low (less than 10 ppm), larger samples must be employed to observe PAH bands. Large samples, especially of higher fractions, introduced a lot of paraffins and N-heterocycles which

resulted in several large, broad absorption bands. These tended to obscure large spectral regions where PAH's might be observed. It also seemed that codeposition of these materials affected the degree of isolation, as evidenced by the broadness of the bands. The problem of interfering substances was the limiting factor in detecting PAH's in several fractions. In principle, however, additional extraction of these oils before they are chromatographed would greatly simplify MI-FT-IR analysis of the HPLC fraction. For instance, extraction with a solvent which could H-bond to N-heterocycles such as indole and skatole could eliminate much of the interfering materials found in Synthoil and shale oil. Despite the complexity of the HPLC fractions analyzed, PAH's in the sub-μg range were still identifiable in some of the fractions. In addition, tentative identification of groups of other compounds present in these oils could be made.

A MI-FT-IR spectrum of a U. S. National Bureau of Standards (NBS) PAH sample was run (Figure 29). It was determined to contain chrysene, benzo[a]pyrene, fluoranthene, and phenanthrene. 2-Methylnaphthalene was too volatile to be detected. Chrysene and benzo[a]pyrene have overlapping major bands at approximately 764 cm^{-1}, but the increased sensitivity of the ultramicro system permits their identification by secondary bands. Chrysene and benzo[a]pyrene were determined quantitatively (see section C, following).

4. Spectral Subtraction

One of the potential advantages of the MI-FT-IR method for the analysis of complex mixtures is the ability to do spectral subtraction utilizing the built-in computer capabilities. Performance of this

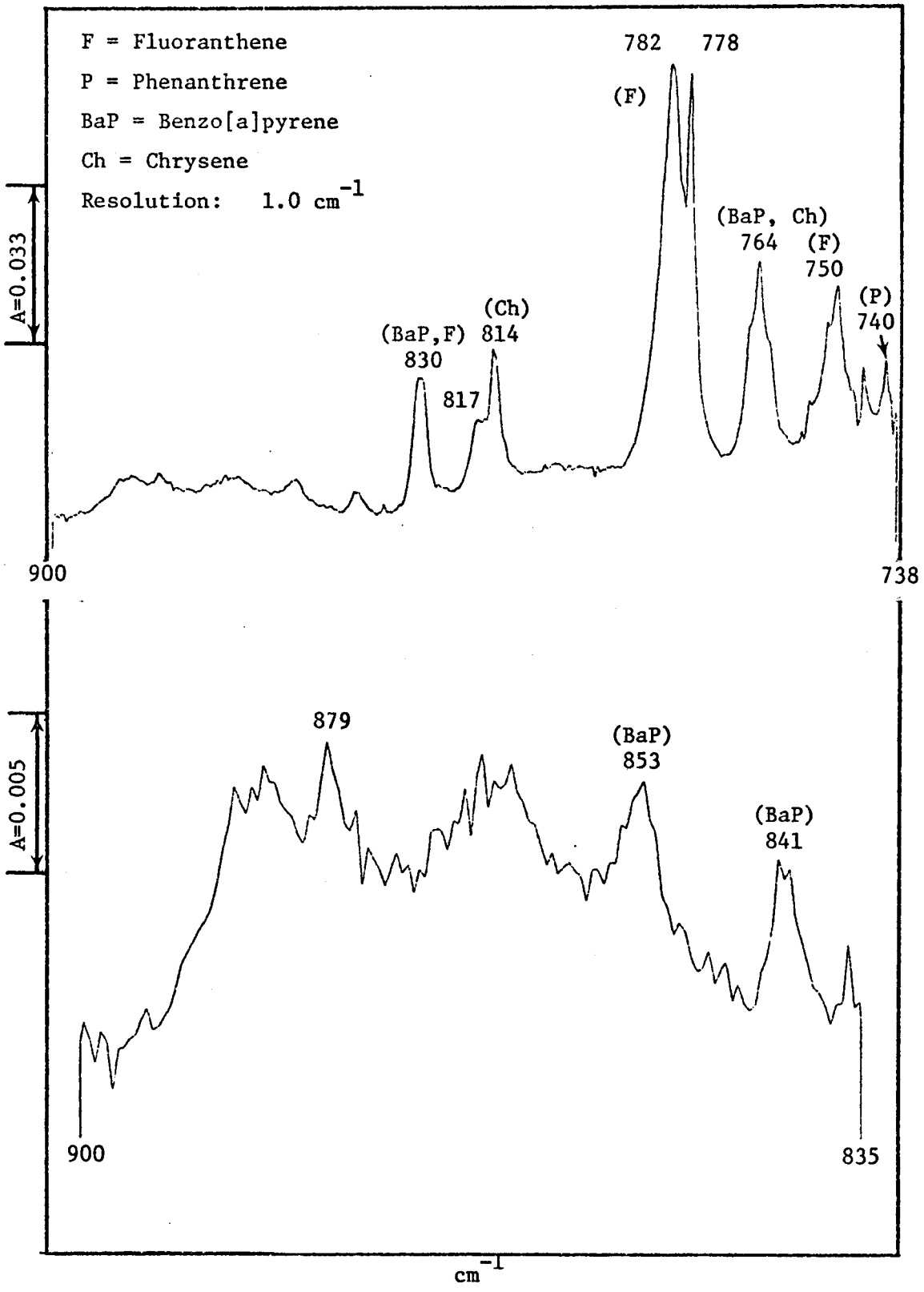


Figure 29. Absorbance spectrum of NBS sample with expanded 900-835 cm^{-1} region.

data manipulation, however, requires high signal to noise ratios and wavelength repeatabilities.[89] It has been shown that MI spectra of PAH's can be accurately reproduced, so that the wavelength repeatability criterion was met. S/N ratios were enhanced by co-addition of spectral scans, and for peak absorbances greater than 0.01, sufficient S/N ratios were obtained to identify a species in an IR difference spectrum.

By accumulating a reference library of PAH spectra, any suspected or known component can be subtracted from a mixture by appropriate scaling of the standard spectrum. This simplified the remaining spectrum, making identification of the other components possible. Straight baselines were advantageous to successful subtraction. The FT-IR's arithmetic package could correct for sloping baselines, so this could be tolerated to some degree.

A six-component mixture was used in order to assess these capabilities of spectral subtraction for MI-FT-IR spectra. A mixture of 50 μg each of benz[a]anthracene (BaA), benzo[e]pyrene (BeP), carbazole (C), phenanthrene (P), anthracene (A), and pyrene (Py) was prepared. Peak absorbances were on the order of 0.05. The mixture spectrum showed distinctive absorption bands for each compound but had a large unresolved peak from 755-750 cm^{-1} which was due to contributions of the major absorption bands of BeP, C, and BaA. At very low levels of these materials, these may be the only bands intense enough for identification. Figures 30 and 31 show the computer unraveling of this peak.

In Figure 30, benz[a]anthracene was subtracted from the mixture. The 755 cm^{-1} band of benzo[e]pyrene remained in the difference spectrum, but no spectral features due to carbazole were detected in this region. Several things should be noted in this series of spectra. The difference

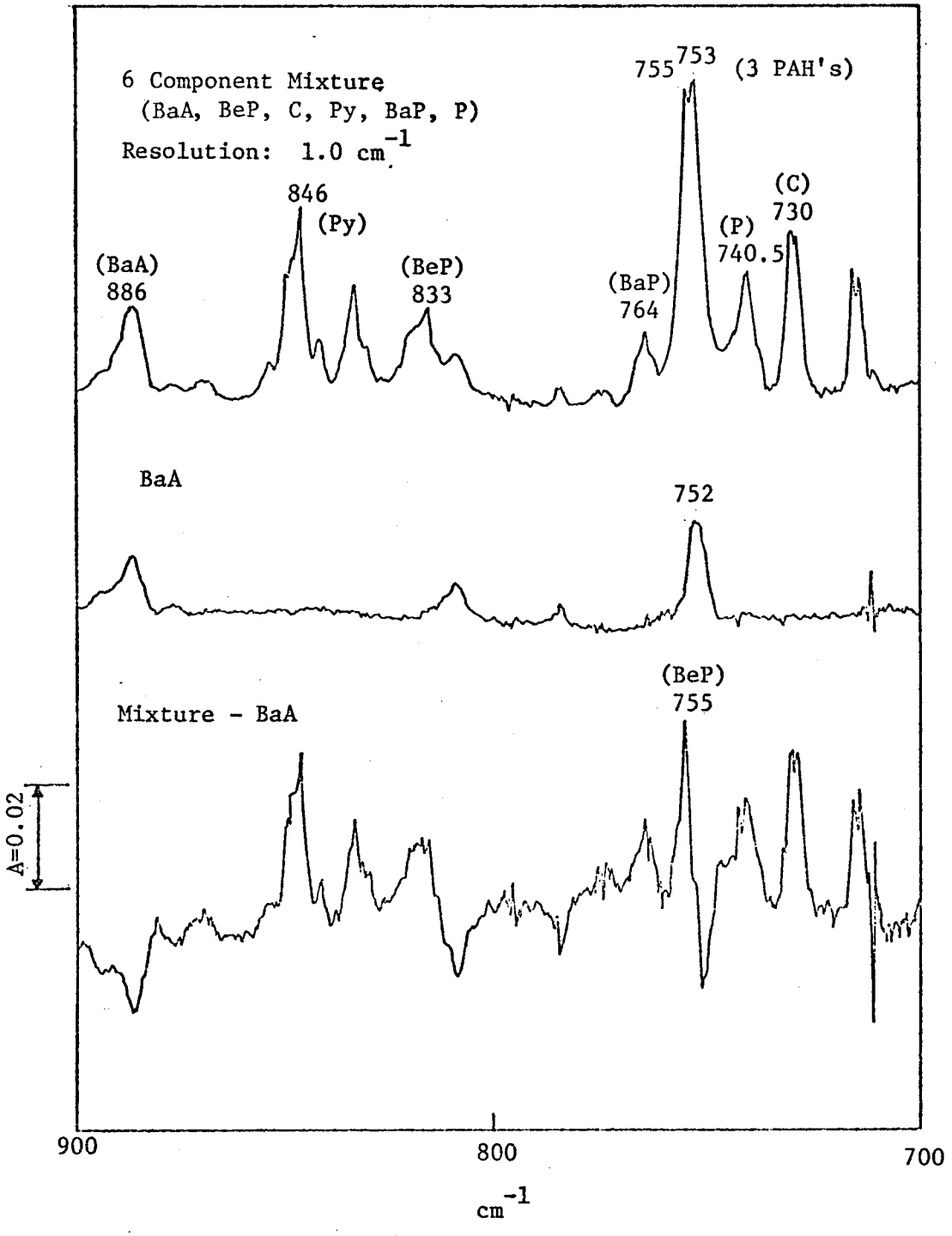


Figure 30. Spectral subtraction of Benz[a]anthracene from a six-component mixture.

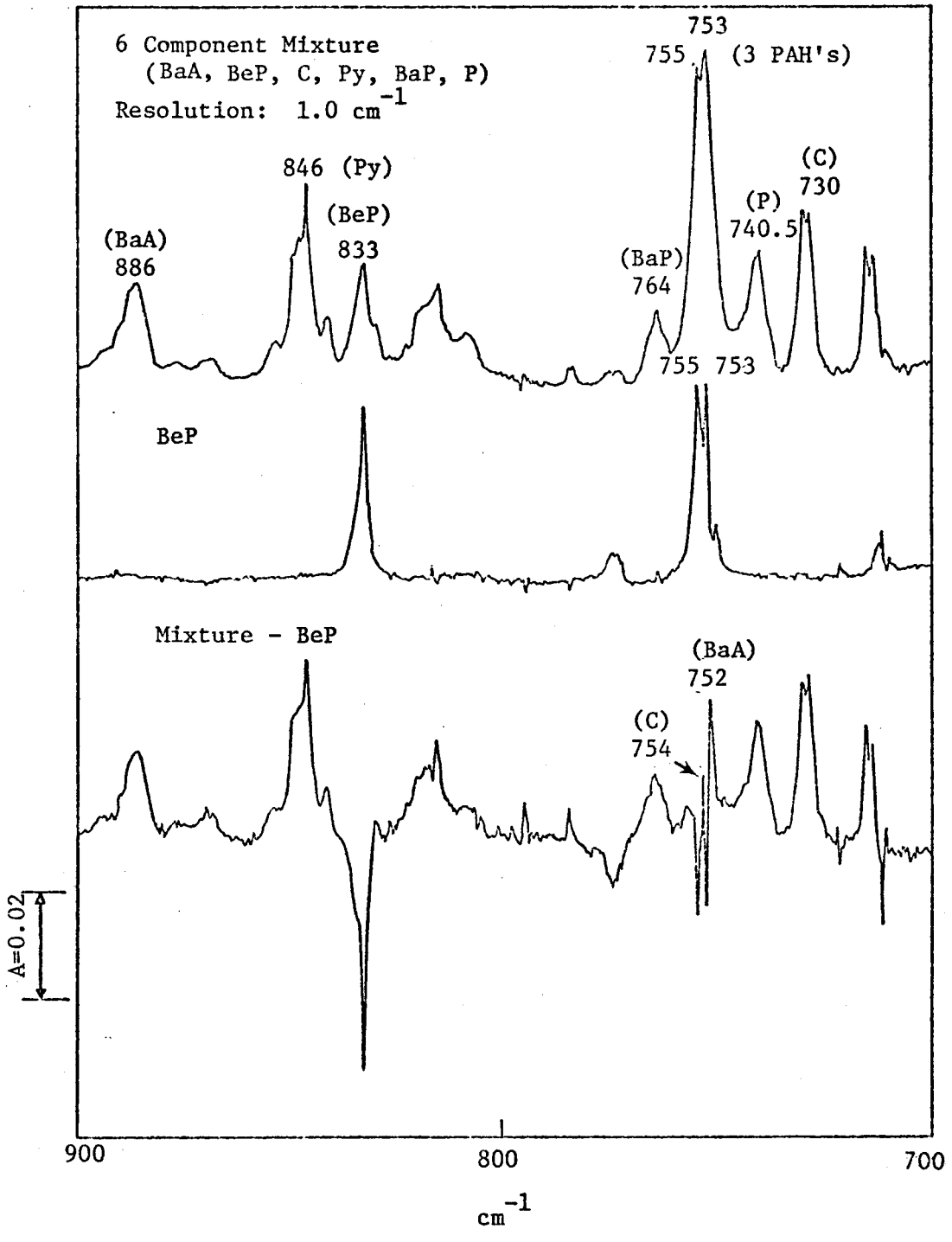


Figure 31. Spectral subtraction of Benzo[e]pyrene from a six-component mixture.

spectrum contains negative peaks which were the result of oversubtraction. This was done deliberately to ensure that the peaks being subtracted were completely eliminated. Also, early in these studies, it was discovered that relative peak heights of absorption bands for single component spectra of the same PAH were not always constant. Oversubtraction compensated for this phenomenon, too. The S/N ratio of the difference spectrum was severely degraded as compared to the original spectra. Because of this, large values of signal to noise ratios were essential in absorbance subtraction to be able to identify components in a difference spectrum. Finally, absorption peaks with overlapping features cannot be separated.

Subtraction of benz[e]pyrene from the mixture was more revealing (Figure 31). The difference spectrum showed spectral features which could be assigned to benz[a]anthracene and carbazole. The shape of the BeP doublet (narrow bandwidth at half-maximum and a "spectral window" between the doublet) was such that these bands were not removed from the mixture spectrum.

Spectral subtraction would be useful if the following conditions were met:

1. standard MI-FT-IR spectra of the PAH's were available,
2. there were some prior knowledge of the composition of the sample,
3. absorbances were large enough to give a S/N ratio in the difference spectrum adequate for peak identification, and
4. peak features of overlapping compounds were sufficiently different.

With the ultramicrosampling system, several PAH's gave peak absorbances greater than 0.01 for sample sizes less than 1.0 μg. Spectral subtraction would be feasible on real mixtures of PAH which are often present at these levels.

C. Quantitative Studies

The utility of MI-FT-IR spectroscopy for quantitative determinations of PAH's was investigated with regard to adherence to Beer's law, linear dynamic range, precision, and detection limits. The three sampling systems — general, micro, and ultramicro — were studied.

To establish the linear working range, plots of absorbance versus quantity of PAH were obtained. The first attempts to generate these plots were done by weighing solid samples and using the general sampling system. The linear dynamic range was approximately one order of magnitude (0.1 mg - 1.0 mg), but problems with sample transfer, weighing, and loading severely limited the reliability of these results.

Using the closed Knudsen cell, the microsampling system, and samples from standard solutions, linear relationships were obtained over almost two decades of sample size.[90] A linear range was obtained from 2 to 50 μg for anthracene. Above 50 μg, using the microsampling system, the plots showed a negative deviation. This was interpreted to indicate that at large PAH concentrations, the large amount of sample present inhibits good isolation. Solute-solute interactions and aggregation were prevalent, resulting in wide bandwidths. This diminishes intensity and causes a flattening of the curve. This was not considered a serious problem, however, since detection of high (above 50 μg) PAH

levels was not an objective of this study. In fact, it is at low concentrations where the utility of this method for environmental samples would lie. The ultramicrosampling system provided the means to extend the working range of this method to a more realistic level.

Beer's law plots for five compounds using the ultramicro system are shown in Figures 32-35. Linear relationships for these compounds were noted over a range of one to two decades. It was found during the establishment of these curves that changing the interferometer's beamsplitter in order to perform other experiments or changing other instrumental alignments could adversely affect the reproducibility of the results. It was essential that the complete calibration curve be completed at one set of instrumental conditions. Because of this and because of the long time necessary to get these relationships (3 to 7 days), standard addition would be the method to use for quantitative work. Once a linear relationship was established, standard addition could be employed for quantitative work. To generate a new calibration curve for each compound each time it was analyzed would be prohibitively time-consuming. The working curves were useful, however, since they did establish the linear range and gave the investigator some indication of the approximate concentration of a PAH. This was helpful in choosing the proper amounts for spiking of an unknown sample concentration.

As with the microsampling system, the higher end of the useful range was determined by where sample interaction affected isolation. Depending on the compound, this occurred from 2 to 10 μg.

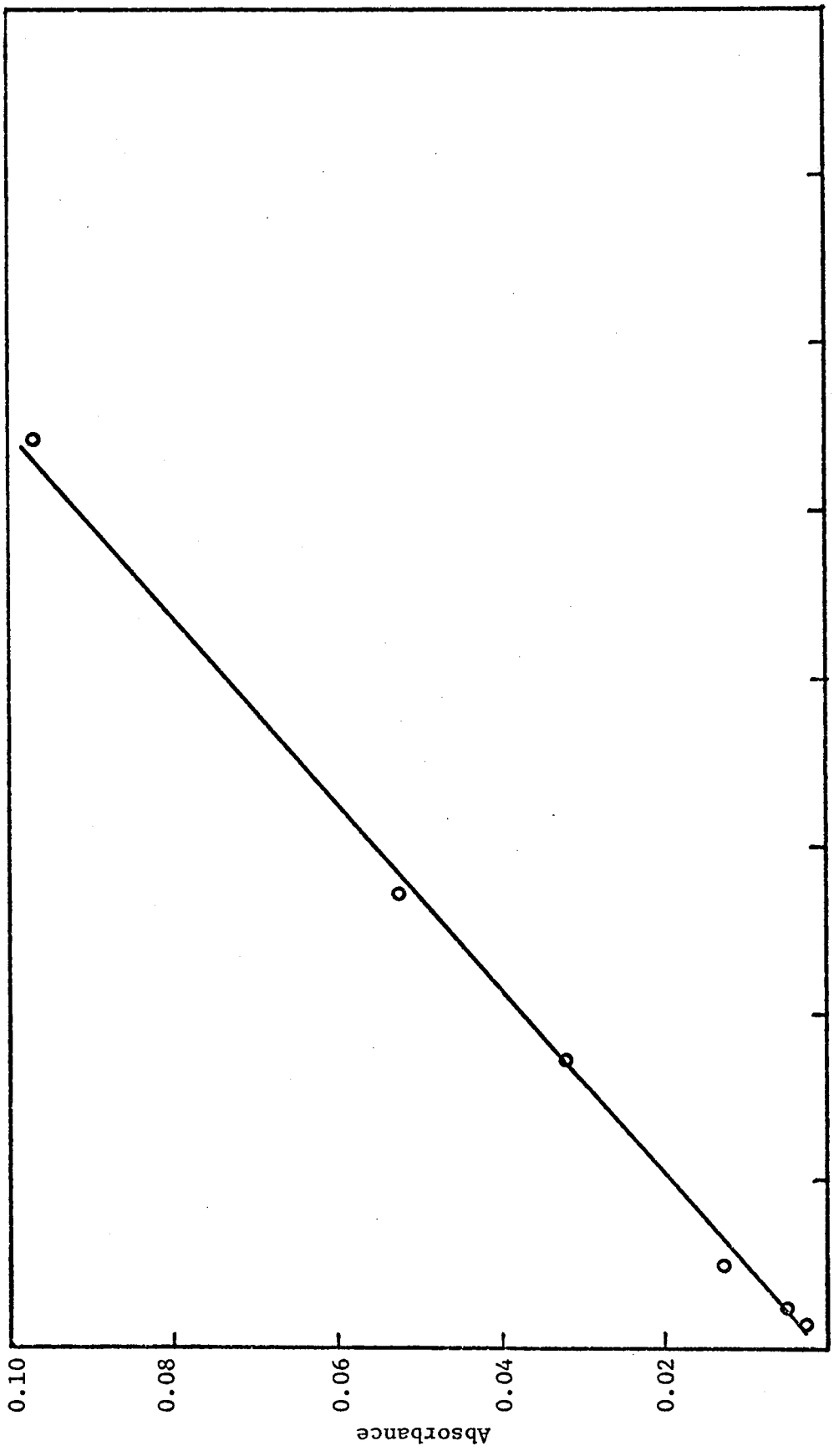


Figure 32. Beer's law plot for the 753 cm^{-1} band of benzo[e]pyrene.

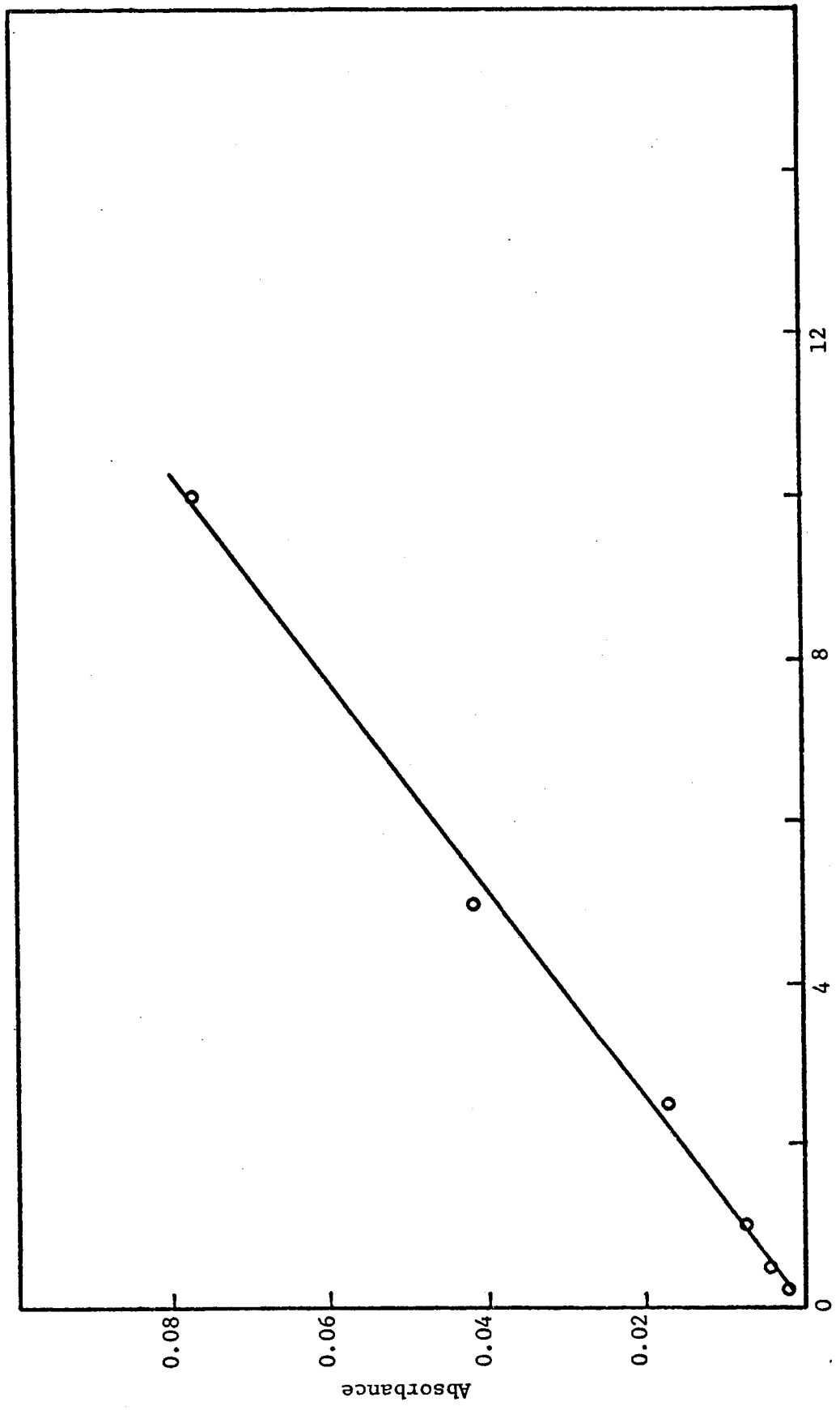


Figure 33. Beer's law plot for the 846 cm^{-1} band of pyrene.

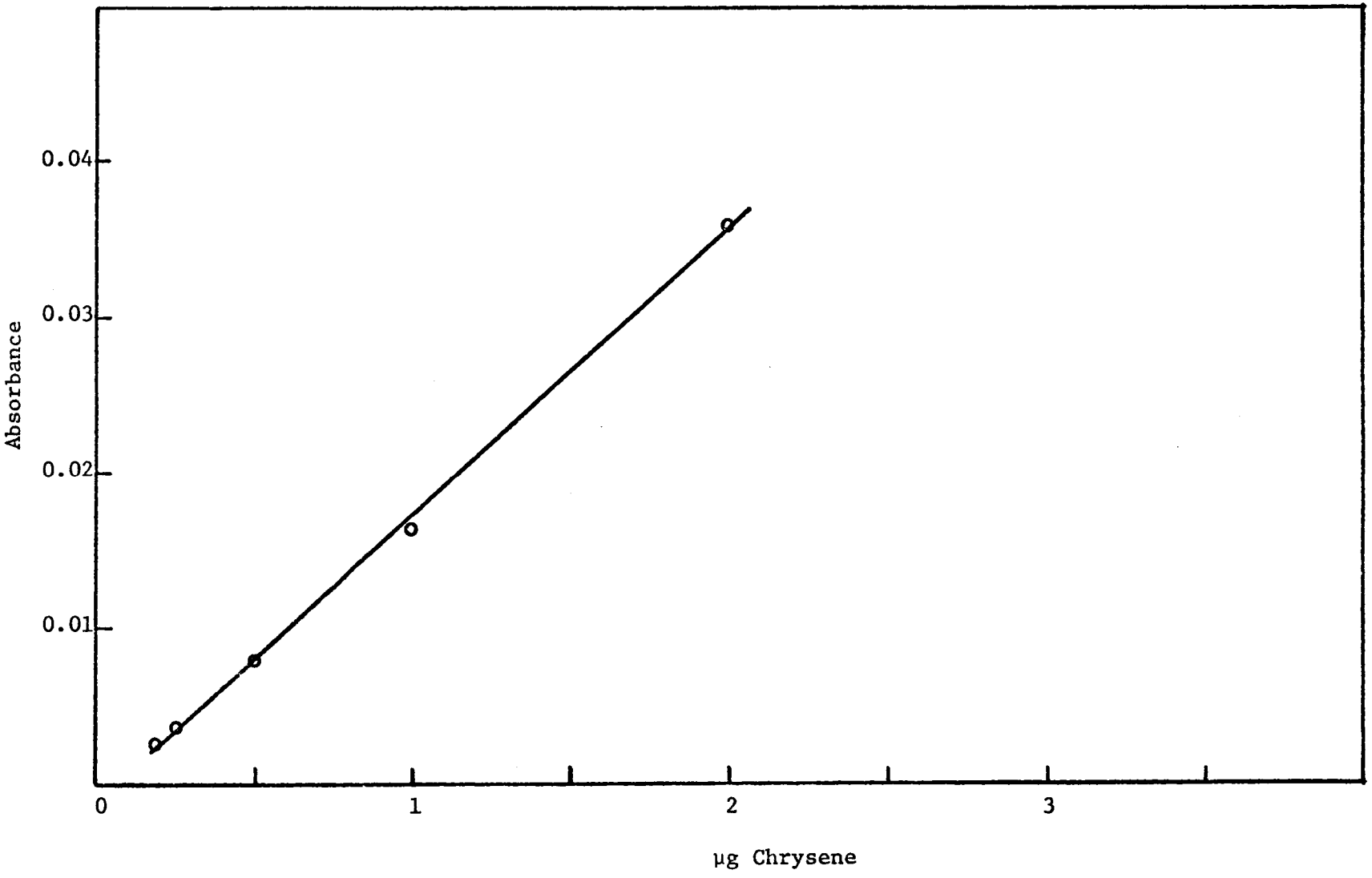


Figure 34. Beer's law plot for the 764 cm^{-1} band of chrysene.

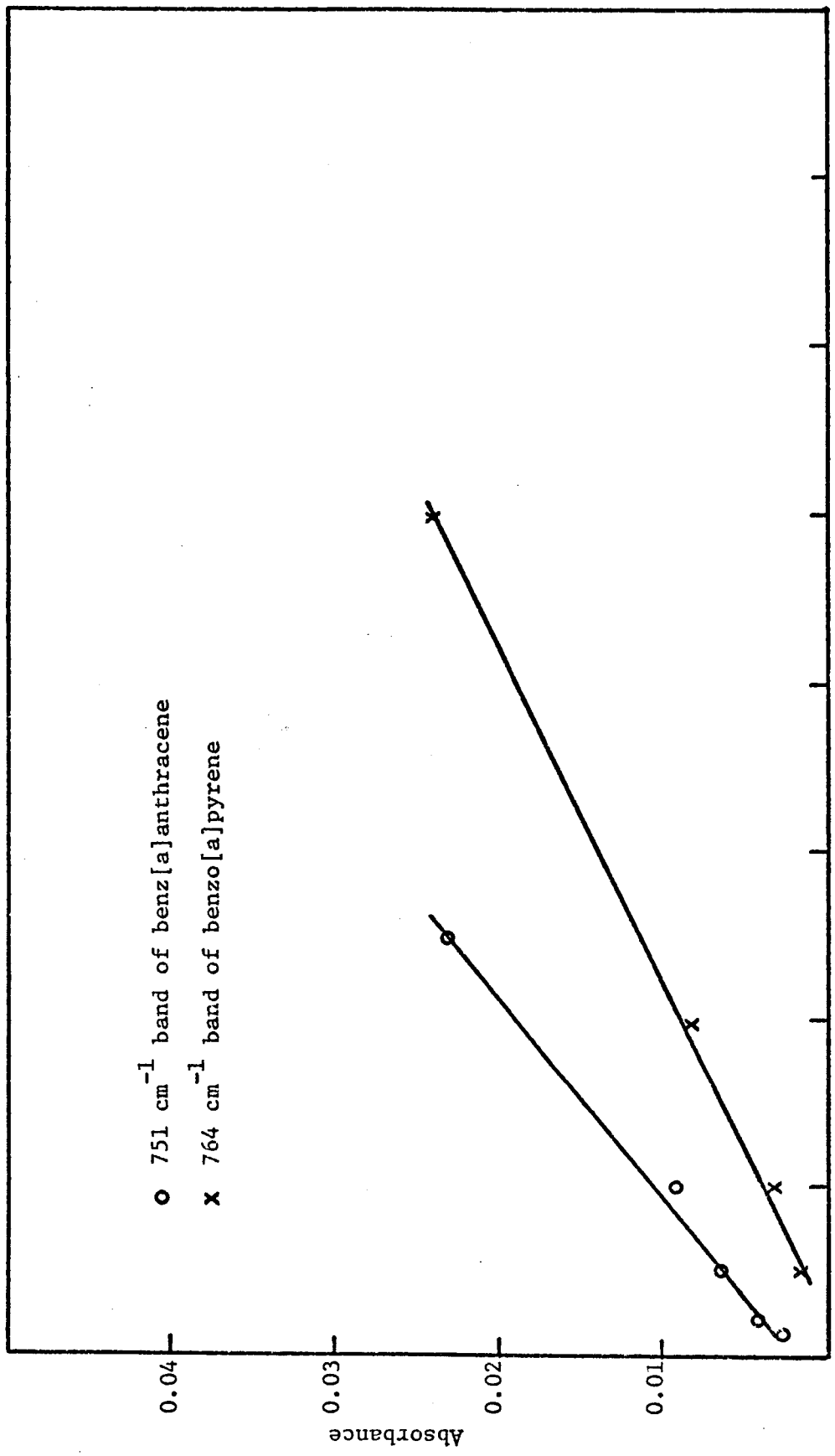


Figure 35. Beer's law plots for benz[a]anthracene and benzo[a]pyrene.

Using the microsampling system, Beer's law plots were obtained for benzo[e]pyrene and pyrene from 10 to 50 μg. If necessary, the combination of the two systems could be employed over a range of approximately three decades.

The detection limits for six PAH's are shown in Table IX. The detection limit is defined as an absorbance of approximately 0.0017 which gave a S/N ratio of 2 for coaddition of 1000 scans collected at a resolution of 1.0 cm^{-1}.

The best detection limit obtained was 50 ng (1.9×10^{-10} moles) for perylene. This is approximately 10 times lower than that for perylene using the microsampling system.[90] This is similar to the lowest detection limit reported for FT-IR.[67] Detection limits for all compounds compared were from five to ten times better by ultramicrosampling. The best detection using the general system was 100 μg for phenanthrene and anthracene.

The reproducibilities of MI-FT-IR absorptions were evaluated from the three sampling systems. As with Beer's law plots, precision by the general system was very poor due to inadequate weighing capabilities for solid samples and collection efficiencies.

Precision for a 5 μg sample of pyrene was determined using the microsampling system. Peak height absorbance and integrated area were compared. The software contained an area calculation based on:[91]

$$I(K) = \Delta\nu/100 \sum_{i=i_o}^{K} \left[D(i) - (TLT + CUR * \nu(i))\right] , \qquad (14)$$

where I(K) = outputted integrated point,

$\Delta\nu$ = the frequency per disk point (frequency between two adjacent points),

TABLE IX

DETECTION LIMITS FOR SIX PAH'S

PAH	Detection Limit
Benzo[e]pyrene	100 ng
Benzo[a]pyrene	500 ng
Perylene	50 ng
Pyrene	200 ng
Chrysene	100 ng
Benz[a]anthracene	200 ng

$\nu(i)$ = the frequency of the disk point D(i), and

i_o = the disk point corresponding to the starting point.

TLT and CUR corrected the absorbance spectrum to a zero absorbance baseline and any sloping baselines. The operator must supply the spectral range. It was hoped that this would compensate for differences in isolation and bandwidths. Peak heights were measured by the baseline method.[92]

Seven different deposits for which both peak heights and integrated absorbance were calculated are shown in Table X. To insure that the whole peak was included, integration was performed over approximately 10 cm^{-1}. The choice of the region over which to integrate was critical to good results, since noise contributed significantly to the area value. Results of this comparison showed little advantage of one method over the other with regard to precision. Integrated area showed only a slight improvement (1% in the relative standard deviation), which was not considered significant. The additional time required to calculate integrated areas was a disadvantage. Personal judgement was necessary with both methods, i.e., drawing baselines for peak height determinations or estimating starting and ending points for area calculations. Using different starting values for area calculations resulted in relative standard deviations which varied as much as 3%.

A major consideration in choosing the absorbance method to be used was its utility in mixtures. As has been seen, peak overlapping can be expected in mixtures of PAH's. Peaks that are not baseline resolved can be accurately identified. The use of integration to quantify compounds in mixtures would be extremely difficult since the shapes of the

TABLE X

COMPARISON OF PEAK HEIGHT AND INTEGRATED AREA METHODS FOR QUANTITATIVE DETERMINATIONS[a]

Sample Number	Peak Height Absorbance[b]	Integrated Area[c]
1	0.0143	0.0735
2	0.0136	0.0812
3	0.0087	0.0600
4	0.0114	0.0654
5	0.0115	0.0666
6	0.0108	0.0494
7	0.0110	0.0665
	RSD[d] = 16.0%	RSD[d] = 15.1%

[a]Five μg samples of pyrene, matrix/sample mole ratio $\sim 10^5$.

[b]846 cm^{-1} band of pyrene.

[c]Area over which integration was performed was from 854 to 843 cm^{-1}.

[d]Relative standard deviation.

peaks would not be certain. The base of the peak for establishing integration limits would be unknown. Peak heights can readily be measured in complex mixtures. Considering all factors, peak height absorbance measurements were adopted as the method of choice for this study.

The main source of error in this reproducibility study was undoubtedly the varying FT-IR instrumental conditions under which these data were obtained. These deposits were used to explore a number of other variables (such as resolution, zero-filling, annealing, band areas) which prolonged the data accumulation over several weeks. Considering the number of instrumental modifications (mainly beamsplitter changes) made during this period, this reproducibility was considered acceptable.

Annealing studies were done on nine different 5 μg samples of pyrene to determine whether this technique would improve precision and reduce band splitting. The deposits were annealed at 25 K for 30 minutes to allow limited diffusion of the N_2 matrix. It was hoped that this would reduce alternate trapping sites and possibly improve quantitative reproducibility. At that time, the nature of the band splitting was unknown.

Inspection of spectra after annealing showed very little improvement in the appearance of the spectra. Relative intensities of split bands changed in some samples but not in others. Splitting was never significantly reduced by annealing. Precision for nine pyrene sample absorbances at 846 cm^{-1} did show improvement due to annealing, as seen in Table XI. These results indicated that annealing might have some analytical utility for this study.

However, annealing effects proved to be complex and unpredictable from sample to sample. Additional splitting of bands would sometimes be

TABLE XI

EFFECT OF ANNEALING ON THE ABSORBANCE OF THE 846 CM^{-1} BAND OF PYRENE

Sample Number	Absorbance[a]	
	Without Annealing	With Annealing[b]
1	0.0143	0.0123
2	0.0136	0.0089
3	0.0108	0.0104
4	0.0087	0.0104
5	0.0114	0.0119
6	0.0115	0.0097
7	0.0108	0.0095
8	0.0110	0.0104
9	0.0098	0.0103
	RSD[c] = 15.3%	RSD[c] = 10.4%

[a]Matrix/sample mole ratio approximately 10^5.

[b]Thirty minutes at 25 K.

[c]Relative standard deviation.

observed which resulted in an overall spectral quality degradation. The temperature controller and cryostat heater frequently malfunctioned, making well-controlled annealing very difficult.

Because annealing was very time-consuming (at least an additional 30 minutes) and the benefits to be gained were few, if any, it was eventually eliminated from the sample preparation scheme.

Precision for the ultramicro system was determined using perylene (Table XII). A 100 ng sample had a precision of 5%; precision for a 1 µg sample was 9%. This is a significant improvement over the microsampling system, which indicates that the poor deposition efficiency (50%) was an important factor in the poorer reproducibility obtained. The sources of error in ultramicrosampling were evaporation of solvent, different alignments of the Knudsen cell in relation to the window spot, and distance of the oven from the window. The greatest contribution to the error was thought to be the oven distance, as some samples were noticed to spray onto the teflon mask when the distance was too large. Precision for some PAH's may also be dependent on the sample size. As Stroupe *et al.*[93] noted in their fluorescence studies, at low levels (1-10 ng region) some PAH's under these conditions vaporize without heating. The amounts lost due to premature vaporization, however, should have little effect on the precision for these compounds. PAH consisting of three or fewer rings would require a coolable cell for accurate work at sub-µg levels. Reproducibility for two other selected points from the Beer's law plots shown in Figure 35 (p 93) gave relative standard deviations of 9.1% for 0.5 µg benz[a]anthracene and 12.5% for 1 µg benzo[a]pyrene (based on four samples each).

TABLE XII

PRECISION USING THE ULTRAMICROSAMPLING SYSTEM

Sample Number	Absorbance[a]	
	100 ng[b]	1 µg[c]
1	0.0048	0.0326
2	0.0045	0.0330
3	0.0044	0.0363
4	0.0043	0.0350
5	0.0042	0.0420
	RSD[d] = 5.2%	RSD[d] = 8.8%

[a] 774 cm^{-1} band of perylene.

[b] Matrix/sample mole ratio approximately 10^6.

[c] Matrix/sample mole ratio approximately 10^5.

[d] Relative standard deviation.

The quantitative determinations of several PAH's in mixtures were done by standard addition. Chrysene and benzo[a]pyrene in the NBS standard were determined to be present at 25 ppm each.

Using the 841 cm^{-1} band of benzo[a]pyrene and the 814 cm^{-1} band of chrysene, linear plots were obtained using two standard additions. The error in these determinations was estimated at $\pm$ 2 ppm. The accepted NBS values were 23.2 ppm for chrysene and 20.4 ppm for benzo[a]pyrene.

D. Comparison with Conventional Sampling Techniques

This study has demonstrated that matrix isolation Fourier transform infrared spectroscopy is superior in several regards to conventional IR sampling techniques. Maximum half-bandwidths for MI-FT-IR spectra are narrower than those attainable by conventional sample preparation.[54] Narrower bands are primarily a function of the small (sub-μg) PAH concentrations and subsequent high matrix to sample mole ratios that can be achieved by matrix isolation. Consequently, more complex mixtures can be analyzed by MI-FT-IR.

The sensitivities of MI-FT-IR surpass those that were obtained in KBr, CS_2, and attenuated total reflectance (ATR) using FT-IR. For pyrene, which was run by both methods, the increase in sensitivity was from 10-35 times better depending on the preparation method.[54] Comparison with work done using a grating IR instrument and beam condensing optics[53] showed enhancements of 5-30 times in the detection limits by MI-FT-IR depending on the compound. Precision for the different methods was comparable.

MI-FT-IR can be utilized over a much wider concentration range than KBr pellets, ATR, or liquid solution using FT-IR.[54] Using one sampling system, the linear dynamic range for the matrix isolation method was comparable to the standard preparation methods (1-1.5 decades). However, with the different sampling arrangements, concentrations of PAH over three decades can be analyzed by MI.

As expected, the position, number, and relative strengths of MI absorption bands were different from those obtained by standard preparation techniques (Table XIII). These differences make it very difficult to utilize existing IR data for the identification of unknown MI-FT-IR peaks. If the presently available data on PAH's obtained in KBr pellets [53,54,92] could be adapted to MI frequencies, the accumulation of a large MI library would not be necessary. Comparison of MI-FT-IR absorption bands with those obtained in KBr yielded the following conclusions:

1. there is no one single factor which can be added to or subtracted from MI bands to correct them to KBr frequencies,
2. the difference between the absorption band positions is frequency-dependent with larger discrepancies between MI and KBr at lower frequencies (900 cm^{-1} or less), and
3. as a result of the frequency dependence, the difference between two spectral bands of the same compound would not be indicative of that compound.

Matrix splitting of absorption bands in MI spectra also complicates identification of a specific PAH without prior documentation of this phenomenon. Without a comprehensive library of MI spectra, unambiguous

TABLE XIII

FT-IR ABSORPTION BAND POSITIONS FOR N_2 AND KBr[a] MATRICES

Pyrene		Anthracene		Phenanthrene	
N_2 cm^{-1}	KBr cm^{-1}	N_2 cm^{-1}	KBr cm^{-1}	N_2 cm^{-1}	KBr cm^{-1}
1436	1434	1451	1449	1462	N[b]
1314	1313	1318	1323	N[b]	1455
1244	1242	N[b]	1273	1432	1429
1185	1185	1151	1148	1304	1302
846[c]	840[c]	1001	998	1249	1244
751	748	960	957	1042	1038
715	709	881	884	1004	999
		733[c]	727[c]	954	948
		N[b]	738	N[b]	885
		N[b]	744	870	872
		603	602	818	819
				740[c]	732[c]
				713	715
				617	617

[a]Source: H. O. Brotherton, M.S. Thesis, The University of Tennessee, Knoxville, 1976.

[b]No comparable band.

[c]Strongest band.

identification of PAH's would be extremely difficult. Thus, with regard to the utilization of available IR data for PAH identification, conventional sample preparation would certainly appear to have an advantage.

The inability to use the large pool of PAH IR data that presently exists may not be as disadvantageous as it first seems. The positive identification of PAH's by MI-FT-IR is dependent on the very accurate determination of band positions. Undoubtedly, most of the IR information accumulated on PAH's has been with a number of different instruments, the majority being grating types. Without the computer-controlled plotting and the advantage of laser reference, the positions of PAH bands in these spectra are poor by comparison. The study by Boiteau et al.,[53] in fact, lists band positions only every five wavenumbers. This degree of accuracy would be inadequate for the determination of complex mixtures at very low PAH levels. Thus, it seems that even if the same matrix (KBr) were used, the differences in the frequencies obtained by FT-IR and a grating instrument would hamper the interchangeability of these data.

CHAPTER IV

SUMMARY

Matrix isolation Fourier transform infrared spectroscopy has been shown to overcome many if not all of the problems which have precluded the use of infrared spectroscopy for the analysis of polycyclic aromatic hydrocarbons. Trapping of PAH's in a low temperature (15 K) inert matrix minimizes solute-solute interactions and freezes out rotational contributions to absorption bands. Consequently, infrared absorption bands of PAH's were narrow (1-3 cm^{-1}) at high matrix to PAH mole ratios, which facilitated the resolution of a spectrum of complex mixtures. Mixtures of up to ten PAH's can be resolved by MI-FT-IR. Where overlapping absorption bands did inhibit compound identification, spectral subtraction proved valuable. Very similar IR absorption bands were identified by spectral subtraction. Use of a rare gas or nitrogen matrix provided a vibrationally transparent matrix over a wide spectral range.

The increased sensitivity of MI-FT-IR has extended the analytical range of infrared spectroscopy to include concentration levels comparable to those of PAH's found in environmental samples. Detection limits as low as 50 ng (2×10^{-10} moles of perylene) have been obtained. The analytical sensitivity of MI-FT-IR was less than that of GC-MS or fluorescence, but the improvements place infrared's capabilities well within the realm of real samples.

Linear relationships between band strength and PAH quantity were established for several PAH's over one to two decades. The low end

of the linear range was determined by the detection limit. Deviations from linearity at high sample concentrations were due to increased solute-solute interactions.

MI-FT-IR offers several advantages over other detection methods commonly used for PAH analysis. Isomers have very different vibrational spectra, which make their resolution an easy task. Mixtures of several isomers were easily resolved by MI-FT-IR. Mass spectrometry does not have the capability to distinguish between PAH isomers. Unlike fluorescence and UV spectroscopy, IR is universal in that compounds other than PAH's can be analyzed. While MI-FT-IR may not be as powerful a tool as mass spectrometry for structural analysis, identification and analysis of many materials is possible.

The Knudsen cell concept of sample preparation by vaporization was shown to have inherent advantages for PAH analysis. The PAH's investigated in this study were grouped by vaporization temperature to form thermal fractions. Separation of PAH's by differential heating was determined to be feasible in this study. PAH's contained in solid samples could possibly be analyzed by direct vaporization.

The MI-FT-IR method developed in this study was not without its drawbacks. The successful implementation of MI-FT-IR was dependent upon continued operation of a variety of complex instrumentation. With this type of system, equipment failures (major and minor) were inevitable. For routine analysis, the reliability of the instrumentation would be crucial. Though the mechanics of an MI experiment could be mastered with time, the instrumental failures were not so easily remedied.

A problem which is related to equipment failures is the less than 100% success rate for an MI experiment. The number of parameters which dictated a "good" run were many, and the failure rate was probably as high as 30%. This has serious consequences for this method's use in routine analysis. In addition, a maximum of only two samples could be examined in an eight-hour day. Cool-down time for the cryostat was 1-1 1/2 hrs., deposition time was 1 hr., collection time was 1 1/2 hr. at a resolution of 1.0 cm^{-1}, and computation took 15 minutes. Time between runs for sample preparation and cleaning was 15-30 minutes.

The cost of the MI-FT-IR instrumentation could be prohibitive ($10,000 for a cryostat and $60,000 or more for the FT-IR spectrometer) for the routine analytical laboratory. However, with the growing market for FT-IR spectrometers because of their multiple applications, they, like mass spectrometers, may well become standard equipment for analytical laboratories in the near future.

Despite some drawbacks, the results of this study have shown that MI-FT-IR can be of significant utility for the analysis of PAH's. The capabilities of MI-FT-IR demonstrated warrant that this method be further investigated to expand the scope of its applicability. In particular, the potential of thermal fractionation should be explored with synthetic mixtures and real samples (i.e. unchromatographed oils and/or particulate extracts). Alkyl-substituted PAH's comprise an important part of the PAH family of compounds. The capability of MI-FT-IR to distinguish between these derivatives needs to be established. Since N-heterocycles are major constituents in synthetic liquid fuels and shale oil, more consideration should be given to this group of compounds in the future. A cryogenic cell for ultramicrosampling needs to be

developed for use with volatile PAH's and other lower boiling organics to complete the technique's sampling capabilities. The potential of MI-FT-IR to simultaneously determine polycyclic aromatic hydrocarbons and other sample constituents present in trace amounts in complex environmental samples is also an important aspect to be further investigated.

LIST OF REFERENCES

LIST OF REFERENCES

1. Division of Medical Science, National Research Council, "Particulate Polycyclic Organic Matter," 1972.

2. W. Giger and M. Blumer, Anal. Chem., 12, 1663 (1974).

3. M. Zander, Intern. J. Environ. Anal. Chem., 4, 111 (1972).

4. G. M. Badger in "Analysis of Carcinogenic Air Pollutants," E. Sawicki and K. Cassell, Jr., eds., Nat. Cancer Inst. Monogr. No. 9, U. S. Dept. of Health, Education, and Welfare, 1962.

5. C. R. Begeman and J. M. Colucci, Soc. Automot. Eng. paper 700469, 1970.

6. C. R. Begeman and J. M. Colucci, Science, 161, 271 (1968).

7. A. Candeli, G. Morozzi, A. Paolacci, and L. Zoccolillo, Atmos. Environ., 9, 843 (1975).

8. M. E. Snook, J. Natl. Cancer Inst., 57, 191 (1976).

9. M. E. Snook, W. J. Chamberlain, R. F. Severson, and O. T. Chortyk, Anal. Chem., 47, 1155 (1975).

10. D. Hoffmann and E. L. Wynder in "Air Pollution," Vol. II, Arthur Stern, ed., Academic Press, New York, N. Y., 1968, pp. 210-211.

11. N. H. Ketcham and R. W. Norton, Arch. Environ. Health, 1, 194 (1960).

12. G. Goldstein, J. Chromatogr., 129, 61 (1976).

13. D. M. Jerina and J. W. Daley, Science, 185, 573 (1974).

14. B. Weinstein, A. M. Jeffrey, K. W. Jennette, S. H. Blobstein, R. G. Harvey, C. Harris, H. Autrup, H. Kasai, K. Nakanishi, Science, 193, 593 (1976).

15. D. L. Whalen and A. M. Ross, J. Am. Chem. Soc., 96, 6814 (1974).

16. N. Nelson in "Inhalation Carcinogenesis," M. G. Hanna, Jr., P. Nettesheim, and J. R. Gilbert, eds., U. S. Atomic Energy Commission, 1970.

17. R. C. Lao, R. S. Thomas, and J. L. Monkman, J. Chromatogr., 112, 681 (1975).

18. J. M. Colucci and C. R. Begemann, Environ. Sci. Technol., 5, 145 (1975).

19. R. C. Pierce and M. Katz, Anal. Chem., 47, 1743 (1975).

20. J. F. Thomas, M. Mukai, and B. D. Tebbens, Environ. Sci. Technol., 2, 33 (1968).

21. E. Sawicki and K. Cassel, Jr., eds.,"Analysis of Carcinogenic Air Pollutants," Nat. Cancer Inst. Monogr., No. 9, U. S. Dept. of Health, Education, and Welfare, 1962.

22. E. Sawicki, Crit. Rev. Anal. Chem., 1, 275 (1970).

23. E. Sawicki, T. W. Stanley, W. C. Elbert, J. Mesker, and S. McPherson, Atmos. Environ., 1, 131 (1967).

24. T. W. Stanley, J. E. Meeker, and M. J. Morgan, Environ. Sci. Technol., 1, 927 (1967).

25. F. A. Gunther and F. Buzzetti, Residue Rev., 9, 90 (1965).

26. E. Hluchán, M. Jenik, and E. Malý, J. Chromatogr., 91, 531 (1974).

27. M. L. Lee, K. D. Bartle, and M. V. Novotny, Anal. Chem., 47, 540 (1975).

28. M. Novotny and R. Farlow, J. Chromatogr., 103, 1 (1975).

29. L. E. Stomberg and G. Widmark, J. Chromatogr., 47, 27 (1970).

30. C. A. Streuli, J. Chromatogr., 56, 219 (1971).

31. J. Frycka, J. Chromatogr., 65, 341, 432 (1972).

32. C. G. Vaughan, B. B. Sheals, and M. J. Whitehouse, J. Chromatogr., 78, 203 (1973).

33. M. A. Fox and S. W. Staley, Anal. Chem., 48, 992 (1976).

34. J. A. Schmidt, R. A. Henry, R. C. Williams, and J. F. Dieckman, J. Chromatogr. Sci., 9, 645 (1971).

35. M. Novotny, M. L. Lee, and K. D. Bartle, J. Chromatogr. Sci., 12, 606 (1974).

36. J. F. Coetzee, G. H. Kazi, and J. C. Spurgeon, Anal. Chem., 48, 2170 (1976).

37. A. P. D'Silva, G. J. Oestreich, and V. A. Fassel, Anal. Chem., 48, 915 (1976).

38. M. L. Lee, M. Novotny, and K. D. Bartle, Anal. Chem., 48, 1566 (1976).

39. E. Clar, "Polycyclic Hydrocarbons," Vols. I and II, Academic Press, New York, N. Y., 1964.

40. P. Wedgwood and R. L. Cooper, Chem. Ind., 1066 (1951).

41. E. Sawicki, Health Lab. Sci., 7 (suppl.), 31 and 45 (1970).

42. A. M. Krstulovic, D. M. Rosie, and P. R. Brown, Anal. Chem., 48, 1383 (1976).

43. H. Boden, J. Chromatogr. Sci., 14, 391 (1976).

44. E. Sawicki, Talanta, 16, 123 (1969).

45. G. Heinrich and H. Güsten, Z. Anal. Chem., 278, 257 (1976).

46. R. C. Lao, R. S. Thomas, H. Oja, and L. Dubois, Anal. Chem., 45, 908 (1973).

47. W. Cautreals and K. Van Cauwenberghe, Atmos. Environ., 10, 447 (1976).

48. J. L. Monkman, Annual Report, International Bank of Polycyclic Aromatic Hydrocarbons, Ottawa, Canada (1973).

49. G. Svehla ed., "Comprehensive Analytical Chemistry," Vol. VI, Analytical Infrared Spectroscopy," Elsevier Scientific Publishing Co., New York, N. Y. 1976.

50. C. G. Cannon and G. B. B. M. Sutherland, Spectrochim. Acta, 4, 373 (1951).

51. J. M. Hume and G. I. Jenkins, Appl. Spectrosc., 18, 161 (1964).

52. P. C. Szap and W. R. Utynok, Appl. Spectrosc., 18, 186 (1964).

53. H. L. Boiteau, M. Robin, and S. Gelot, J. Eur. Toxicol., 5, 293 (1972).

54. H. O. Brotherton, M. S. Thesis, The University of Tennessee, Knoxville, Tennessee, 1976.

55. A. A. Michelson, Philos. Mag., 34, 280 (1892).

56. P. Griffiths, Anal. Chem., 46, 645A (1974).

57. J. Cuthbert, J. Phys. E., 7, 328 (1974).

58. M. J. D. Low, Anal. Chem., 41, 97A (1969).

59. J. Bates, Science, 191, 31 (1976).

60. R. J. Bell, "Introductory Fourier Transform Spectroscopy," Academic Press, New York, N. Y., 1972, pp. 23-25.

61. P. R. Griffiths in "Chemical Analysis," Vol. 43, P. J. Elving, J. D. Winefordner, and I. M. Kolthoff, eds., Chemical Infrared Fourier Transform Spectroscopy, John Wiley and Sons, New York, N. Y., 1975, pp 9-23, 89-92.

62. G. Horlick, Appl. Spectrosc., 22, 617 (1968).

63. G. Horlick, Anal. Chem., 43, 61A (1971).

64. R. Ramirez, Electronics, 47, 96 (1975).

65. J. L. Koenig, Appl. Spectrosc., 29, 293 (1975).

66. P. R. Griffiths and F. Block, Appl. Spectrosc., 27, 432 (1973).

67. D. H. Anderson and T. H. Wilson, Anal. Chem., 47, 2482 (1975).

68. E. D. Becker and T. C. Farrar, Science, 178, 361 (1972).

69. J. L. Koenig, Am. Lab., 6, 9 (1974).

70. J. L. Koenig, FTS/IR Notes No. 20, DigiLab Inc., November 1975.

71. H. E. Hallam, ed., "Vibrational Spectroscopy of Trapped Species," John Wiley and Sons, London, 1973.

72. S. Craddock and A. J. Hinchcliffe, "Matrix Isolation," Cambridge University Press, Cambridge, 1975.

73. B. Meyer, "Low Temperature Spectroscopy," American Elsevier Publishing Co., New York, N. Y., 1971.

74. M. J. Linevsky, J. Chem. Phys., 34, 1956 (1961).

75. L. Bajema, M. Gouterman, and B. Meyer, J. of Mol. Spectrosc., 27, 225 (1968).

76. S. T. King, J. Phys. Chem., 74, 2133 (1970).

77. A. Snelson in "Vibrational Spectroscopy of Trapped Species," H. E. Hallam, ed., John Wiley and Sons, London, 1973, pp. 203-244.

78. J. L. Monkman, L. Dubois and C. J. Baker, Pure Appl. Chem., 24, 731 (1971).

79. G. C. Pimentel, J. Chem. Phys., 22, 1943 (1954).

80. A. J. Barnes and H. E. Hallam, Quart. Rev. Chem. Soc., 23, 392 (1969).

81. M. M. Rochkind, Spectrochim. Acta, 27A, 566 (1971).

82. A. Snelson, J. Phys. Chem., 70, 1919 (1969).

83. D. F. Ball and C. J. Purnell, Intern. J. Environ. Stud., 9, 131 (1976).

84. Operator's Manual, Spectrim™ Spectrometric Sample Conditioner, Cryogenic Technology, Inc., January, 1973.

85. N. B. Colthup, L. H. Daly, and S. E. Wiberley, "Introduction to Infrared and Raman Spectroscopy," Academic Press, New York, N. Y., 1964.

86. E. Knozinger, Angew. Chem., 15, 25 (1976).

87. W. D. Shults, ed., "Preliminary Results: Chemical and Biological Examination of Coal-Derived Materials," Oak Ridge National Laboratory, 1976.

88. G. Mamantov, E. L. Wehry, R. R. Kemmerer, E. R. Hinton, R. C. Stroupe, and G. Goldstein, "Characterization of Mixtures of Polycyclic Aromatic Hydrocarbons by Liquid Chromatography and Matrix Isolation Spectroscopy," abstract of paper presented at the 173rd ACS National Meeting, New Orleans, La., March, 1977.

89. T. Hirschfeld, Appl. Spectrosc., 30, 552 (1976).

90. G. Mamantov, E. L. Wehry, R. R. Kemmerer, and E. R. Hinton, Anal. Chem., 49, 86 (1977).

91. Digilab FTS® - IR System Operator Manual, 1975.

92. H. H. Willard, L. L. Merritt, and J. A. Dean, "Instrumental Methods of Analysis," 5th ed., D. Van Nostrand, Princeton, N. J., 1974, p 170.

93. R. C. Stroupe, E. L. Wehry, G. Mamantov, P. Toukousbalides, and R. B. Dickinson, Anal. Chem., in press.

APPENDIX

APPENDIX

Structures for the polycyclic aromatic hydrocarbons used in this study are shown in Table XIV. The carcinogenic properties of these compounds are denoted by the National Research Council (NRC) designations.[1]

Standard matrix isolation Fourier transform infrared spectra are presented in Figures 36-40. The spectral region shown, 1500-500 cm^{-1}, contained the characteristic absorption bands for the compounds studied.

Spectra of phenanthrene and benz[a]anthracene, shown in Figures 41 and 42, include the C-H stretching region, 3100-3000 cm^{-1}. These spectra are representative of all MI-FT-IR spectra of PAH's in that they contain few, if any, characteristic absorption bands above 1500 cm^{-1}.

The expanded region from 900-700 cm^{-1} for the standard spectra contained the strongest IR absorption bands (Figures 43-47). Maximum half-band widths at a nitrogen to PAH mole ratio of approximately 10^3 ranged from 4-8 cm^{-1}.

TABLE XIV

STRUCTURES OF POLYCYCLIC AROMATIC HYDROCARBONS

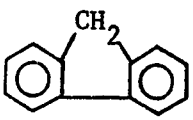
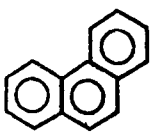
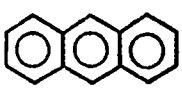
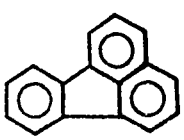
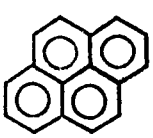
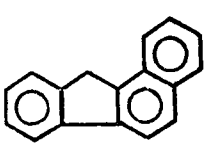
Compound	Empirical Formula	Structure	Carcinogen[a]
Acenaphthene	$C_{13}H_{10}$		-
Fluorene	$C_{13}H_{10}$		-
Phenanthrene	$C_{14}H_{10}$		-
Anthracene	$C_{14}H_{10}$		-
Fluoranthene	$C_{16}H_{10}$		-
Pyrene	$C_{16}H_{12}$		-
Benzo[a]fluorene (1,2-Benzfluorene)	$C_{17}H_{12}$		-

TABLE XIV (Continued)

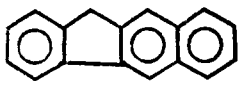
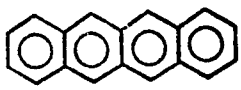
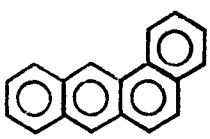
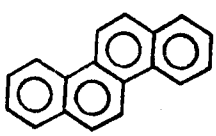
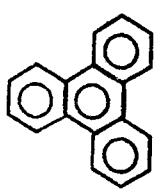
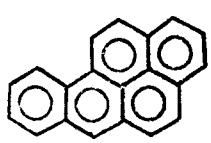
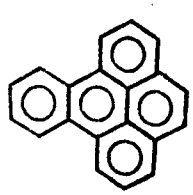
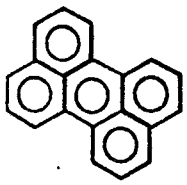
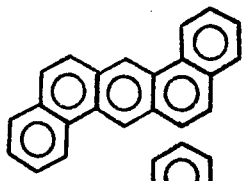
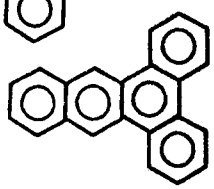
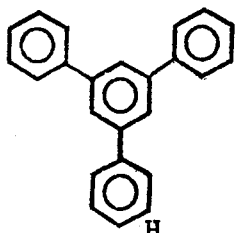
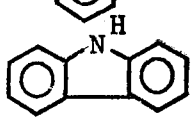
Compound	Empirical Formula	Structure	Carcinogen[a]
Benzo[b]fluorene	$C_{17}H_{12}$		-
Napthacene (Tetracene)	$C_{18}H_{12}$		-
Benz[a]anthracene (1,2-Benzanthracene)	$C_{18}H_{12}$		+
Chrysene	$C_{18}H_{12}$		±
Triphenylene (9,10-Benzphenanthrene)	$C_{18}H_{12}$		-
Benzo[a]pyrene (4,5-Benzpyrene)	$C_{20}H_{12}$		+++
Benzo[e]pyrene (1,2-Benzpyrene)	$C_{20}H_{12}$		-

TABLE XIV (Continued)

Compound	Empirical Formula	Structure	Carcinogen[a]
Perylene	$C_{20}H_{12}$		-
Dibenz[a,h]anthracene (1,2,5,6-Dibenzanthracene)	$C_{22}H_{14}$		++++
Dibenz[a,c]anthracene (1,2,3,4-Dibenzanthracene)	$C_{22}H_{14}$		+
1,3,5-Triphenylbenzene[b]	$C_{24}H_{18}$		-
Carbazole[b]	$C_{12}H_9N$		-

[a]NRC designation:[1] - not carcinogenic, ± uncertain or not carcinogenic, + carcinogenic, ++, +++, ++++ strongly carcinogenic.

[b]Not a PAH but often found in mixtures of PAH's in real samples.

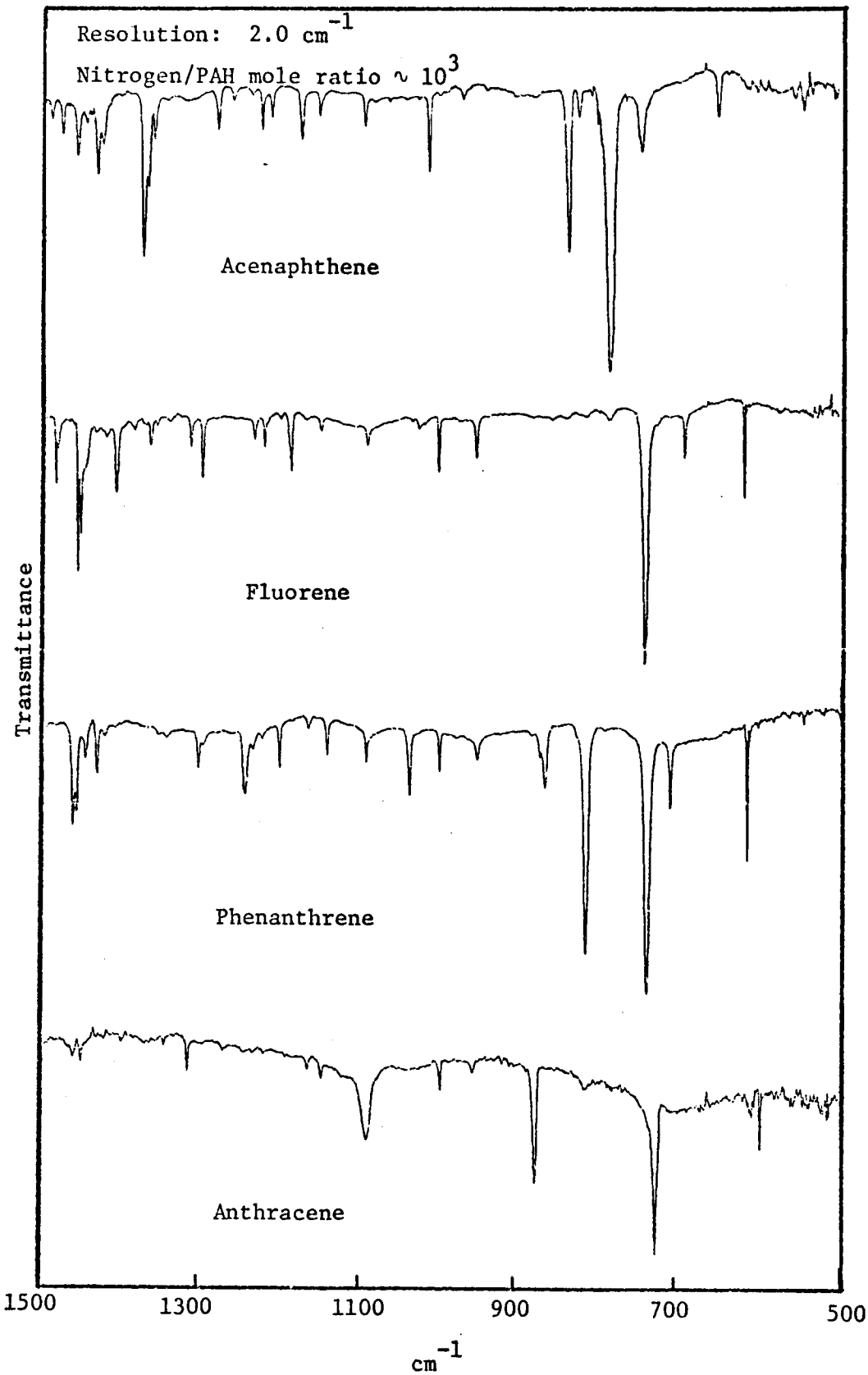


Figure 36. Transmittance MI-FT-IR spectra of acenaphthene, fluorene, phenanthrene, and anthracene.

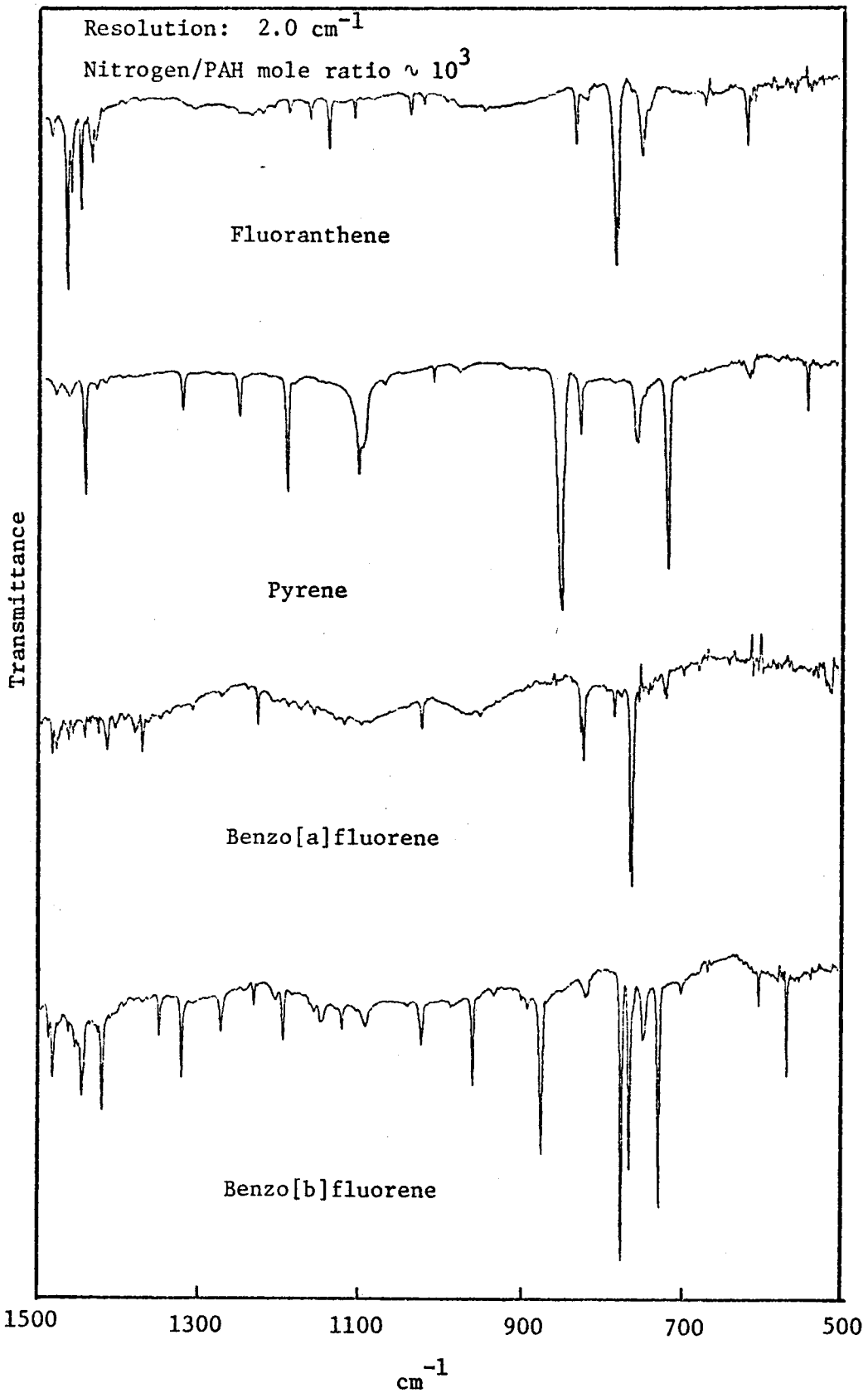


Figure 37. Transmittance MI-FT-IR spectra of fluoranthene, pyrene, benzo[a]fluorene, and benzo[b]fluorene.

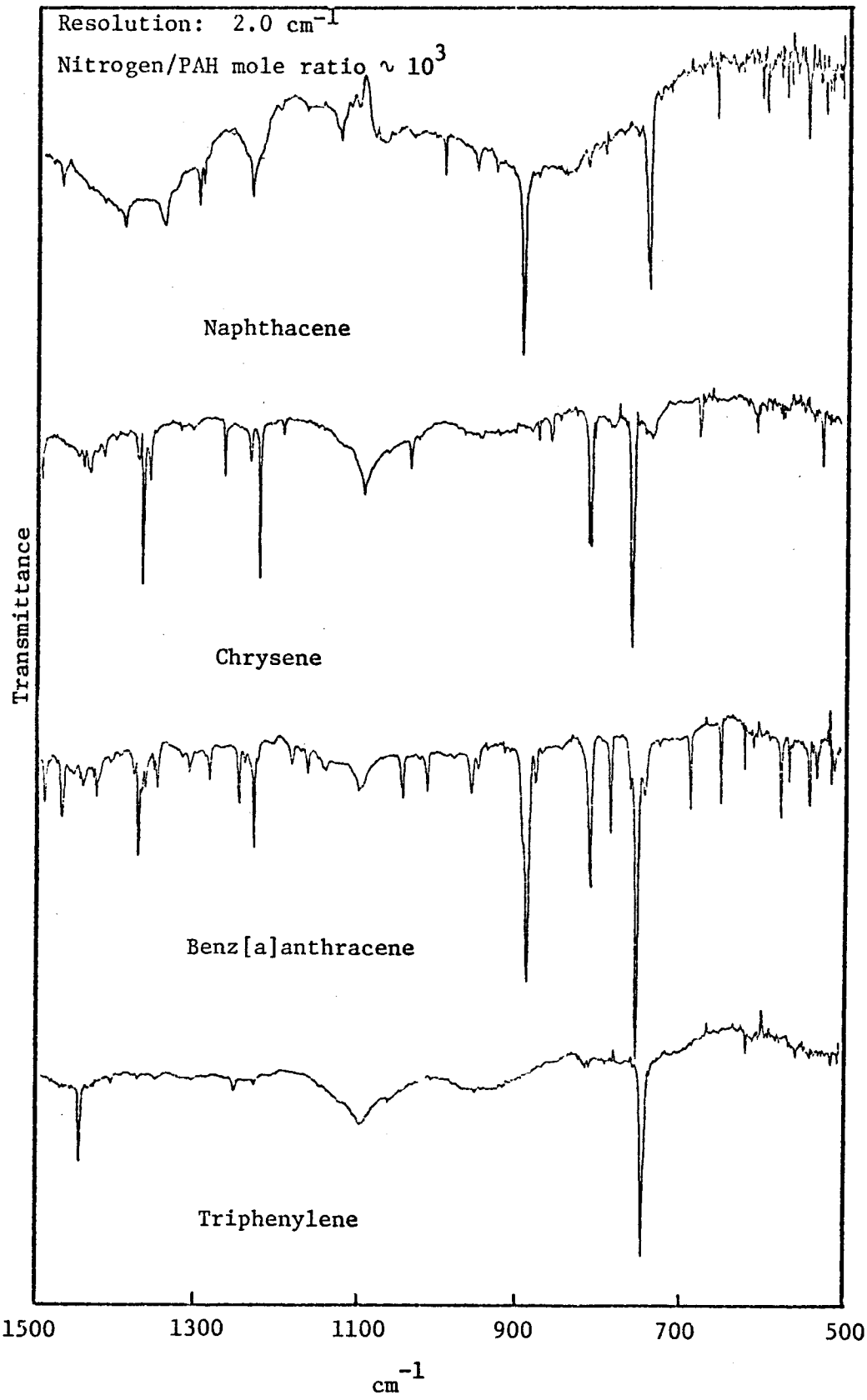


Figure 38. Transmittance MI-FT-IR spectra of naphthacene, chrysene, benz[a]anthracene, and triphenylene.

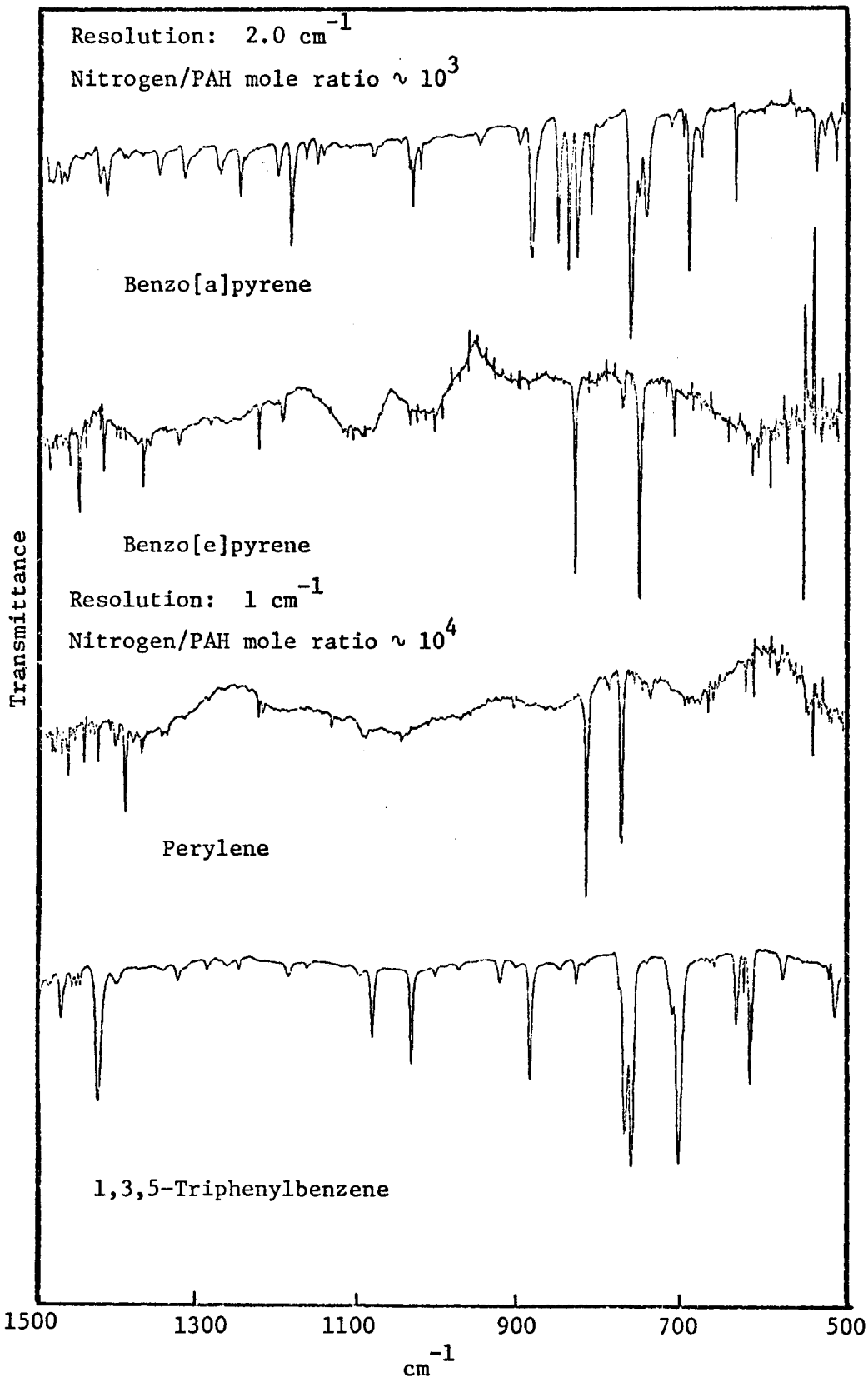


Figure 39. Transmittance MI-FT-IR spectra of benzo[a]pyrene, benzo[e]pyrene, perylene, and 1,3,5-triphenylbenzene.

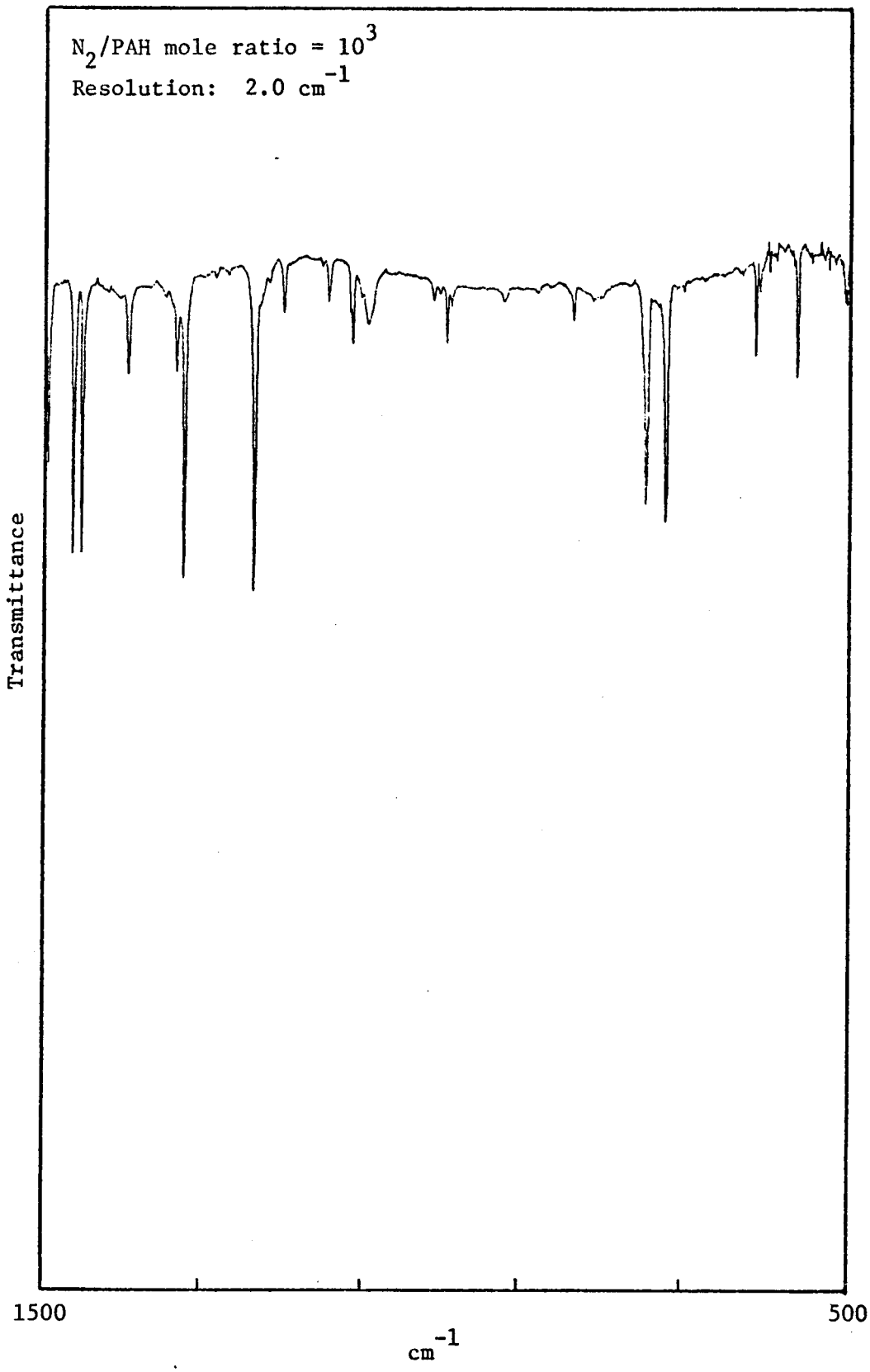


Figure 40. Transmittance MI-FT-IR spectrum of carbazole.

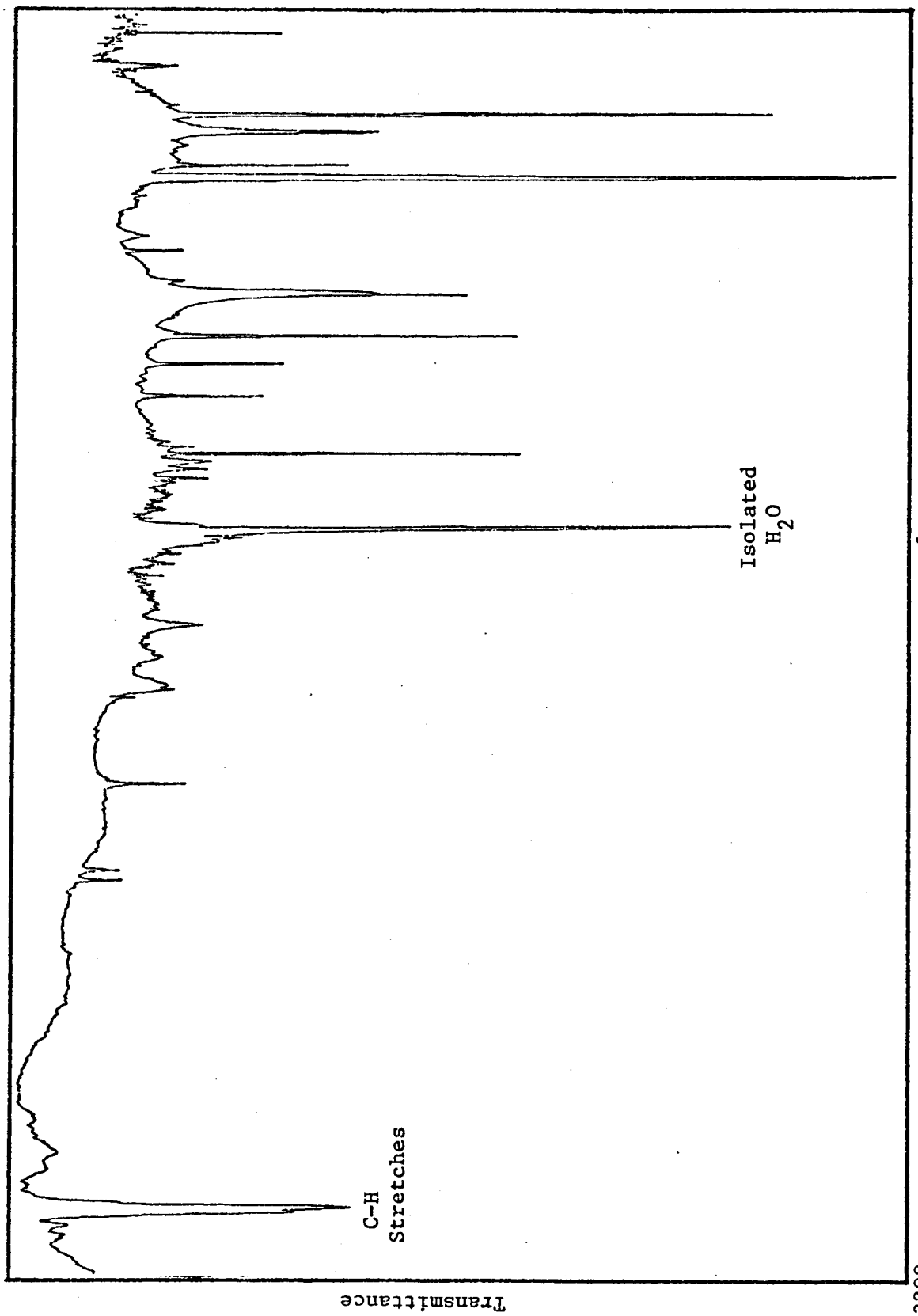


Figure 41. Transmittance spectrum of pyrene, 3200-500 cm^{-1}.

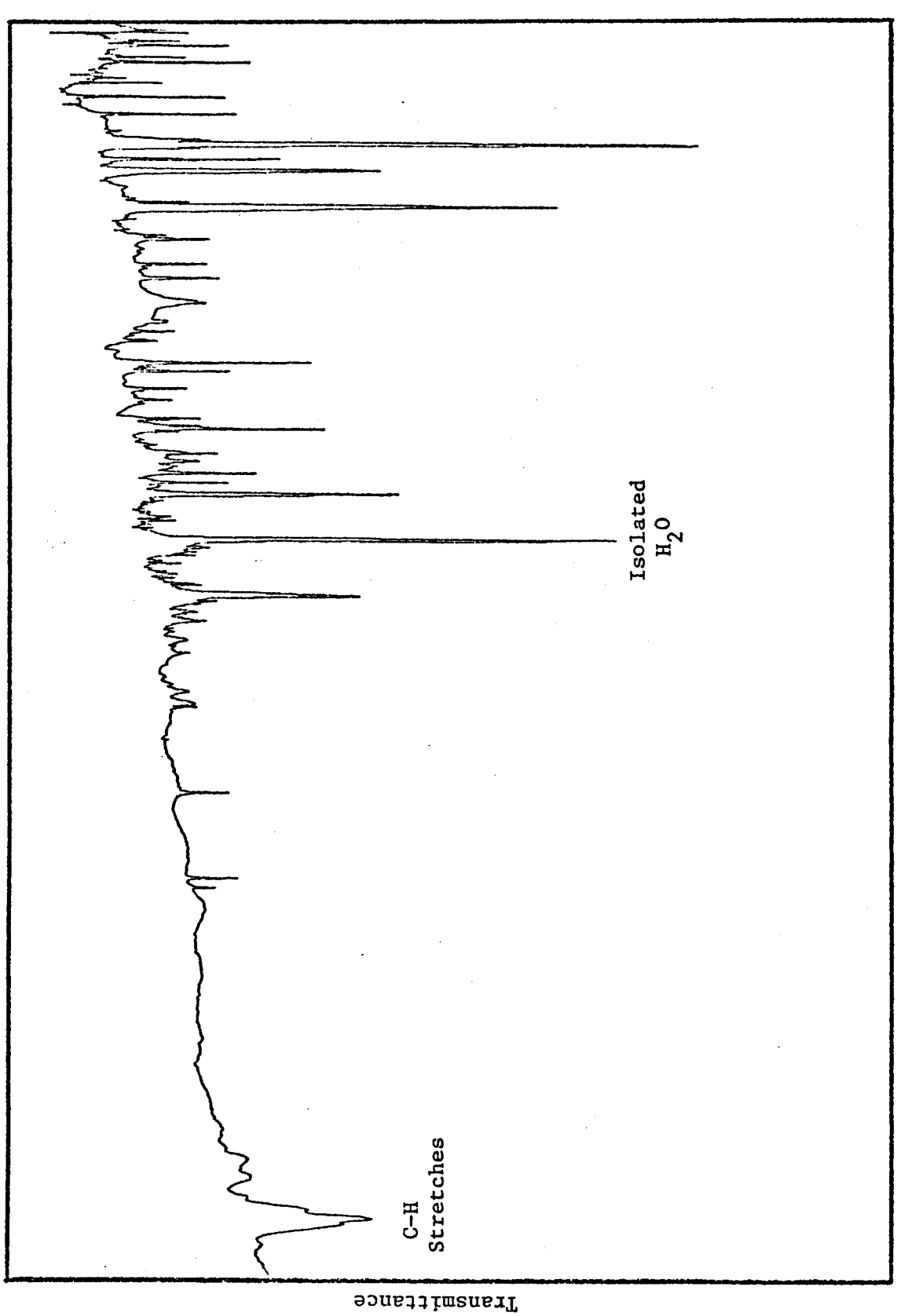


Figure 42. Transmittance spectrum of benz[a]anthracene, 3200-500 cm^{-1}.

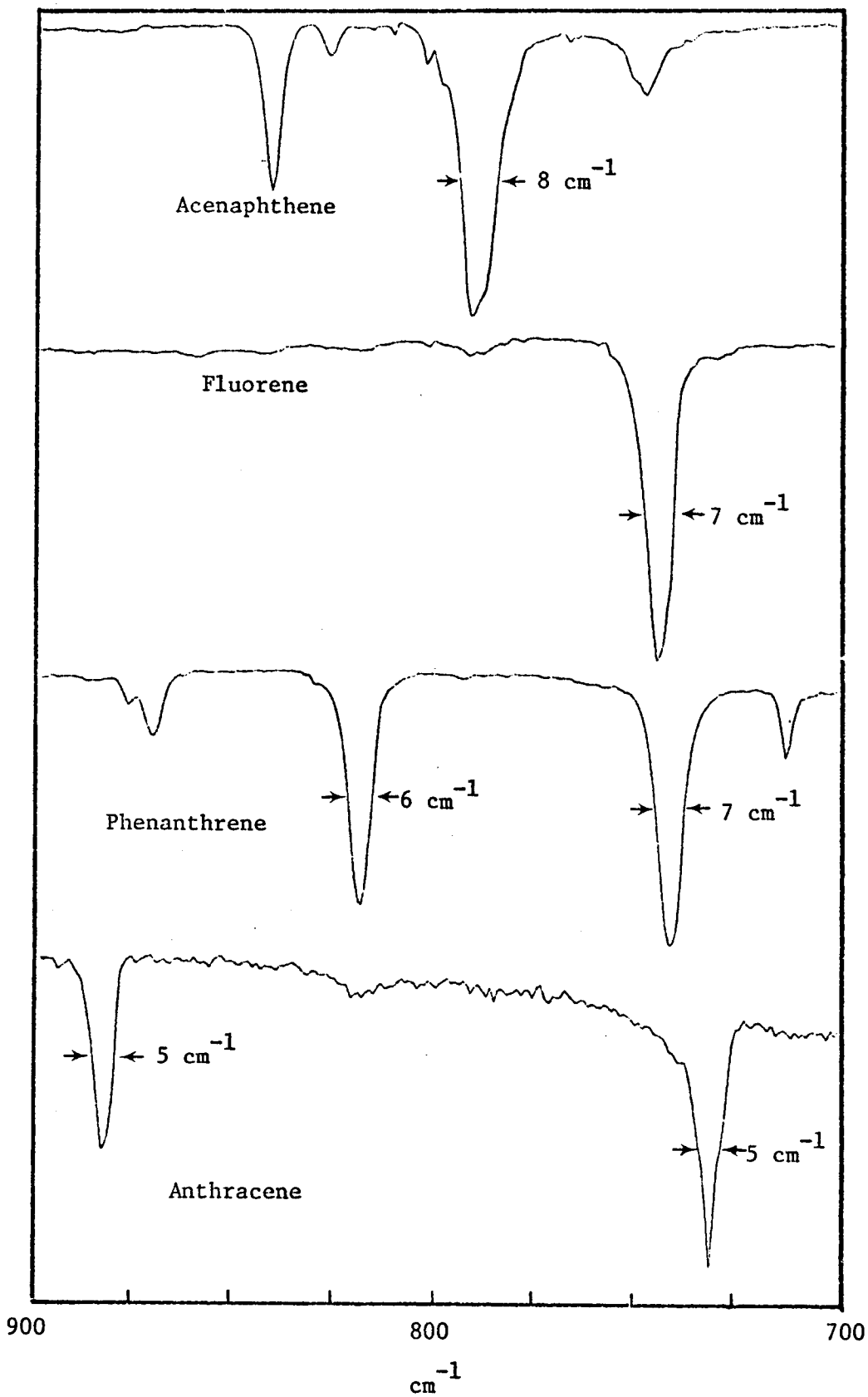


Figure 43. Expanded spectra for the compounds shown in Figure 36, p 121, 900-700 cm^{-1}.

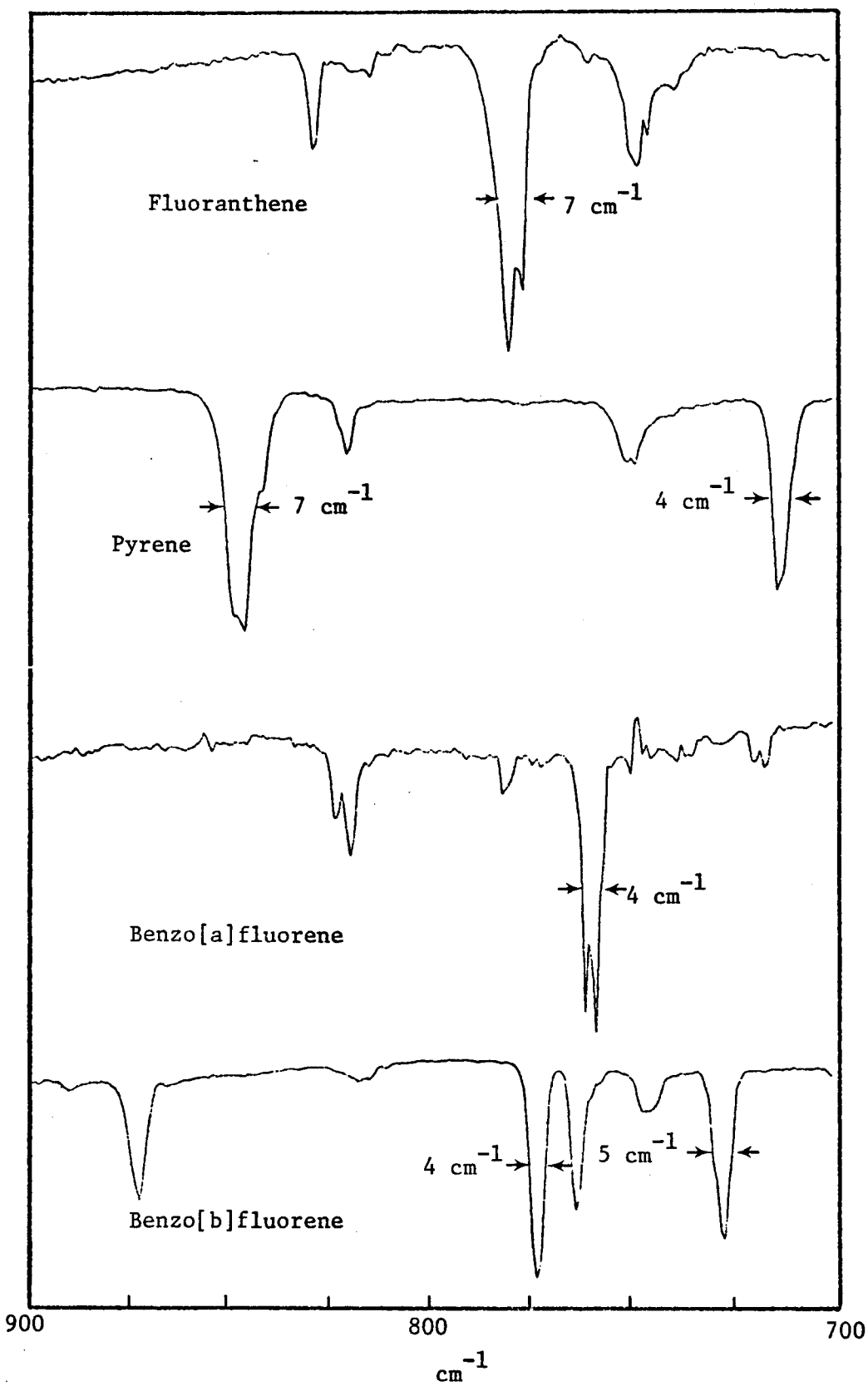


Figure 44. Expanded spectra for the compounds shown in Figure 37, p 122, 900-700 cm^{-1}.

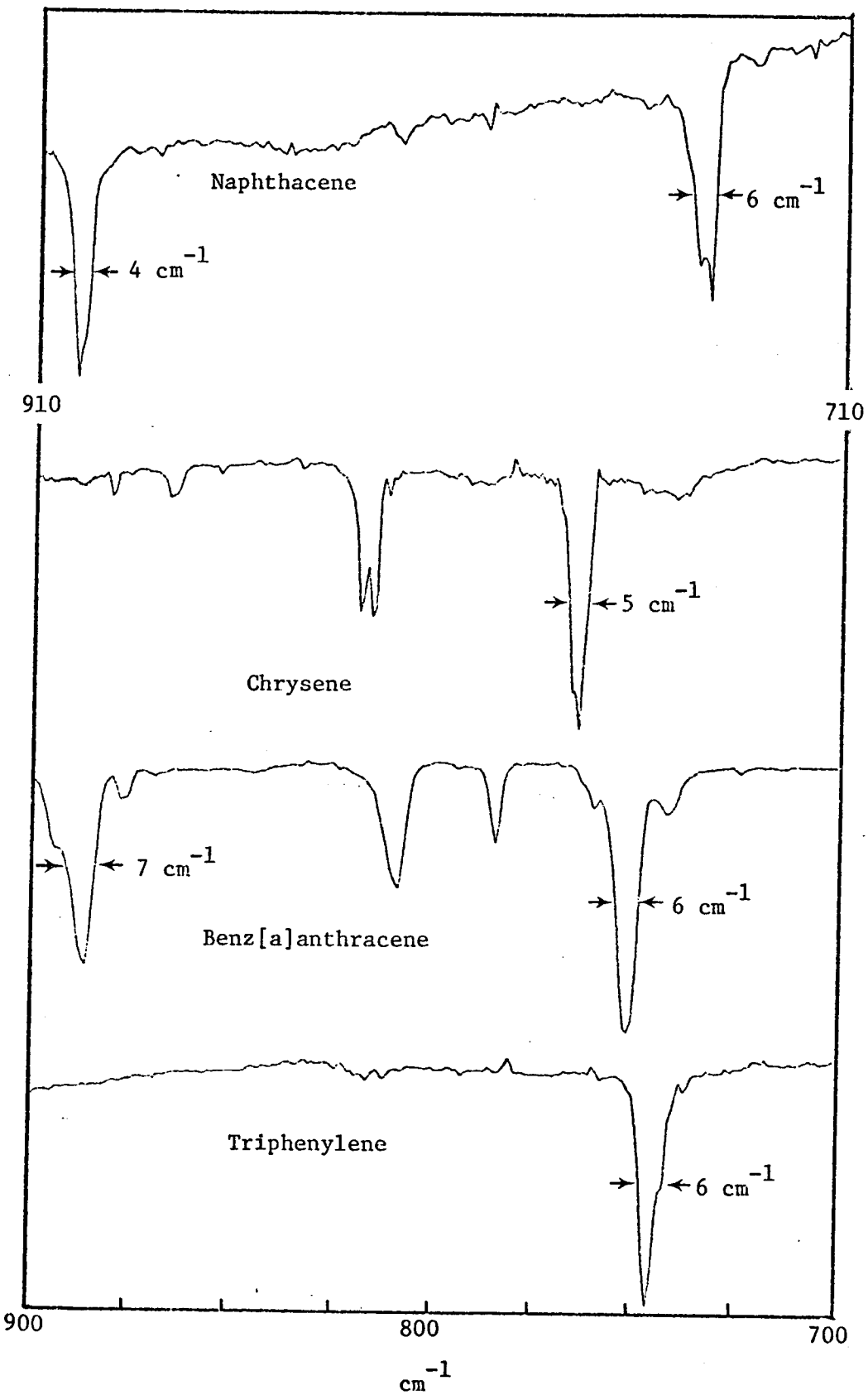


Figure 45. Expanded spectra for the compounds shown in Figure 38, p 123, 900-700 cm^{-1}.

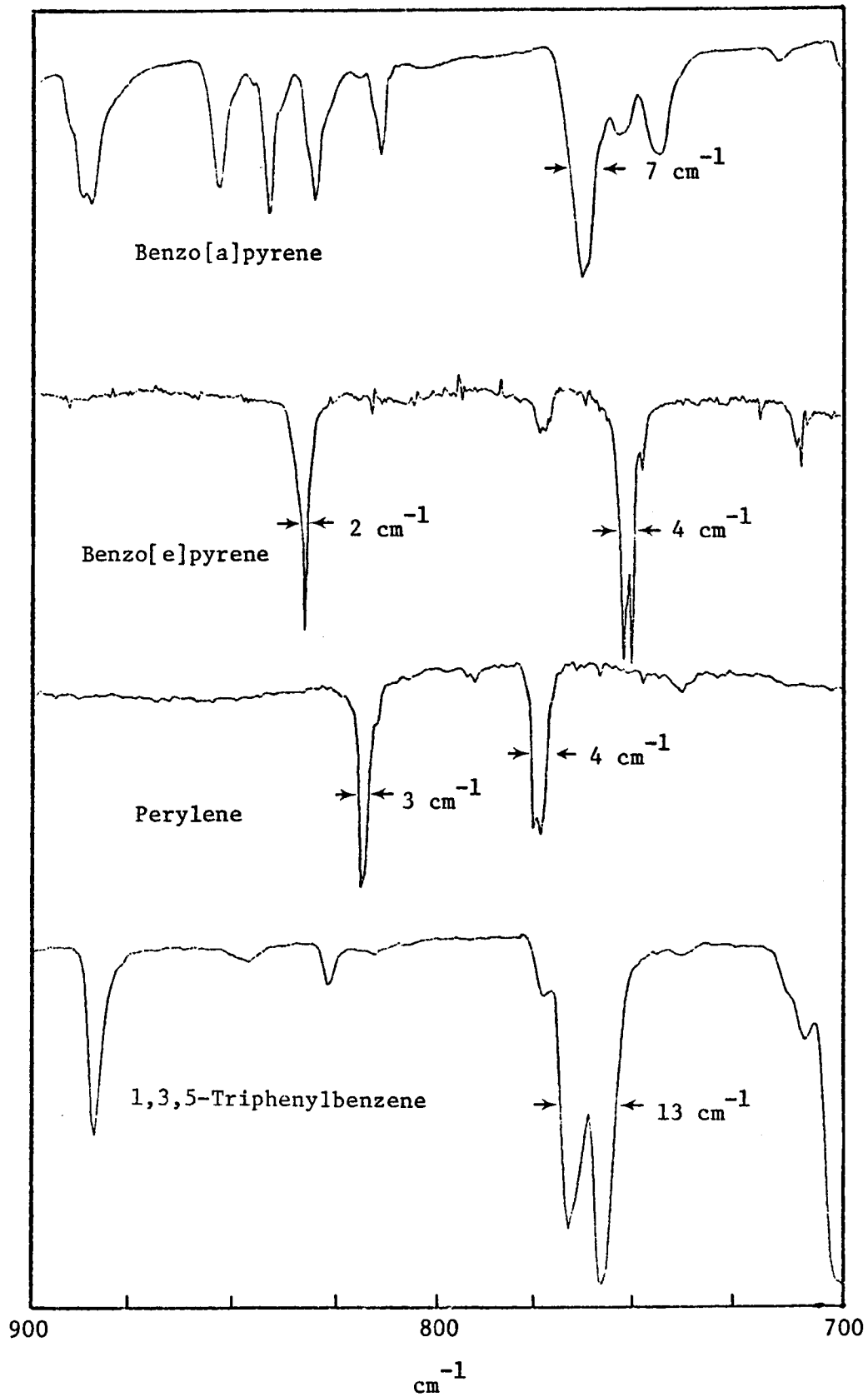


Figure 46. Expanded spectra for the compounds shown in Figure 39, p 124, 900-700 cm^{-1}.

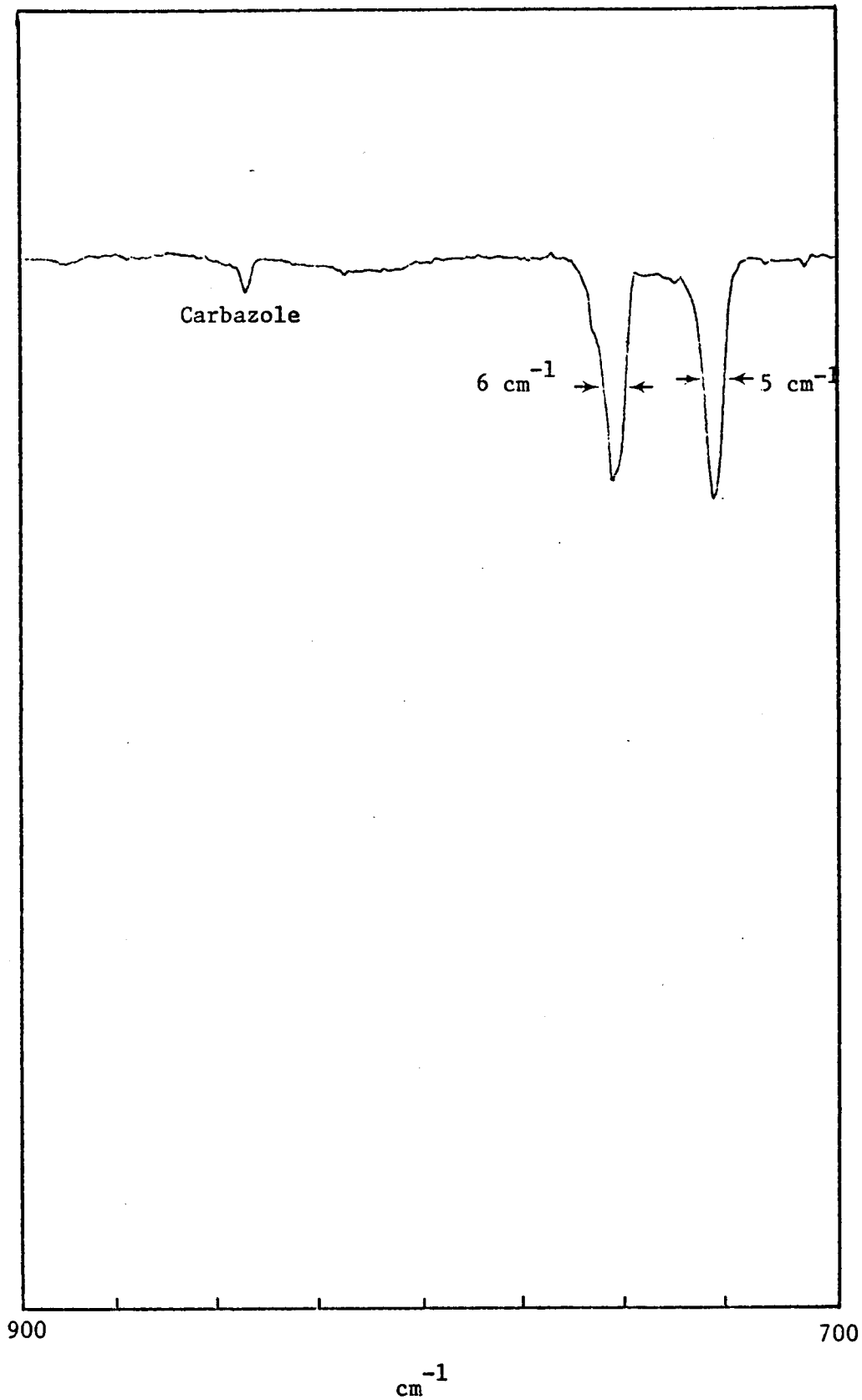


Figure 47. Expanded spectrum for carbazole, 900-700 cm^{-1}.

VITA

Richard Ray Kemmerer was born in Ridgway, Pennsylvania on October 10, 1947. He attended public schools in Johnsonburg, Pennsylvania and graduated from Johnsonburg Area High School in 1965. He entered the Pennsylvania State University in September 1965, and received the Bachelor of Science degree in Chemistry in June 1969.

He began graduate studies in chemistry at Syracuse University in September 1969. His studies were interrupted after one year when he was drafted into the United States Army. Upon completion of his military service, he returned to Syracuse University, where he received the Master of Science degree in Environmental Science in May 1973.

He entered the Graduate School at the University of Tennessee in September 1973, and received the Doctor of Philosophy degree with a major in Chemistry in June 1976. He is a member of the American Chemical Society.

During the course of his graduate study, he has coauthored several articles. The most recent of these has appeared in Analytical Chemistry.